NEW EXCAVATION TECHNOLOGIES FOR UNDERGROUND CONSTRUCTION:
Linear Cutting Machine Tests on Microwave-Irradiated Granodiorite

FINAL PROJECT REPORT

Shrey Arora[1]
Rennie B. Kaunda[1]
[1] Colorado School of Mines,

Sponsorship
(UTC-UTI and Earth Mechanics Institute))

For

University Transportation Center for
Underground Transportation Infrastructure
(UTC-UTI)

March 24, 2018

DISCLAIMER

The contents of this report reflect the views of the authors, who are responsible for the facts and the accuracy of the information presented herein. This document is disseminated in the interest of information exchange. The report is funded, partially or entirely, by a grant from the U.S. Department of Transportation's University Transportation Centers Program. However, the U.S. Government assumes no liability for the contents or use thereof.

Technical Report Documentation Page

1. Report No. UCT-UTI-001	2. Government Accession No.	3. Recipient's Catalog No.
4. Title and Subtitle: NEW EXCAVATION TECHNOLOGIES FOR UNDERGROUND CONSTRUCTION: Linear cutting machine tests on microwave-irradiated granodiorite		5. Report Date: March 24, 2018 6. Performing Organization Code
7. Author(s): Shrey Arora and Rennie B. Kaunda		8. Performing Organization Report No. UTC-UTI-001
9. Performing Organization Name and Address University Transportation Center for Underground Transportation Infrastructure (UTC-UTI) Colorado School of Mines Coolbaugh 308, 1012 14th St., Golden, CO 80401		10. Work Unit No. (TRAIS) 11. Contract or Grant No. 69A3551747118
12. Sponsoring Agency Name and Address United States of America Department of Transportation Research and Innovative Technology Administration		13. Type of Report and Period Covered Final Project Report (14. Sponsoring Agency Code
15. Supplementary Notes Report also available at: https://zenodo.org/communities/utc-uti		
16. Abstract Recent breakthroughs in thermally induced rock fragmentation research indicate the feasibility of utilization of microwaves during rock excavation and tunneling. Unfortunately, few studies have been conducted to systematically assess energy requirements if these emerging technologies were implemented. Additional potential payoffs from the development of such excavation technologies include minimal disturbance to neighboring infrastructure during excavation. The main challenge with current excavation techniques is that it is extremely expensive to break up and move large volumes of rock during blasting, drilling or mechanical excavation in difficult rock. The objective of this project is to measure the specific energy requirements for representative hard rock which has been weakened by microwave irradiation. Granodiorite rock blocks were collected from Boulder, Colorado and prepared at a local quarry. Three of the rock blocks were placed inside a commercial microwave and heated for 30 seconds, 100 seconds and 200 seconds. The four blocks were cast in concrete inside a fabricated metallic box and allowed to cure at the Earth Mechanics Institute (EMI) at Colorado School of Mines. Large scale linear cutting tests were conducted on the four blocks using a single disc cutter. During each linear cutting pass, displacements, horizontal and vertical cutting forces were measured by a computer monitoring system connected to the large scale linear cutting machine. The specific energies required during each cut were then calculated, compiled and analyzed. Further cutting tests are recommended to improve the statistical significance of the findings and to quantify the actual specific energy reductions after microwave preconditioning.		
17. Key Words Rock Excavation; Thermal, Microwave, Linear Cutting, Specific Energy, TBM		18. Distribution Statement No restrictions.

19. Security Classification (of this report) Unclassified	20. Security Classification (of this page) Unclassified	21. No of Pages 82	22. Price NA

TABLE OF CONTENTS

List of Figures

List of Tables

List of Abbreviations

CSM: Colorado School of Mines
EMI: Earth Mechanics Institute
LCM: Linear Cutting Machine
LVDT: Linear Variable Displacement Transducer
SE: Specific Energy
TAL: Thermally Assisted Liberation
TBM: Tunnel Boring Machine
UTC-UTI: University Transportation Center for Underground Transportation Infrastructure

EXECUTIVE SUMMARY

The objective of this project is to measure the specific energy requirements for representative hard rock which has been weakened by microwave irradiation. Granodiorite rock blocks were collected from Boulder, Colorado and prepared at a local quarry. Three of the rock blocks were placed inside a commercial microwave and heated for 30 seconds, 100 seconds and 200 seconds. The four blocks were cast in concrete inside a fabricated metallic box and allowed to cure at the Earth Mechanics Institute (EMI) at Colorado School of Mines. Large scale linear cutting tests were conducted on the four blocks using a single disc cutter. During each linear cutting pass, displacements, horizontal and vertical cutting forces were measured by a computer monitoring system connected to the large scale linear cutting machine. The specific energies required during each cut were then calculated, compiled and analyzed. Further cutting tests are recommended to improve the statistical significance of the findings and to quantify the actual specific energy reductions after microwave preconditioning.

CHAPTER 1 - INTRODUCTION

High energy requirements precluded the practical application of thermal energy to fragment rock and were deemed uneconomical a few decades ago (Kumar, 1968, Carstens et al., 1970, Heuze, 1983, Lau et al., 1991). A major challenge was the conceptual application of energy intensive rock fragmentation processes such as thermal spalling, or melting of intact rock (e.g. Carstens et al., 1970), and wherefore considered a major hurdle in making the technology available for industry use. However, recent studies have shown advances in thermal rock-weakening principles which were previously overlooked (Whittles et al., 2003, Jones et al., 2005, Toifl et al., 2014, Toilfl et al., 2015, Meisels et al., 2015, Zuo et al., 2015, Hassani et al., 2016). These studies, in conjunction with microstructural studies and numerical modeling, point to the observation that if differential heat absorption can be induced such that sufficient high tensile stresses are mobilized through: 1) differential thermal absorption due to mechanical rock microstructure heterogeneities and 2) mineralogical heterogeneities (e.g. Meisels et al., 2015), significant rock weakening can occur. The research in this area has taken a crucial step by acknowledging the theory of microwave heating as viable source of generating differential stresses and strains in rock. The theory suggests that the different mineral constituents assembled within a rock substance will respond differently to irradiation, and at different heating rates and temperatures because of their individual absorption properties. The differential absorption would cause the development of an inhomogeneous state of stress within the same rock - especially along grain boundaries, such as absorbing grains in a non-microwave absorbing matrix (e.g., Whittles et al. 2003; Jones et al. 2005, 2007). More recently, Meisels, et al. (2015) have shown that tensile stresses form along grain boundaries in a multi-phase system when heated with microwaves, and may exceed the tensile strength of the grains leading to significant additional damage to the material.

The role of alternate excavation technologies for hard rock tunneling purposes cannot be ignored as the demand, cost and the depth at which these projects are carried out have increased over time. To this end, researchers have contemplated the application of microwaves for pre-treatment of rock to reduce the cost of mechanical excavation. Laboratory experiments such as large-scale linear cutting of bulk rock blocks can help evaluate the energy requirements during rock excavation. A linear cutting machine (LCM) is a device that provides a "direct measure of rock cuttability" for different simulated field conditions. The machine has the capability to measure the load acting on a single cutter while making a cut on an actual rock. With the help of various sensors mounted on this machine and because of the large scale of the tests, a direct assessment of machine performance can be made in terms of specific energy. Specific energy is the amount of energy spent to excavate a unit volume of rock. For the study described in this report, four samples of boulder granodiorite rock were first subjected to microwave for different exposure time (30 sec., 100 sec., 200 sec., and untreated). The samples were then subjected to linear cutting machine test to determine the specific energy associated with cutting/excavating these preconditioned rocks.

CHAPTER 2 - LITERATURE REVIEW

2.1 Review of Microwave Damage of Rock

The use of thermal energy to facilitate rock fracturing can be traced back to ancient time when "fire setting" was used to fracture rocks long before technologies such as blasting became popular (Fitzgibbon and Veasey, 1990). Scientific research carried out in the early 19th century focused around investigating the role of thermally assisted liberation (TAL) as a means for improving the overall efficiency of a mineral processing plant which spends a considerable amount of energy on crushing and grinding of ores (Wonnacott and Bills, 1990; Lytle et al., 1992). The process at that time involved conventional heating of an object and then subjecting it to air quenching. Despite these attempts at establishing TAL as a tool for preconditioning the rock, the technology could not become popular as it was not economically feasible (Somani et al., 2017). This is largely attributed to the fact that the resulting heat transfer mechanism (conduction, convection, and radiation) inside the rock is a slow process and results in poorly developed fractures in the more economic zone of operation.

The focus on ramping up the heating time made researchers in the field consider microwaves as a new source of TAL. Several research studies have shown that microwave irradiation can enhance rock fragmentation by selectively heating the constitutive minerals (Whittles et al., 2003, Jones et al. 2004, Ali and Bradshaw, 2009, Hartlieb et al., 2012, and others). The microwave absorbing mineral in a non-absorbing matrix, results in the development of differential thermal stresses and subsequent fracturing along mineral boundaries during irradiation. Along with providing an efficient solution of selective heating of minerals, microwave irradiation has the added advantage of producing thermal response (reduction in strength due to artificially induced fractures) in a shorter duration as compared to conventional heating techniques.

Whittles et al. (2003) used finite element simulations to demonstrate that an increase in absorbed microwave energy by some mineral results in the creation of greater (Figure 1). Their study used a theoretical ore consisting of a microwave absorbing pyrite mineral in a low-absorbing calcite matrix. They also concluded that with an increase in absorbed energy, the desired level of rock fracturing can be achieved at a lower energy input. Jones et al. (2005) with the help of similar approach as described earlier, concluded that stresses observed along the mineral boundary were predominantly shear and tensile in nature. The particle size was shown to influence the overall fracturing process. A decrease in size of mineral was accompanied by an increase by microwave energy required for sufficient fracturing of the rock.

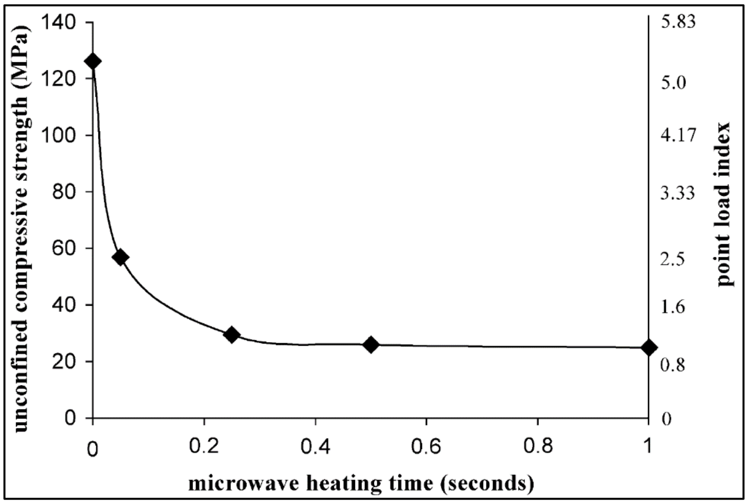

Figure 1 Effect of microwave heating time on the unconfined compressive strength of the theoretical calcite and pyrite sample (Whittles et al., 2003).

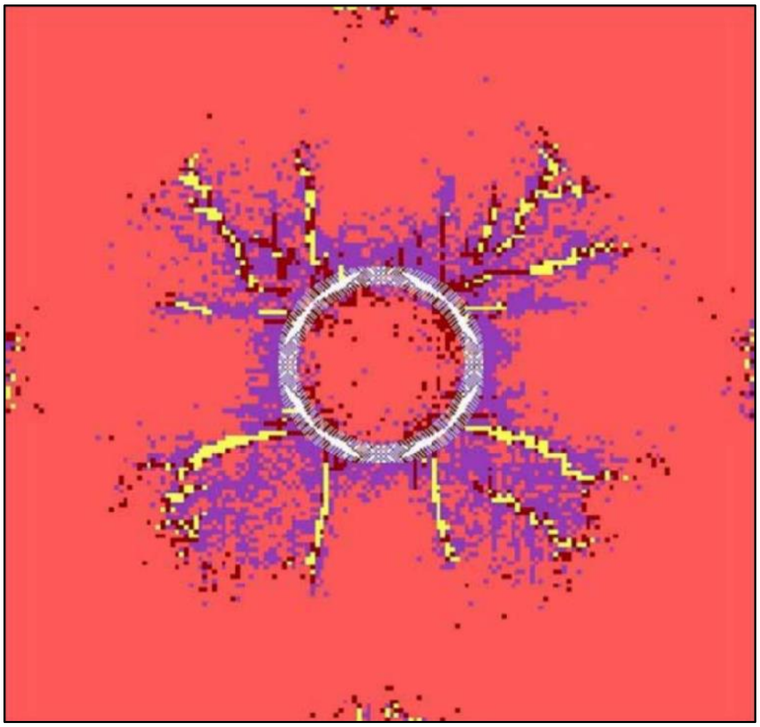

Figure 2 Extensive tensile cracks formed around pyrite discs in a calcite matrix after 1000 micro-seconds (Jones, 2005).

Further, significant research has been performed in the mineral processing domain to highlight the importance of differential thermal gradients in rock damage. These works have shown that by harnessing the dielectric properties of rock constituents, which respond differently to microwave irradiation, differential stresses can be generated (e.g. Amankwah and Pickles 2009; Samouhos et al. 2012). Peak temperature has been chosen as an indicator by many workers (e.g. Walkiewicz et al. 1988) for microwave absorption, and was demonstrated that the peak temperature differs strongly depending on the irradiated mineral. In addition, several experimental studies with low power microwave irradiation have been carried demonstrating that:

- certain types of rock such as magnesite, andesite, dolomite, siderite and travertine can be cracked significantly as result of microwave irradiation (Murová et al. 2000);
- basalt reduces its strength expressed by point load testing and p-wave velocity measurements (Satish et al. 2006; Peinsitt et al. 2010; Hartlieb et al. 2012).
- it is feasible to apply microwave heating to cause damage in granite and sandstone samples (Sikong and Bunsin, 2009 and Peinsitt et al., 2010).
- microwave irradiation of ore can also be effective at enhancing mineral processing applications (Vorster et al., 2001, Rizmanoski, 2011, Kingman et al., 2004, Figure 3).

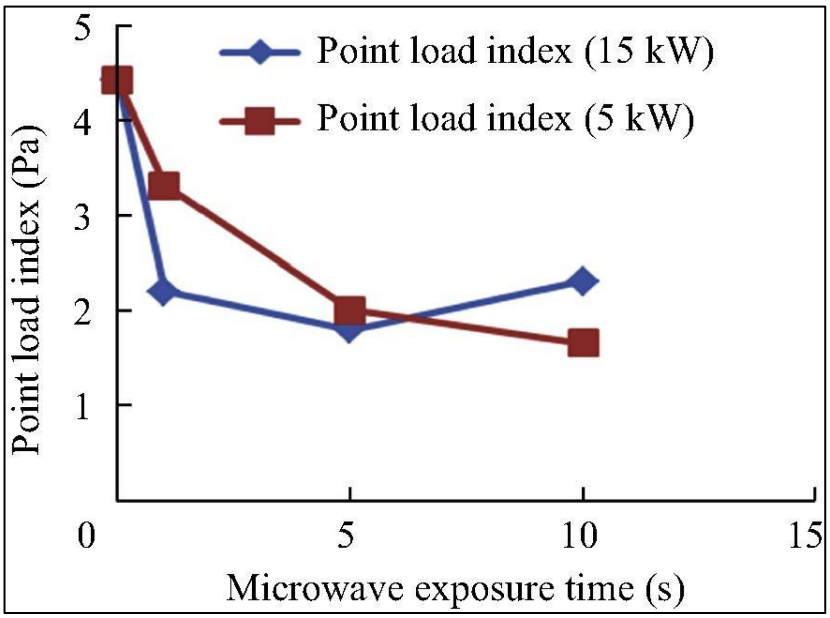

Figure 3 Point load index for different rated power and exposure time for a lead-zinc ore sample (Kingman et al., 2004).

In addition, conventional heating of rock has been investigated for the purposes of understanding fundamental rock behavior in many studies, and the occurrence of microcracks and microcavities was reported in thermally stressed samples (e.g., Zhang et al. 2001; Keshavarz et al. 2010; Yin et al. 2012, Balme et al. 2004). In these previous studies, questions pertaining to damage accumulation, and how the cracks are aligned with respect to mineralogy, and the overall effects on strength degradation remain unclear. Given that rock material consists of a broad variety of minerals, each of which behave differently when exposed to heat. Spatial confinement, possible grain interactions phase changes, recrystallization and coincident volumetric changes, e.g., for example thermal expansion all lead to different behavior for the same rock type (e.g. Reś et al. 2003).

Hassani et al. (2016) carried out a series of laboratory tests to determine the effects of microwave irradiation on the strength reduction of three hard rocks namely norite, basalt, and granite. The experiment al results indicated that the tensile and uniaxial strength of the three types of rocks reduced with increasing exposure time and the power level at which the microwave was operated. It was also concluded that operating power levels play a significant role in increasing the amount of damage caused to the rocks. With the help of empirical equations (Eq. 1), it was shown that the penetration per revolution (P_{REV}) of disc cutter mounted on a Tunnel Boring Machine will increase as the exposure time increases (Figure 4).

$$P_{REV} = 624 \frac{F_n}{\sigma_{BT}} \quad \text{(Eq. 1)}$$

where, F_n = is the thrust force applied by the disc cutter (N) (the normal force in response to the applied thrust), σBT is the Brazilian tensile strength (BTS) of rock (MPa).

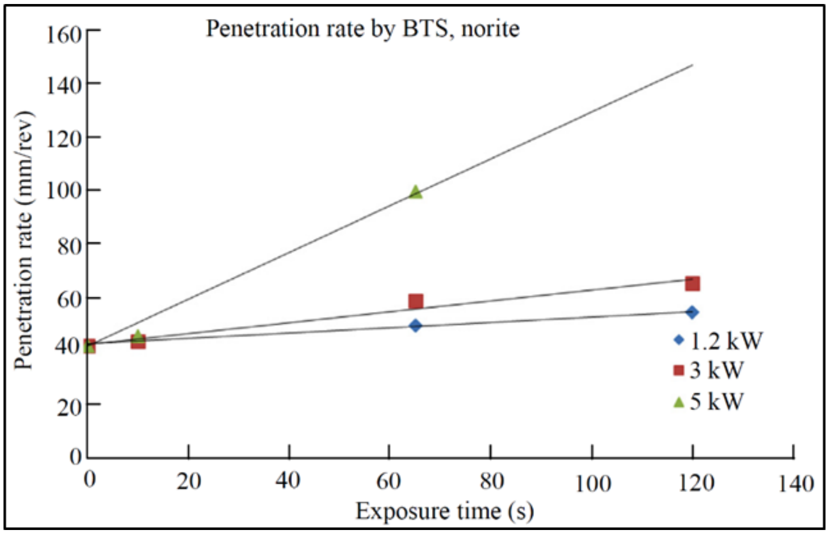

Figure 4 Estimated penetration rate of a TBM into norite vs. microwave treatment (Hassani et al., 2016)

2.2 Review of Linear Cutting Machine Test

There exist different types of rock excavation technologies today which are frequently used in civil and mining engineering projects. These technologies rely on fracturing and disintegration of rock using different methodologies and machines. One of the most important machines that is in use today is the Tunnel Boring Machine (TBM) as shown in Figure 5.

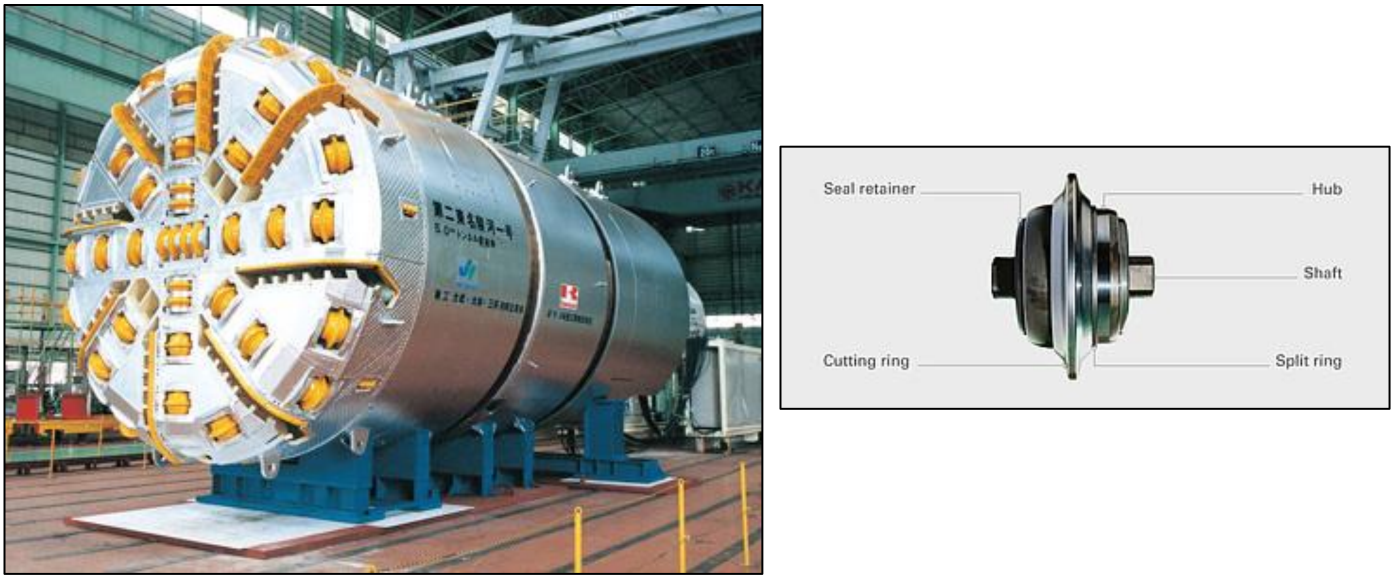

Figure 5 Tunnel Boring Machine: (a) General view of TBM face, (b) TBM disc cutters

The TBM cuts the rock with the help of disc cutter mounted at its face which rotates as the machine is pushed forward into the virgin rock. TBM machines have been employed on various successful projects. However, there is still a need to improve their performance and make them adapt to efficiently work in any rock condition to achieve an optimum advance rate.

Performance of a TBM is essentially governed by the rock breakage mechanism caused by rolling disc on the surface of rock. As the cutters penetrate the rock, a crushed zone develops beneath it (Figure 6). Further, radial cracks develop around these crushed zones and propagate into the rock. These cracks then join with adjacent cracks from another cutter to form rock chips that fallout from the face of the excavation. The forces that develop on the cutter disk are schematically shown in Figure 7. There are three vector components of force as indicated: i.e. the normal force, rolling force and side force. An estimate of these forces can be obtained either through experiments or theoretically.

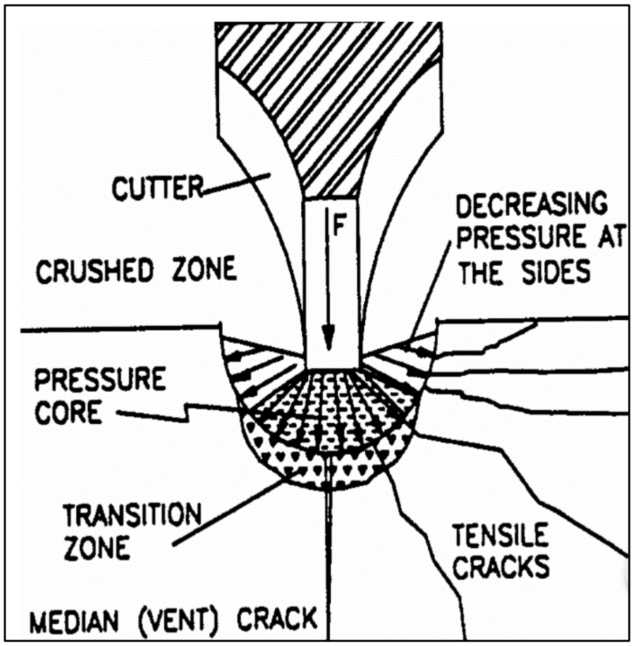

Figure 6 Rock failure mechanism during cutting with a disc cutter (Asbury et. al, 2002)

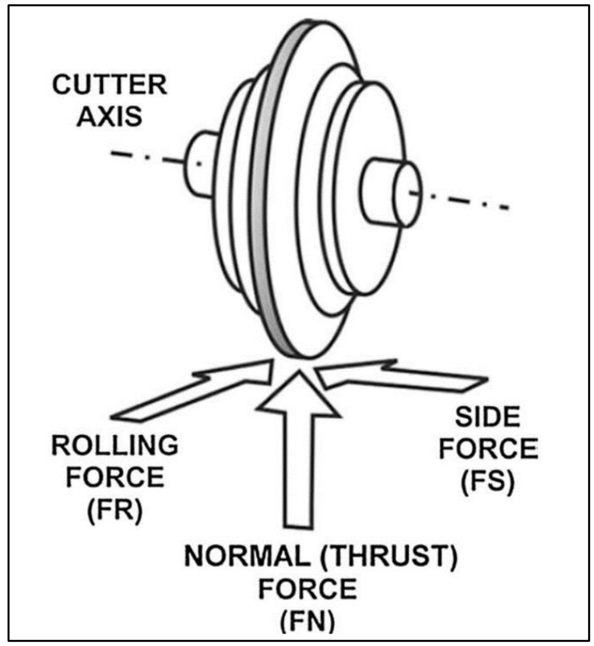

Figure 7 Forces acting on disc cutter (Labra et. al, 2017)

An estimation of the three force components and performance prediction of a cutter mounted on a TBM can be made on a laboratory scale. Colorado School of Mines developed the first ever Linear Cutting Machine (LCM) (Figure 8) in the early 1970's that could provide a measurement of cutting forces and rock cuttability for a given set parameters (i.e. cutter spacing, cutter penetration, cutter thrust and cutting speed).

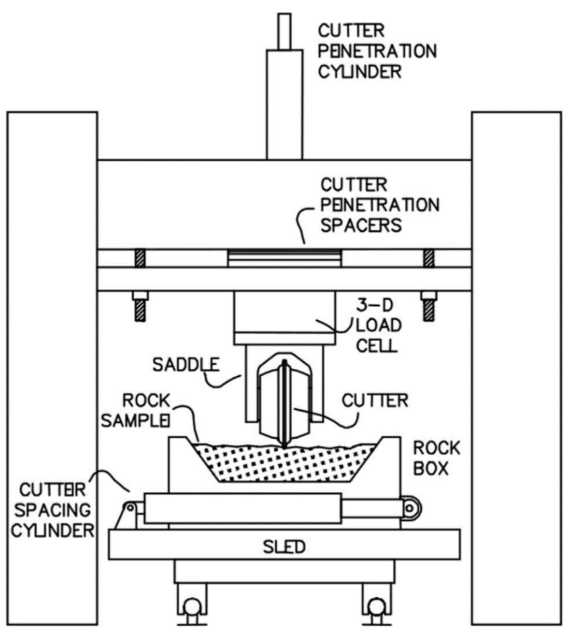

Figure 8 Linear cutting machine (Colorado School of Mines)

Once the forces are determined, the concept of specific energy (*SE*) is used to assess cutting efficiency of a single disc cutter. *SE* is defined as the amount of energy required to excavate a unit volume of rocks and is defined as:

$$SE = \frac{F_r\, L}{V} \qquad \text{(Eq. 2)}$$

where *Fr* is the rolling force, *L* the cutting distance, and *V* the cutting volume. Equation 2 can also be expressed in terms of the penetration depth *p* and spacing between disc cutters *s* where *V* = *Pls* and then rewritten as:

$$SE = \frac{F_r\, L}{pLs} = \frac{F_r}{ps} \qquad \text{(Eq. 3)}$$

Further, *SE* can be used to predict TBM performance (Bilgin et al., 1999, 2014). The net production rate (*NPR*) of an excavating machine can then be expressed as following:

$$NPR = \frac{kP}{V} \qquad \text{(Eq. 2)}$$

where k is the energy transfer ratio from the cutting head to the tunnel face, k is usually taken as equal to 0.8 for TBM, and P (in kW) is the power used to excavate rock expressed in terms of the TBM torque T (in kNm), and the rotational velocity of the cutterhead N (in revolutions/sec) as follows:

$$P = 2\pi NT \qquad \text{(Eq. 3)}$$

CHAPTER 3 – METHODOLOGY

The main objective of the research work presented in this report was to observe the reduction in specific energy or the ease in cuttability of microwave irradiated rock blocks. The main hypothesis of this research is: a reduction in specific energy will be observed in rock blocks irradiated by microwaves, and the reduction in specific energy is proportional to the length of microwave irradiation. Consequentially, the following methodology was adopted to test the presented hypothesis, as summarized by the following set of tasks:

1. Granodiorite rock specimen were collected and cut into rectangular blocks.
2. The granodiorite blocks were then subjected to microwave irradiation at three different exposure durations (untreated, 30 secs, 100 secs, and 200 secs).
3. The untreated and treated blocks were then cast in concrete and allowed to cure, and
4. Large-scale linear cutting tests were performed on the concrete-cast rock blocks, while measuring the cutting forces required to cut several lines across the blocks.

3.1 Specimen Collection and Preparation

The rock samples used for this study were collected from Boulder Canyon Trailhead, located approximately 2.5 miles west of Boulder, Colorado along the state highway 119 (Figure 9).

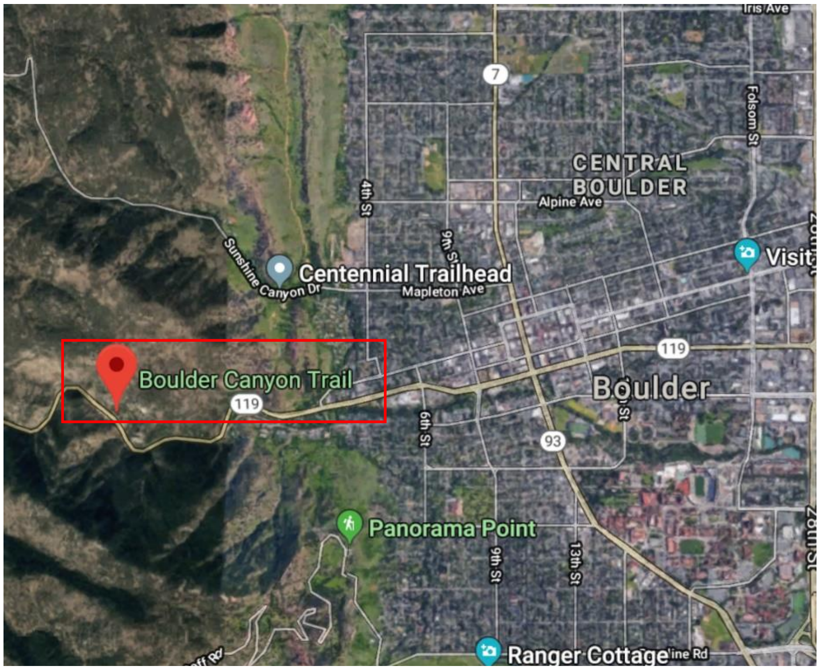

Figure 9 Specimen collection location.

The rock type consists of Boulder creek granodiorite which belong to the Boulder Creek batholith of Precambrian age. The granodiorite is generally a coarser grained mafic rock and is summarized in Table 1.

Table 1 Properties of Granodiorite rock

Rock	**Composition**	**Notes**
Granodiorite	- Quartz > 20% - Feldspar = Na/Ca plagioclase - Biotite + amphibole = 10-25%	- An intermediate rock with high quartz and mafic content - Salt and pepper appearance

The granodiorite rock boulders collected from the site were then transported to a local dimensional stone quarry to be cut in to four rectangular blocks (Figure 10). These blocks had the following dimensions (L x W x H): 12 inches x 11 inches x 7.5 inches.

Figure 10 Example of prepared rectangular rock blocks used for this study

3.2 Microwave Treatment of Specimen

The prepared rock blocks were then transported to CSM for microwave treatment. The Rocks Mechanics Laboratory facility at CSM has a commercial size microwave oven that can operate at 2.45 GHz and 3kW power.

Figure 11 The Amana Commercial microwave oven used for this study.

Three of the specimens were treated for 30 secs, 100 secs and 200 secs at 3kW and the temperature was recorded at the visible face inside the microwave chamber. The fourth rock block was left untreated.

3.3 Linear Cutting Machine Test Set-Up

Upon microwave treatment, rock blocks were cast in concrete, allowed to cure and subjected to linear cutting experiments. The LCM at Colorado School of Mines (Figure 12) consists of a large stiff reaction frame with a cutter assembly mounted on it. The forces acting on the cutter is measured via a tri-axial load frame installed between the cutter and frame. A linear variable displacement transducer (LVDT) is installed on the piston that pushes the tray with a heavy steel box containing the rock sample. The rock sample is cast in concrete within this box (Figure 13) which provides the necessary confinement during testing and to prevent the sample from disintegration under the high cutter loads.

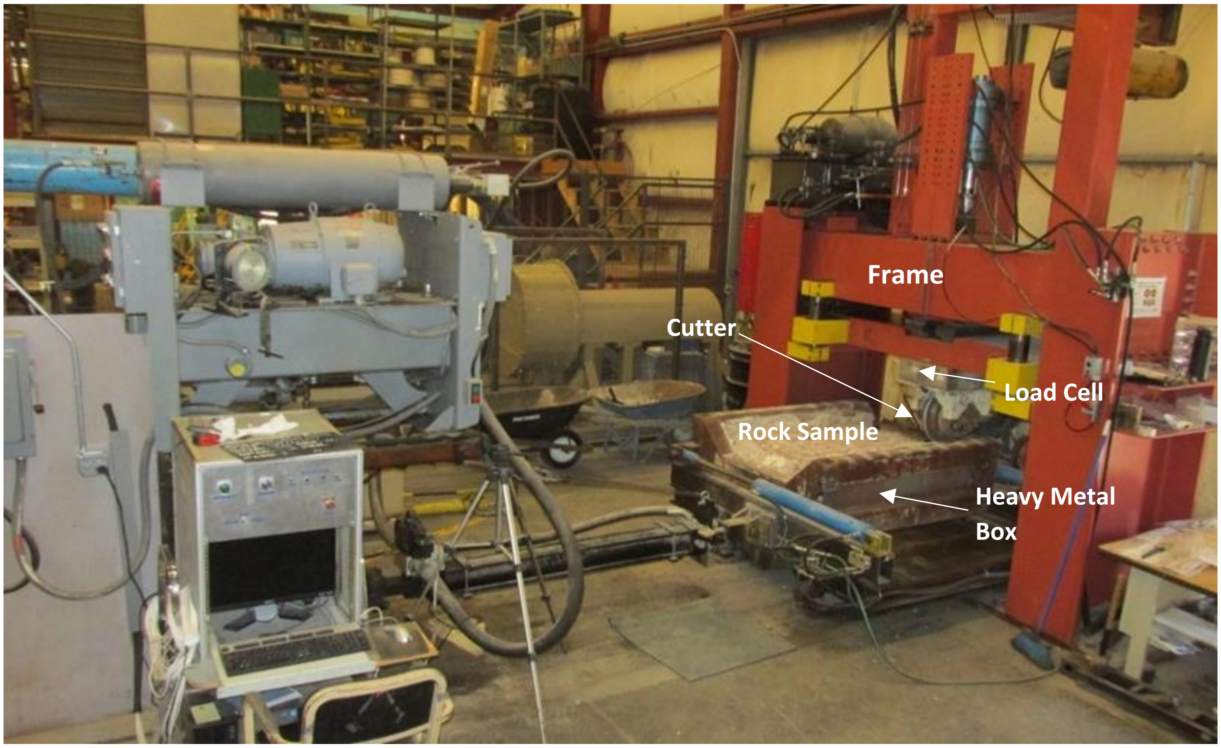

Figure 132 The LCM set up at the Earth Mechanics Institute at Colorado School of Mines

(a) (b)

Figure 14 (a) Rock specimen placed 5 inches apart inside the metal box, (b) After concrete has been casted.

The test is run by pushing the sample through the cutter using a servo controlled hydraulic actuator. Each test is run at a given penetration depth, and constant velocity. The load cell mounted on top of the cutter records the three forces as described earlier. The effect of multiple cutters on an actual TBM cutterhead is achieved by moving the rock box sideways by a specified spacing and the repeating the test. The repetition simulates the coalescence of radial cracks emanating from adjacent cutting sites and the formation of rock chips. It should be noted here that during actual fields conditions, the cutter on a TBM operates on irregular rock surface left behind by previous cutting action. The previous cutting action is replicated in the laboratory by performing conditioning of the rock sample, where essentially the sample is preliminarily run through the cutter without recording any measurements.

Figure 14 shows the configuration of specimens and the number of cutting lines used for each pass during the current project. One pass is considered as the cutting of samples along each of these lines for a desired penetration depth. For the next pass, the cutter is then moved down by adding metal plate spacers (with thickness equal to the desired penetration depth) between the cutter head and metal frame.

Lines 1, 4,6,7,8 and 13 were excluded from the analysis as they were close to the interface between specimen and concrete confinement, and would have yielded unreliable results. The spacing between each cutting line was 2 inches for the entirety of this experiment. A total of three conditioning passes were carried out before the actual test, which consisted of three passes each with 0.1-inch penetration of the cutter head, followed by three more passes but with 0.2-inch penetration.

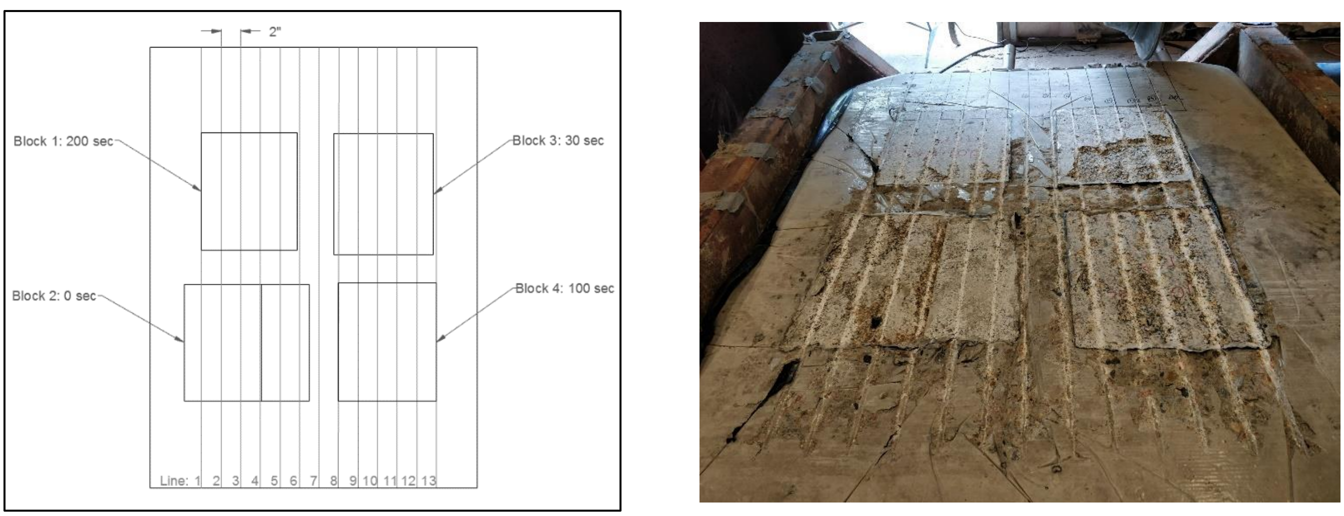

(a) (b)

Figure 15 (a) Specimen and cutting line configuration adopted for LCM test, (b) cutting lines after conditioning.

CHAPTER 4 – RESULTS AND DISCUSSION

As discussed in the preceding sections, three of the granodiorite rock blocks were first subjected to microwave irradiation prior to conducting the large-scale LCM testing. Each rectangular block was exposed to different durations of microwave irradiation, and temperatures were recorded before and after the test using an infrared thermometer. Table 1 summarizes the recorded temperature and Figure 15 shows the location on the specimen where those readings were taken.

Table 2 Temperature readings before and after microwave heating of the specimens.

Irradiation Time (sec)	Temperature Readings (°C) (Before/After)				
	Corner 1	Corner 2	Corner 3	Corner 4	Center
30	20.5/21	20.5/21	20.5/21.1	20.5/21.3	20.5/21.1
100	20/27.5	20/24.4	20.5/24.5	20.5/26.2	20.1/24.4
200	19.9/31.5	20/31.2	20.1/30.9	20.4/30.9	20.3/30.8

Next LCM tests were then conducted on the irradiated rock blocks. During the linear cutting, each pass of the test was documented (videography and photography), and the results of the test (forces recorded by sensors) were stored on a desktop computer. The captured linear cutting forces required to cut each line were analyzed to compute the specific energy required for each cut by the cutter disc using Equations 2 and 3 and are summarized on Figure 16. Table 3 summarizes the computed specific energy in hp-hr/yd^3 for each pass and each specimen. The linear cutting forces used to compute the specific energy shown in Figure 16 have been compiled and presented in Appendix A.

Table 3 Computed specific energy from LCM test using the cutting forces presented in Appendix A.

		Conditioning		0.1" Penetration			0.2" Penetration		
Cumulative cut depth:		0.2	0.3	0.4	0.5	0.6	0.8	1	1.2
Exposure Time (s)	0	2	10	11	5	6	8	8	10
	30	2	10	5	2	6	10	8	8
	100	15	12	15	10	13	14	13	8
	200	1	7	12	12	8	7	10	12
		Specific Energy (hp-hr)/yd^3							

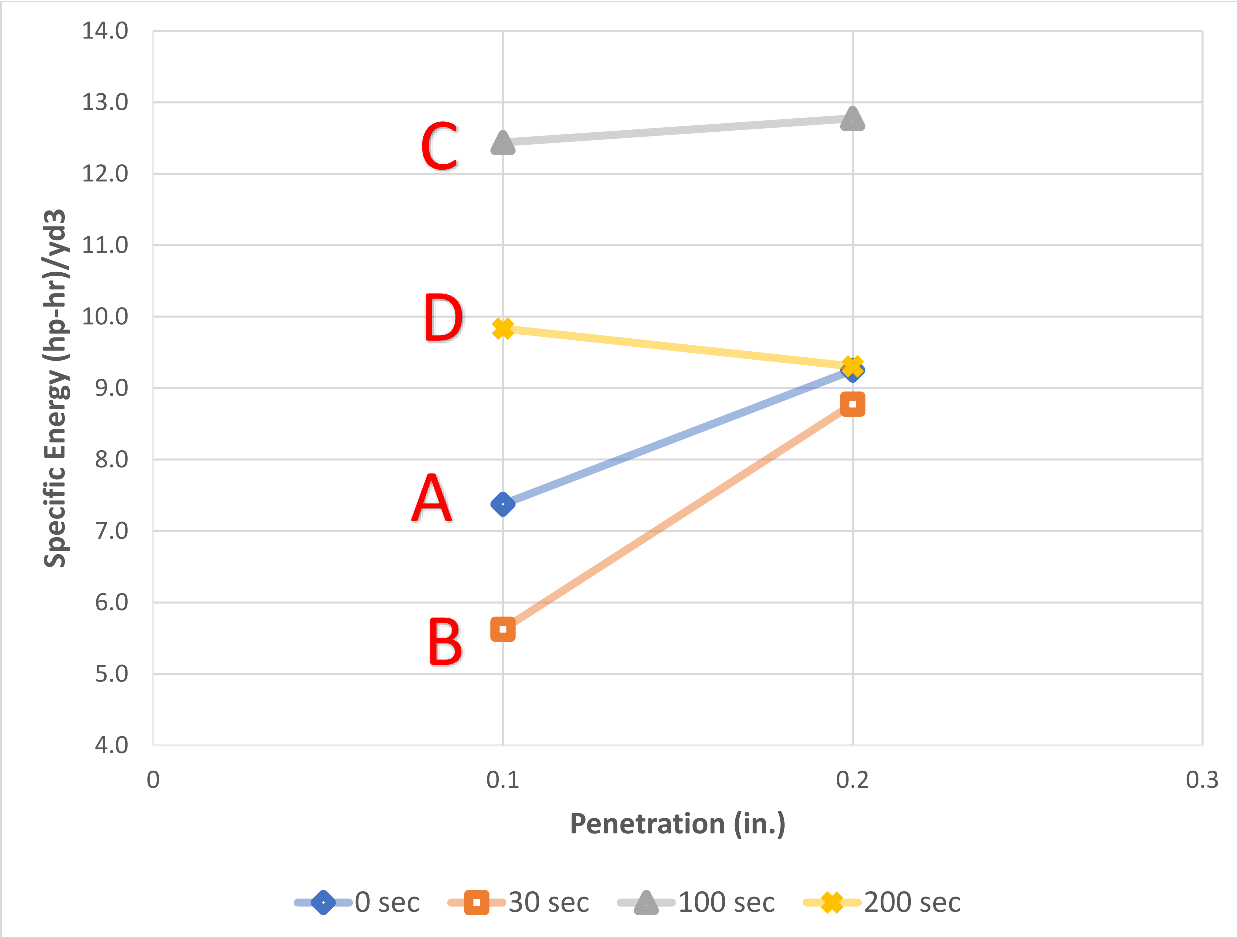

Figure 17 Graphs showing the average specific energy required for each rock block for a given cut penetration depth. All the forces required to compute the specific energies at each cut penetration are presented in Appendix A

According to the current research hypothesis a decrease in specific energy would be expected with increasing microwave irradiation exposure time. However, the damage caused by microwave irradiation can vary depending upon the depth of penetration by the microwaves into the rock interior in addition to the initial condition and intact strengths of individual rock blocks. Figure 16 shows that the rock block treated with microwaves for 30 seconds had the lowest average specific energy requirements of all the rock specimens. On the other hand, the block treated for 100 seconds required the highest average specific energy. In addition, variability in specific energy requirements at a cut penetration of 0.1 for all rock blocks was more significant than at a cut penetration of 0.2 for Blocks A, B and D; implying less influence of microwave induced strength degradation at relatively deeper rock depths.

The characteristics of the cutting forces presented in Appendix A also provide some useful insights. As seen in the graphs of the distance to the peak force for each block, the peak force is approximately in the same location of each block. The distance to the peak force in Block A is in the 35-37-inch range from the edges of the rock block. The distance to the peak force for the Block B is in the 19-21-inch range, and in the 34-36-inch range for Block C. The distance to the peak force for Block D is approximately in the 15-18-inch range. When looking at all the distances to the peak forces for each block and accounting for the placement of the blocks in the concrete-casts, the location of the peak forces in the rock blocks can be justified. It is clear that the range of all the peak forces lies in the center of each rock block, including Block A, i.e. the rock block that was not pre-treated at all. Therefore, the strongest part of the individual blocks was always the center of the block.

While there is no apparent correlation between the rock blocks and the minimum cutting forces, there appears to be a correlation in the location of the minimum forces. Similar to the location of the peak forces along each cut, each block had a specific range where minimum cutting forces were observed. Block A had the first minimum force in the 30-32-inch range and the minimum force in the 34-36-inch range from the edges of the rock block. Block B had the first minimum force in the 15-17-inch range and the second minimum force in the 20-23-inch range. Block C had the first minimum force in the 29-32-inch range and the second minimum force in the 35-37-inch range. Finally, Block D had the first minimum force in the 15-17-inch range and the second minimum force in the 18-21-inch range. It can be inferred that all rock blocks had the first minimum cutting force at an approximate distance of 2-3 inches from one edge of the block, and a second minimum cutting force at a similar location on the opposite edge of the block. Another noticeable feature occurred during the conditioning cuts and the early runs. During cutting, some blocks recorded instantaneous zero forces applied at certain discrete locations, which would seem to indicate the cutting edge did not even contact the surface of the block at those points. Rock Block D was the exception to this observation and displayed no instantaneous forces with a zero reading. On the other hand, Block C followed by Block B displayed the most frequent zero force instantaneous readings at certain discrete points. It is possible that the blocks where the observation was dominant were not perfectly flat, creating uneven horizontal surfaces in certain locations where the disc cutter intersected the rock block.

The following future investigations are suggested based on the analysis of the current LCM test results. A low specific energy was required for the specimen exposed for 200 secs as compared to the other test blocks. However, this trend could be observed only until a total cumulative penetration depth 0.3 inches. It is possible that that the microwaves did not penetrate deeper than 0.3 inches, but statistical validity is required to validate whether this feature was not a function of microwave power density, or duration of exposure at a fixed power density. Given the large size required to prepare rock blocks, it is impossible ensure that all the irradiated and cut samples have the exact same initial conditions. For instance, it is possible that a departure from the initial hypothesis could be explained as a result of each individual rock bloc having undergone different degrees of weathering prior to microwave irradiation. As such, initially weaker rocks would undergo relatively less weakening compared to initially relatively stronger rocks. Therefore, repeatability of the reported LCM testing herein would add statistical validity and confidence to the reported experimental results and conclusions.

REFERENCES

Kumar, A. "The effect of stress rate and temperature on the strength of basalt and granite." *Geophysics* 33, no. 3 (1968): 501-510.

Carstens, J. P., W. R. Davison, and C. A. Brown. "An Evaluation Of Heat-Weaking Hard Rock As An Assist To Mechanical Tunneling." In *The 12th US Symposium on Rock Mechanics (USRMS)*. American Rock Mechanics Association, 1970.

Heuze, F. E. "High-temperature mechanical, physical and thermal properties of granitic rocks—a review." In *International Journal of Rock Mechanics and Mining Sciences & Geomechanics Abstracts*, vol. 20, no. 1, pp. 3-10. Pergamon, 1983.

Lau, J. S. O., R. Jackson, and B. Gorski. "The effects of temperature and pressure on the mechanical properties of Lac du Bonnet grey granite." In *The 32nd US Symposium on Rock Mechanics (USRMS)*. American Rock Mechanics Association, 1991.

Whittles, D. N., S. W. Kingman, and D. J. Reddish. "Application of numerical modelling for prediction of the influence of power density on microwave-assisted breakage." *International Journal of Mineral Processing* 68, no. 1 (2003): 71-91.

Jones, D. A., S. W. Kingman, D. N. Whittles, and I. S. Lowndes. "Understanding microwave assisted breakage." *Minerals engineering* 18, no. 7 (2005): 659-669.

Toifl, M., R. Meisels, P. Hartlieb, F. Kuchar, and T. Antretter. "Microwave Absorption and its Thermo-mechanical Consequences in Heterogeneous Rocks." *Geomechanics from Micro to Macro* (2014): 1545-1550.

Toifl, Michael, Ronald Meisels, Philipp Hartlieb, Friedemar Kuchar, and Thomas Antretter. "3D numerical study on microwave induced stresses in inhomogeneous hard rocks." *Minerals Engineering* 90 (2016): 29-42.

Meisels, R., M. Toifl, P. Hartlieb, F. Kuchar, and T. Antretter. "Microwave propagation and absorption and its thermo-mechanical consequences in heterogeneous rocks." *International Journal of Mineral Processing* 135 (2015): 40-51.

Zuo, J.P., Wang, X.S., Mao,D.Q., and Wang, C. L. "Effect of TM coupled load on cracking behavior and reliability analysis of double-notched crustal rock." (2015).

Hassani, F., Nekoovaght, P.M., and Gharib, N. "The influence of microwave irradiation on rocks for microwave-assisted underground excavation." *Journal of Rock Mechanics and Geotechnical Engineering* 8, no. 1 (2016): 1-15.

Jones, D. A., S. W. Kingman, D. N. Whittles, and I. S. Lowndes. "The influence of microwave energy delivery method on strength reduction in ore samples." *Chemical Engineering and Processing: Process Intensification* 46, no. 4 (2007): 291-299.

Amankwah, R. K., and C. A. Pickles. "Microwave roasting of a carbonaceous sulphidic gold concentrate." *Minerals Engineering* 22, no. 13 (2009): 1095-1101.

Samouhos, Michail, Maria Taxiarchou, Ron Hutcheon, and Eamonn Devlin. "Microwave reduction of a nickeliferous laterite ore." Minerals Engineering 34 (2012): 19-29.

Walkiewicz, J. W., G. Kazonich, and S. L. McGill. "Microwave heating characteristics of selected minerals and compounds." *Miner. Metall. Process* 5, no. 1 (1988): 39-42.

Murová, I.; Lovás, M.; Jakabský, S. "The influence of microwave radiation on the failure of rocks." *Acta Montanistica Slovaca* 5, no. 3 (2000): 283–285.

Satish, H., J. Ouellet, V. Raghavan, and P. Radziszewski. "Investigating microwave assisted rock breakage for possible space mining applications." *Mining technology* 115, no. 1 (2006): 34-40.

Peinsitt, Thomas, Friedemar Kuchar, Philipp Hartlieb, Peter Moser, Hubert Kargl, Uwe Restner, and Nikolaus Sifferlinger. "Microwave heating of dry and water saturated basalt, granite and sandstone." *International Journal of Mining and Mineral Engineering* 2, no. 1 (2010): 18-29.
Hartlieb, P., M. Leindl, F. Kuchar, T. Antretter, and P. Moser. "Damage of basalt induced by microwave irradiation." *Minerals Engineering* 31 (2012): 82-89.

Sikong, Lek, and Thiti Bunsin. "Mechanical property and cutting rate of microwave treated granite rock." *Sonklanakarin Journal of Science and Technology* 31, no. 4 (2009): 447.

Vorster, W., N. A. Rowson, and S. W. Kingman. "The effect of microwave radiation upon the processing of Neves Corvo copper ore." *International Journal of Mineral Processing* 63, no. 1 (2001): 29-44.

Rizmanoski, Vladimir. "The effect of microwave pretreatment on impact breakage of copper ore." *Minerals Engineering* 24, no. 14 (2011): 1609-1618.

Kingman, S. W., K. Jackson, A. Cumbane, S. M. Bradshaw, N. A. Rowson, and R. Greenwood. "Recent developments in microwave-assisted comminution." *International Journal of Mineral Processing* 74, no. 1 (2004): 71-83.

Zhang, Z. X., J. Yu, S. Q. Kou, and P-A. Lindqvist. "Effects of high temperatures on dynamic rock fracture." *International Journal of Rock Mechanics and Mining Sciences* 38, no. 2 (2001): 211-225.

Keshavarz, M., F. L. Pellet, and B. Loret. "Damage and changes in mechanical properties of a gabbro thermally loaded up to 1,000 C." *Pure and Applied Geophysics* 167, no. 12 (2010): 1511-1523.

Yin, Tubing, Xibing Li, Kaiwen Xia, and Sheng Huang. "Effect of thermal treatment on the dynamic fracture toughness of Laurentian granite." *Rock mechanics and rock engineering* 45, no. 6 (2012): 1087-1094.

Balme, M. R., V. Rocchi, C. Jones, P. R. Sammonds, P. G. Meredith, and S. Boon. "Fracture toughness measurements on igneous rocks using a high-pressure, high-temperature rock fracture mechanics cell." *Journal of Volcanology and Geothermal Research* 132, no. 2 (2004): 159-172.

Reś, Janusz; Wladzielczyk, K.; Ghose, Ajoy K. (2003): Environment-friendly techniques of rock breaking. Lisse: Balkema.

Fitzgibbon, K. E., and T. J. Veasey. "Thermally assisted liberation-a review." Minerals Engineering 3.1-2 (1990): 181-185.

Lytle, J., N. Choi, and K. Prisbrey. "Influence of preheating on grindability of coal." International journal of mineral processing 36.1-2 (1992): 107-112.

Wonnacott, G., and B. A. Wills. "Optimisation of thermally assisted liberation of a tin ore with the aid of computer simulation." Minerals Engineering 3.1-2 (1990): 187-198.

Somani, Aditya, et al. "Pre-treatment of rocks prior to comminution–A critical review of present practices." International Journal of Mining Science and Technology 27.2 (2017): 339-348.

Asbury, B., M. Cigla, and C. Balci. "Design methodology, testing and evaluation of a continuous miner cutterhead for dust reduction in underground coal mining." 2002 SME Annual Meeting. 2002.

Labra, Carlos, Jerzy Rojek, and Eugenio Oñate. "Discrete/Finite Element Modelling of Rock Cutting with a TBM Disc Cutter." Rock Mechanics and Rock Engineering50.3 (2017): 621-638.

APPENDIX A: Plots of Linear Cutting Forces

Conditioning Passes:

Pass 2-line 2

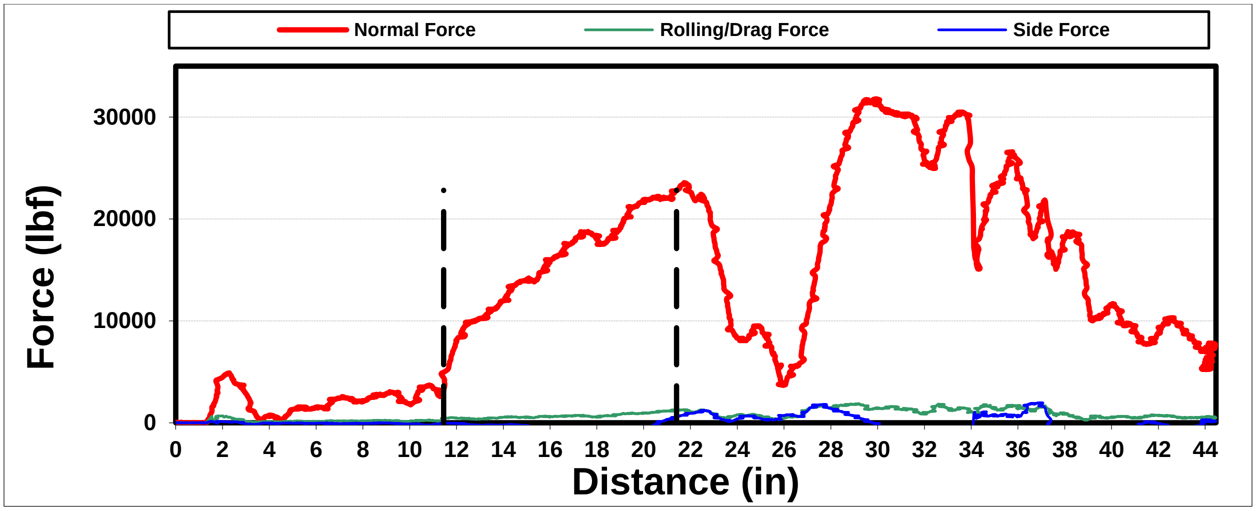

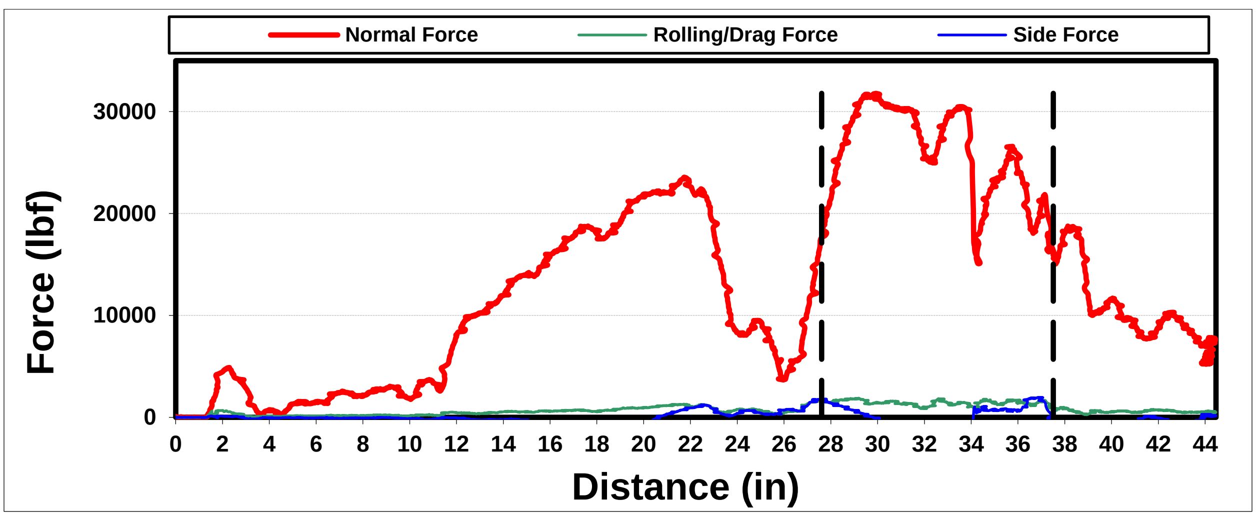

Pass 2 Line 3

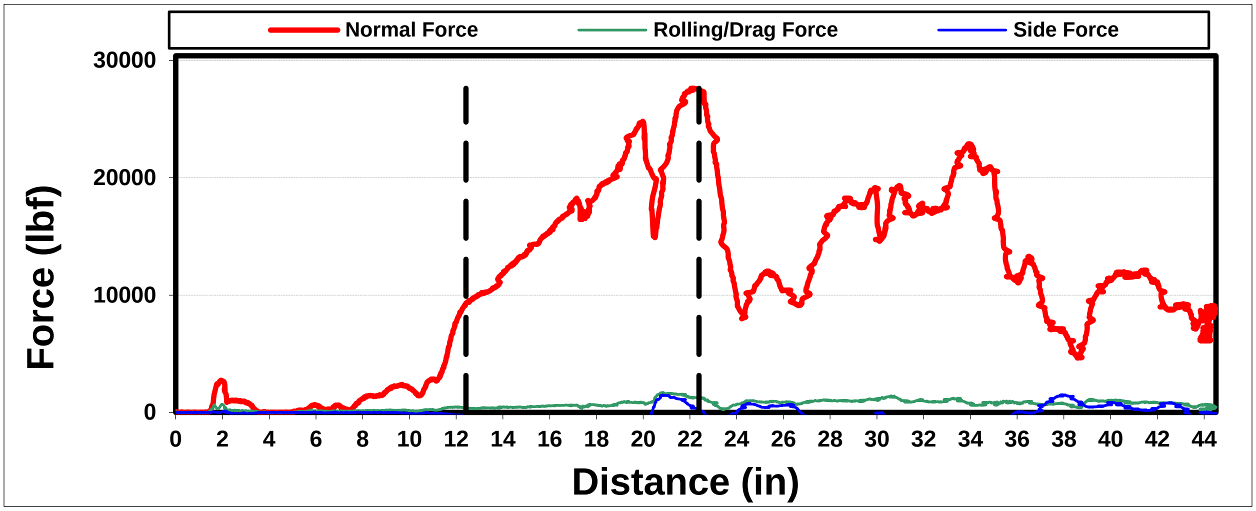

Normal Force
Rolling/Drag Force
Side Force
Force (lbf)
30000
20000
10000
0
0 2 4 6 8 10 12 14 16 18 20 22 24 26 28 30 32 34 36 38 40 42 44
Distance (in)

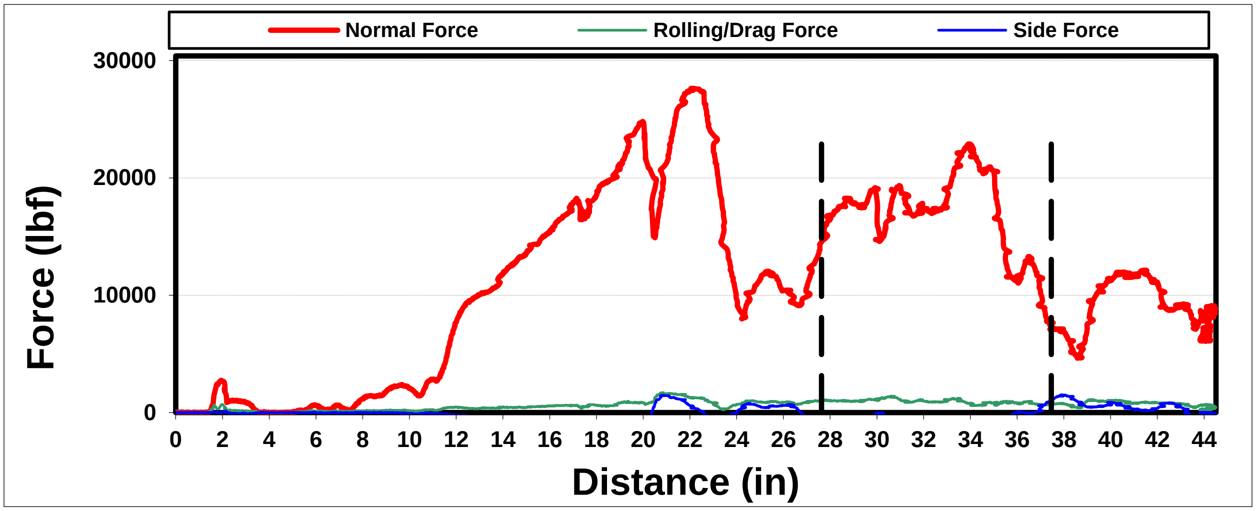

Normal Force
Rolling/Drag Force
Side Force
Force (lbf)
30000
20000
10000
0
0 2 4 6 8 10 12 14 16 18 20 22 24 26 28 30 32 34 36 38 40 42 44
Distance (in)

Pass 2 Line 5

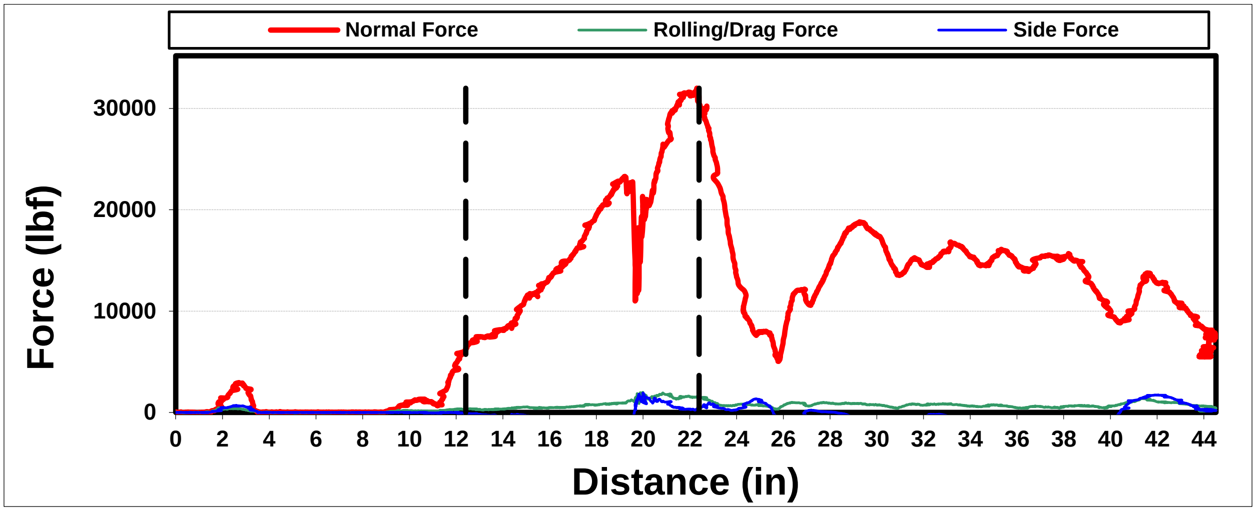
Normal Force
Rolling/Drag Force
Side Force
Force (lbf)
30000
20000
10000
0
0 2 4 6 8 10 12 14 16 18 20 22 24 26 28 30 32 34 36 38 40 42 44
Distance (in)

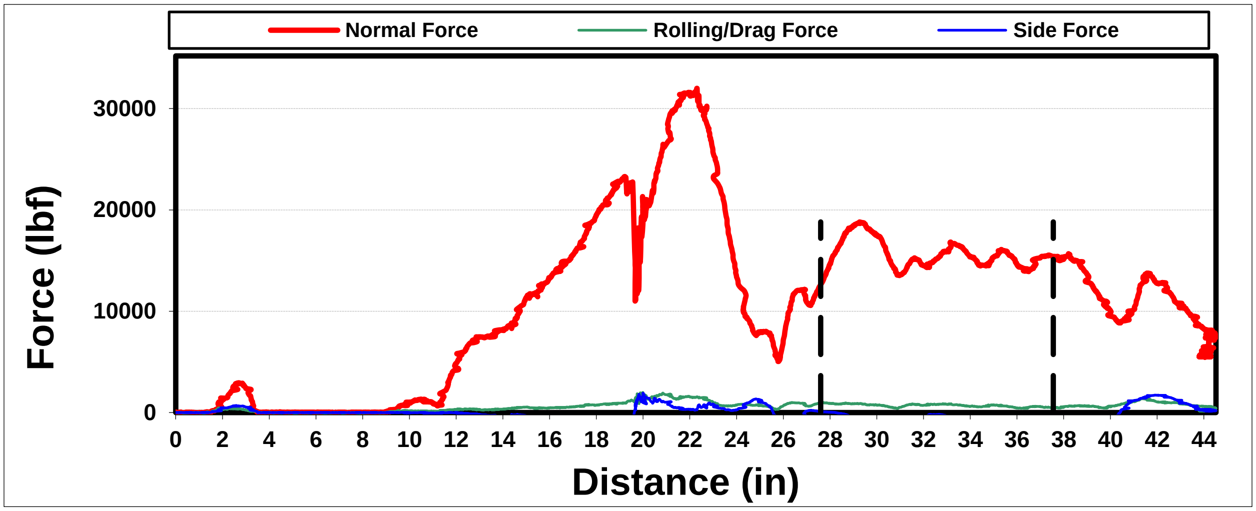
Normal Force
Rolling/Drag Force
Side Force
Force (lbf)
30000
20000
10000
0
0 2 4 6 8 10 12 14 16 18 20 22 24 26 28 30 32 34 36 38 40 42 44
Distance (in)

Pass 2 Line 9

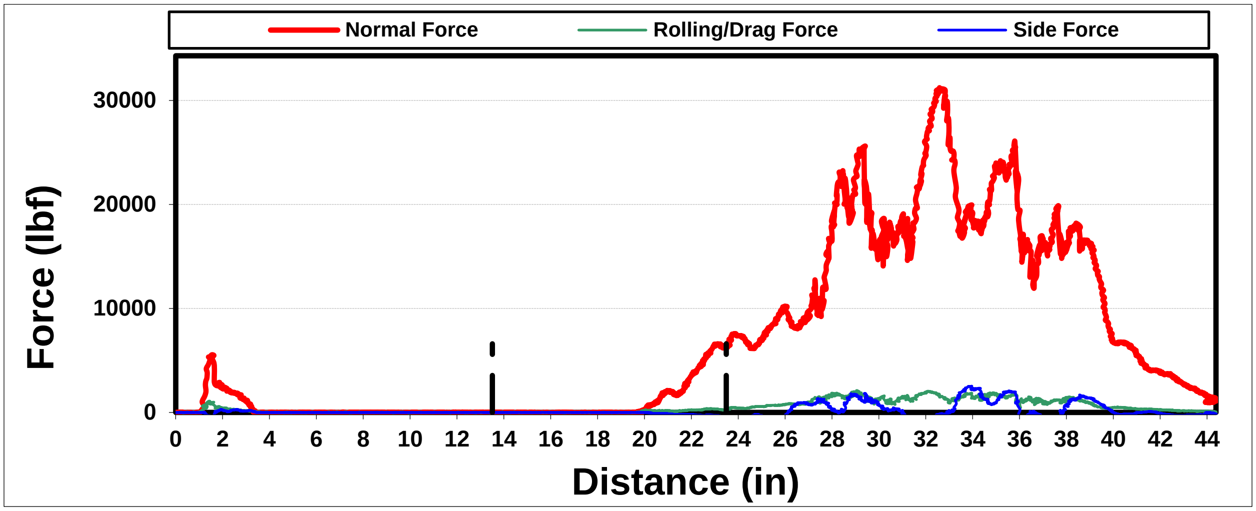
Normal Force
Rolling/Drag Force
Side Force
Force (lbf)
30000
20000
10000
0
0 2 4 6 8 10 12 14 16 18 20 22 24 26 28 30 32 34 36 38 40 42 44
Distance (in)

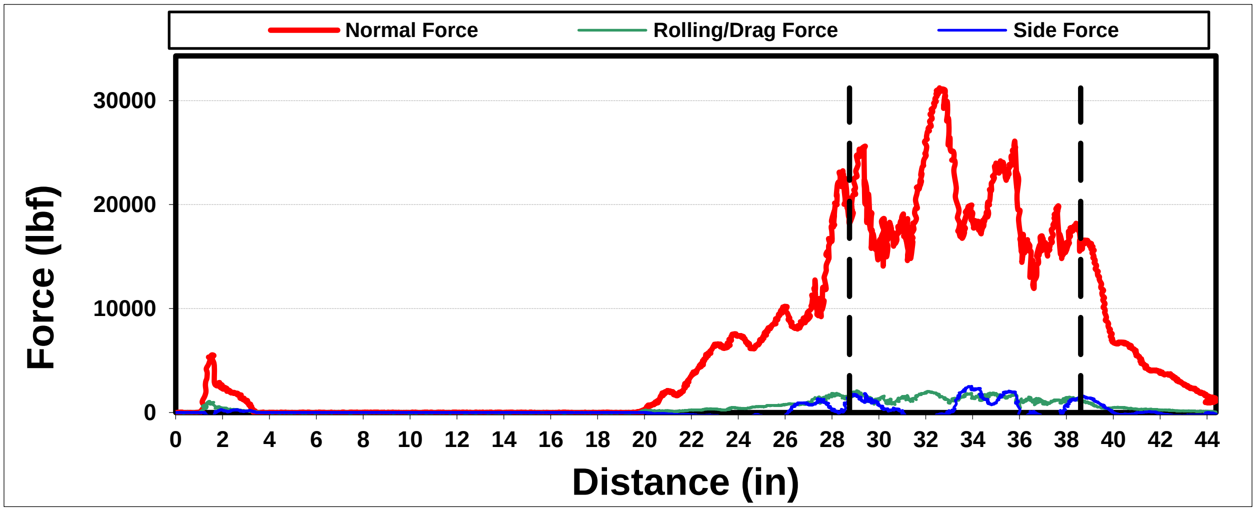
Normal Force
Rolling/Drag Force
Side Force
Force (lbf)
30000
20000
10000
0
0 2 4 6 8 10 12 14 16 18 20 22 24 26 28 30 32 34 36 38 40 42 44
Distance (in)

Pass 2 Line 10

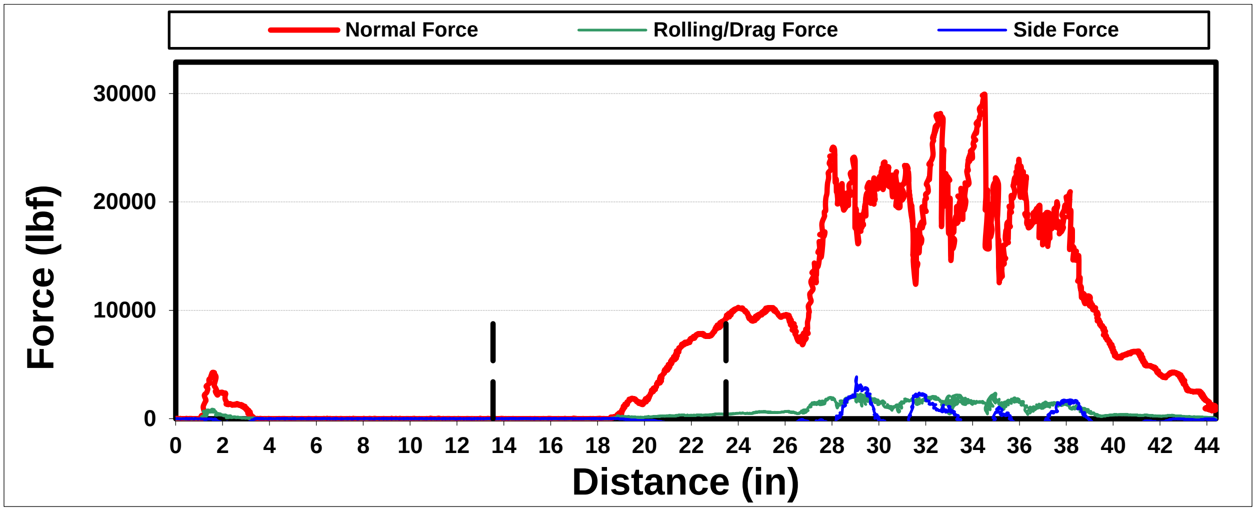

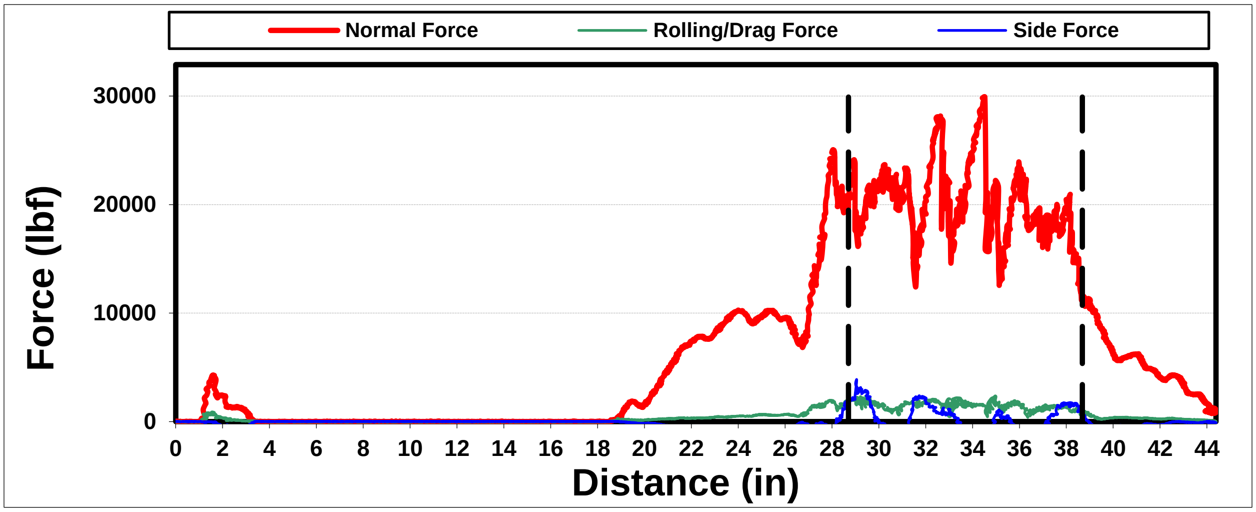

Pass 2 Line 11

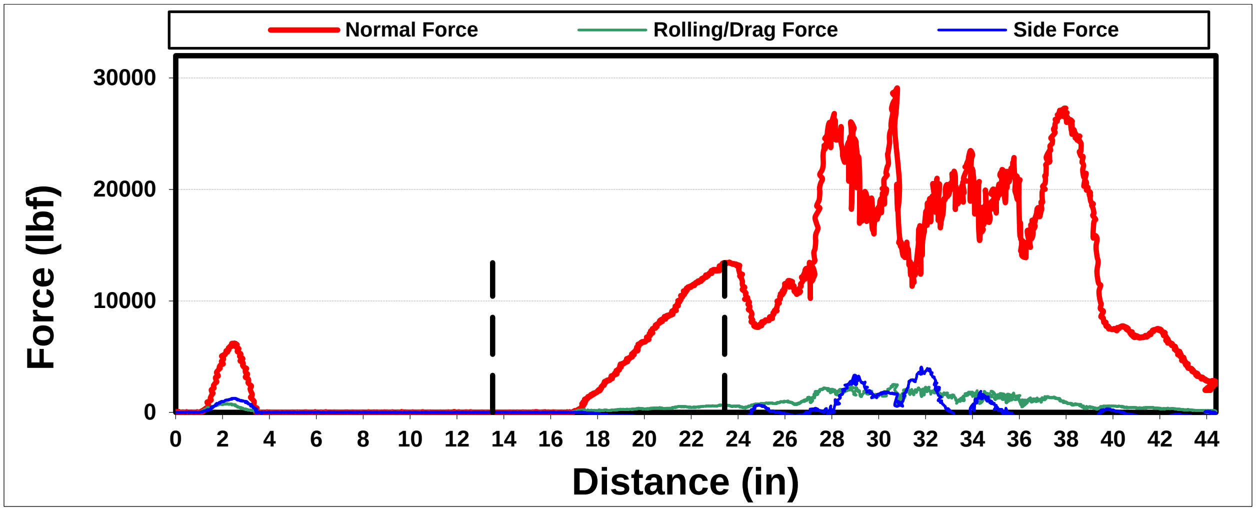

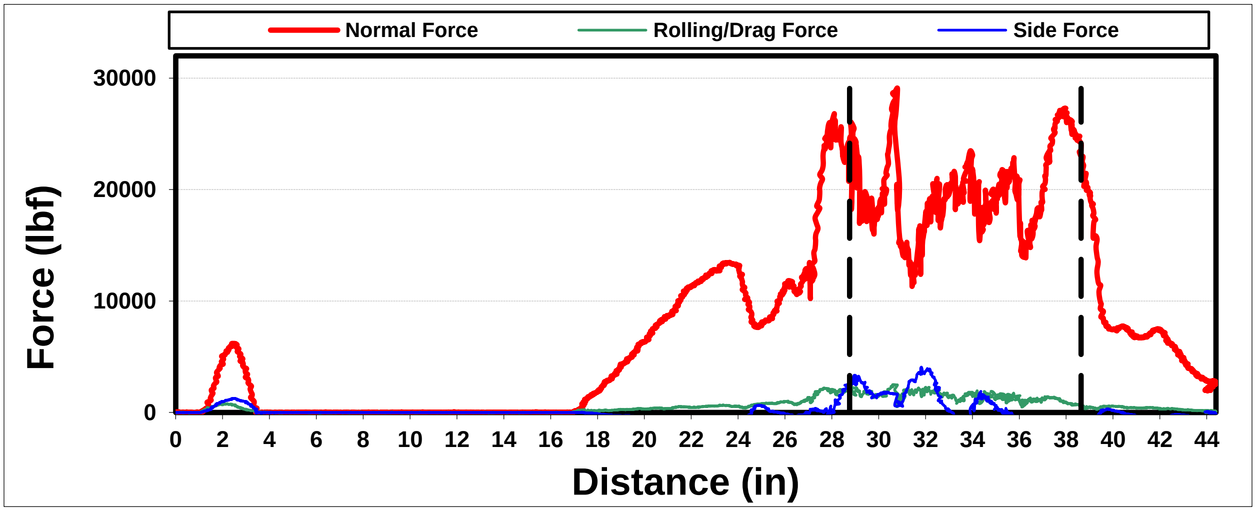

Pass 2 Line 12

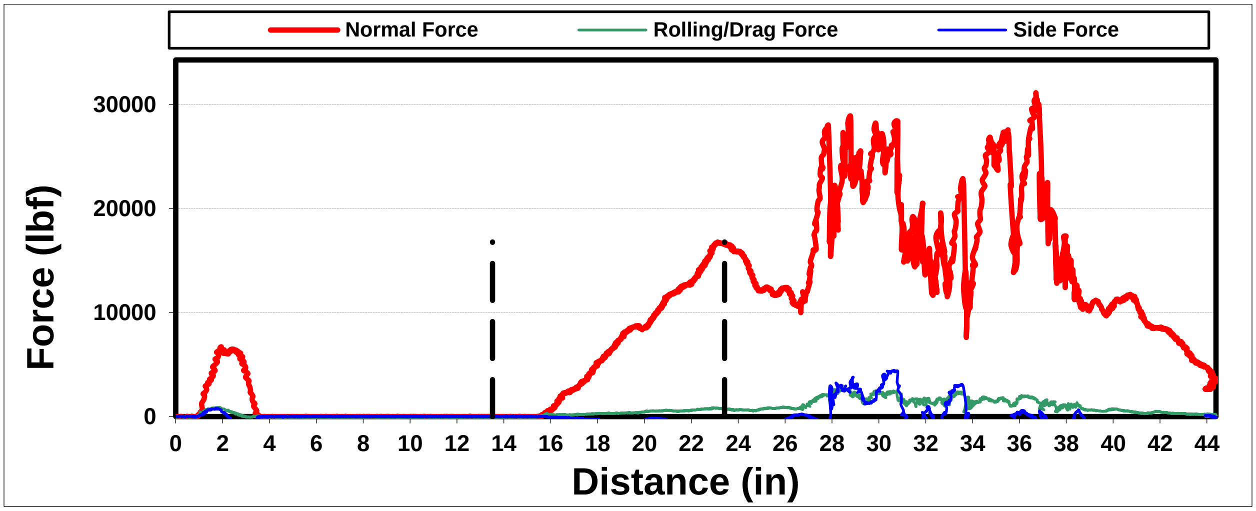

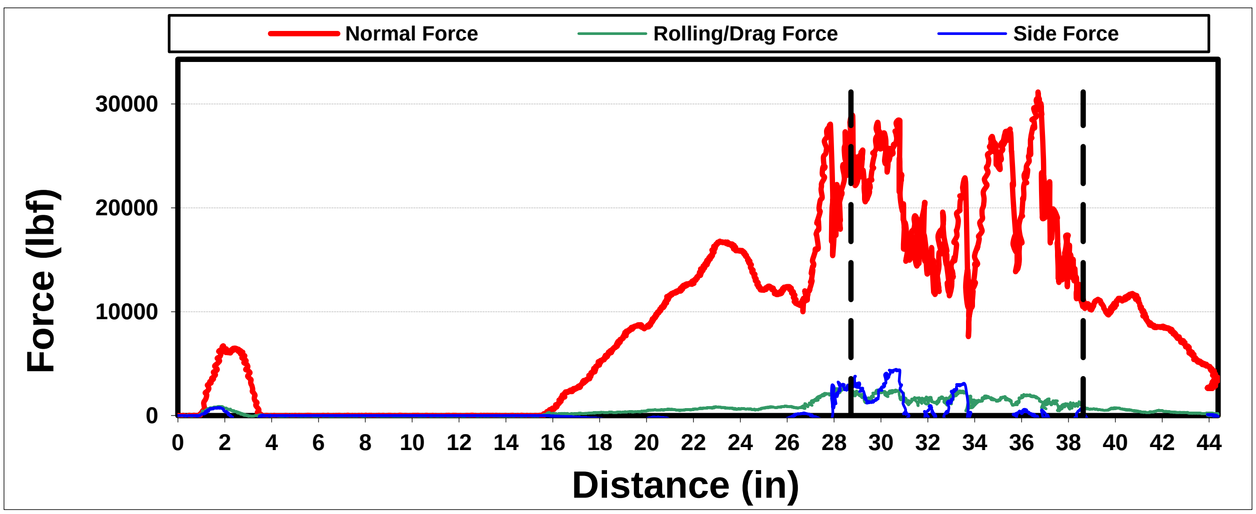

Pass 3 Line 2

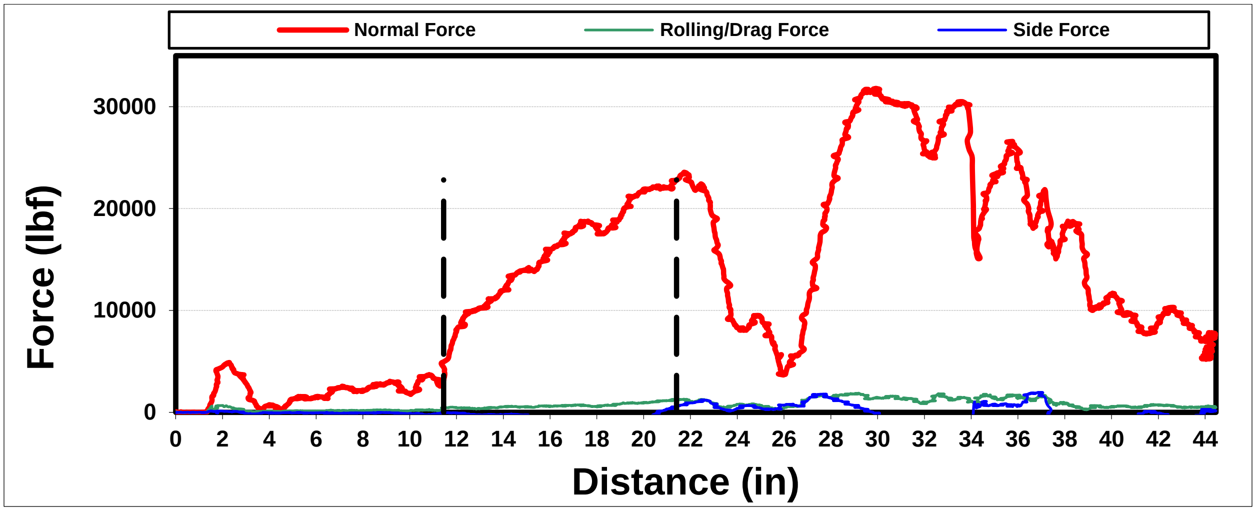

Normal Force
Rolling/Drag Force
Side Force
Force (lbf)
30000
20000
10000
0
0 2 4 6 8 10 12 14 16 18 20 22 24 26 28 30 32 34 36 38 40 42 44
Distance (in)

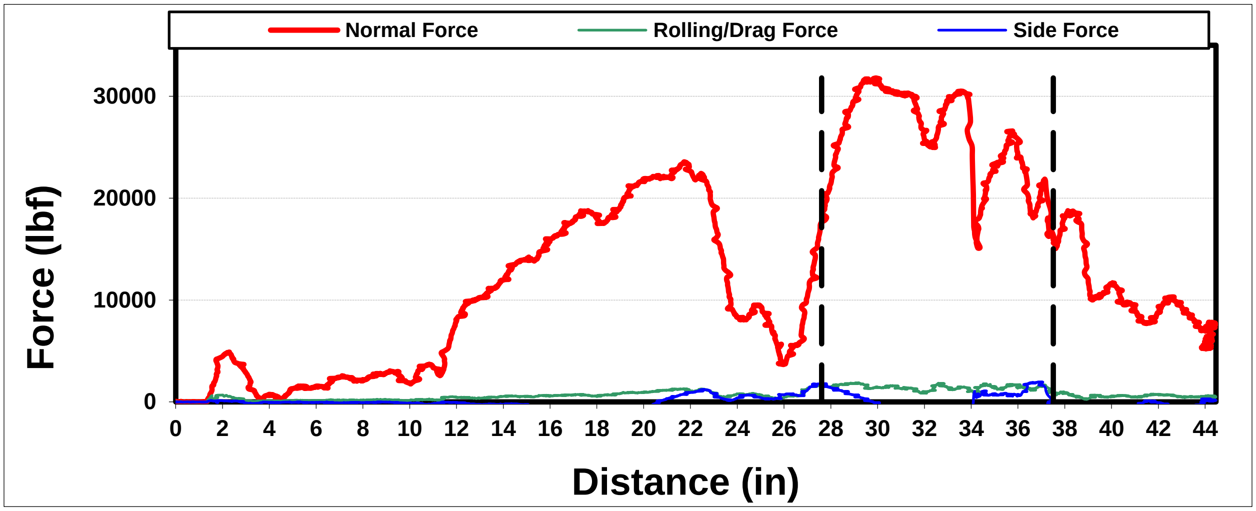

Normal Force
Rolling/Drag Force
Side Force
Force (lbf)
30000
20000
10000
0
0 2 4 6 8 10 12 14 16 18 20 22 24 26 28 30 32 34 36 38 40 42 44
Distance (in)

Pass 3 Line 3

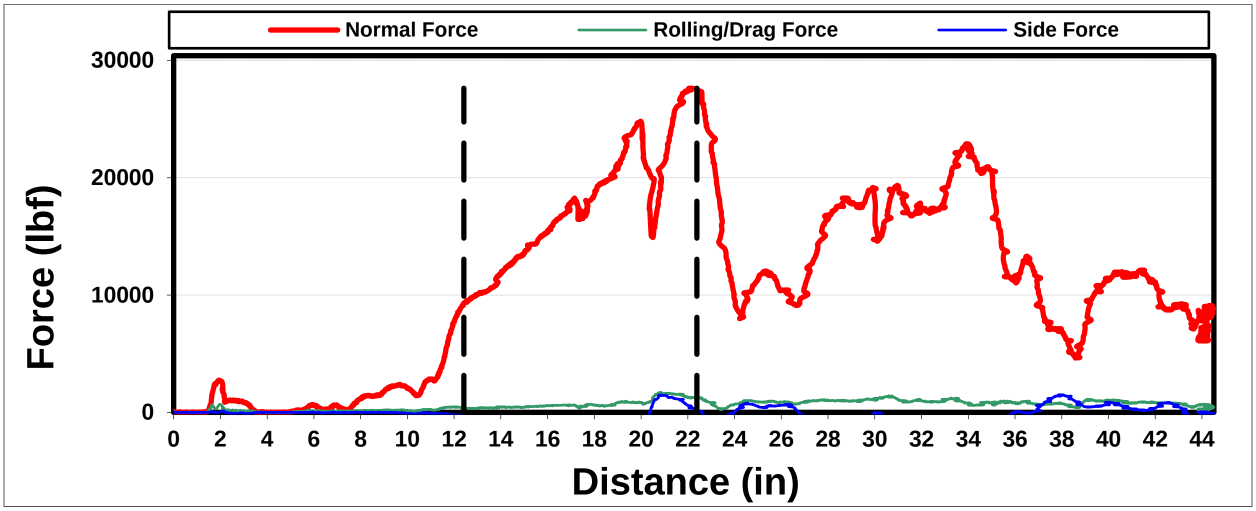
Normal Force
Rolling/Drag Force
Side Force
Force (lbf)
Distance (in)

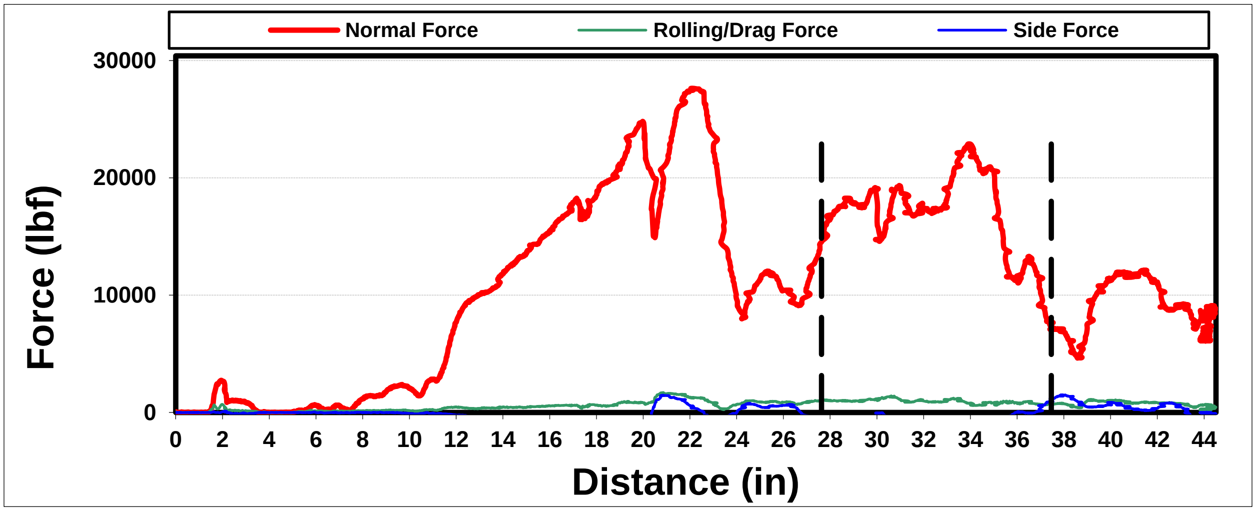
Normal Force
Rolling/Drag Force
Side Force
Force (lbf)
Distance (in)

Pass 3 Line 5

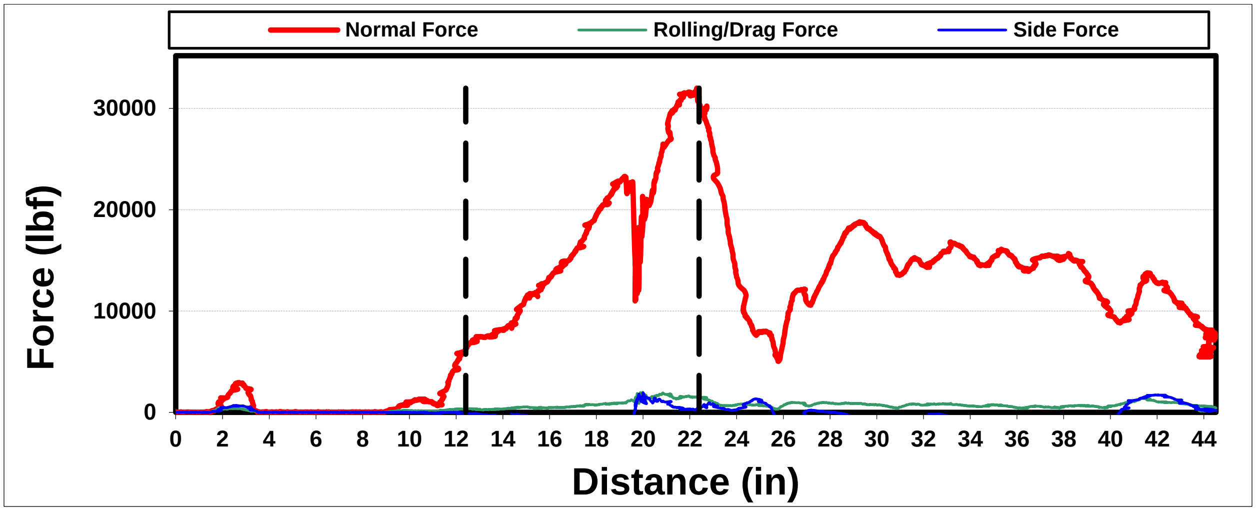

Normal Force
Rolling/Drag Force
Side Force
Force (lbf)
30000
20000
10000
0
0 2 4 6 8 10 12 14 16 18 20 22 24 26 28 30 32 34 36 38 40 42 44
Distance (in)

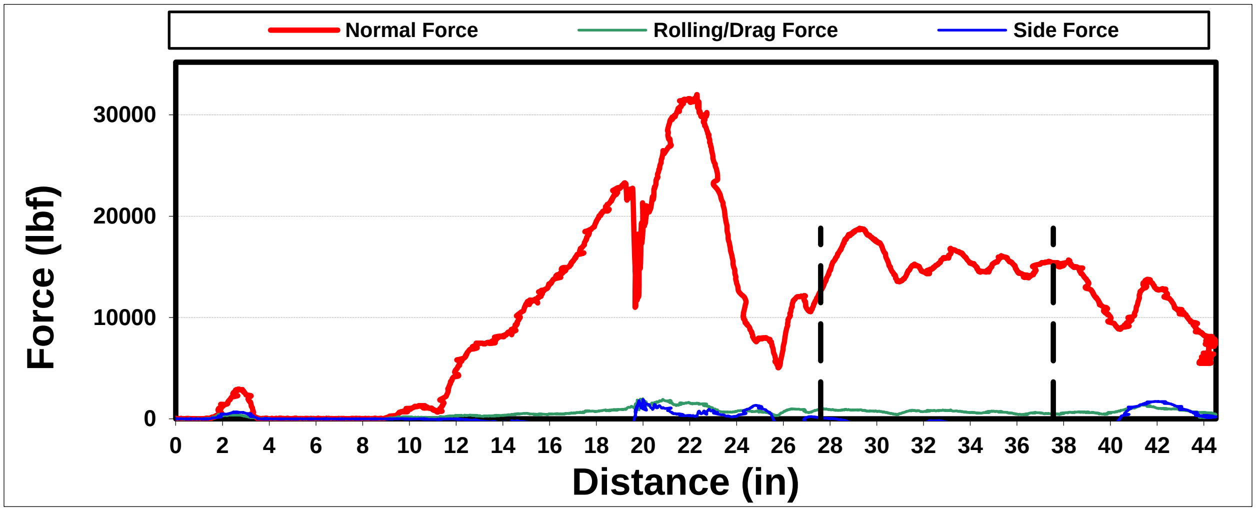

Normal Force
Rolling/Drag Force
Side Force
Force (lbf)
30000
20000
10000
0
0 2 4 6 8 10 12 14 16 18 20 22 24 26 28 30 32 34 36 38 40 42 44
Distance (in)

Pass 3 Line 9

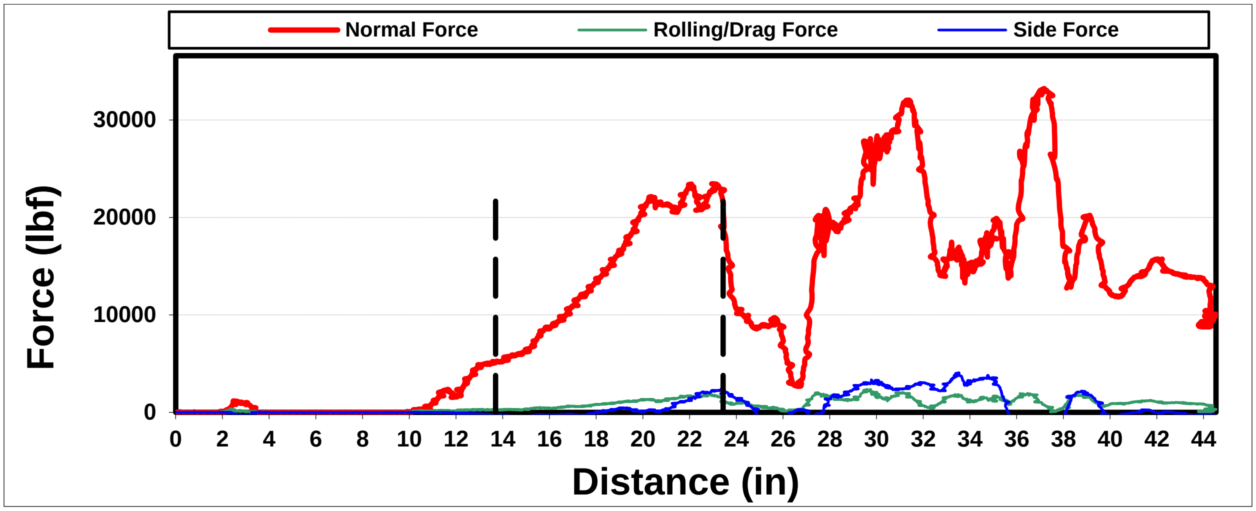

Normal Force
Rolling/Drag Force
Side Force
Force (lbf)
30000
20000
10000
0
0 2 4 6 8 10 12 14 16 18 20 22 24 26 28 30 32 34 36 38 40 42 44
Distance (in)

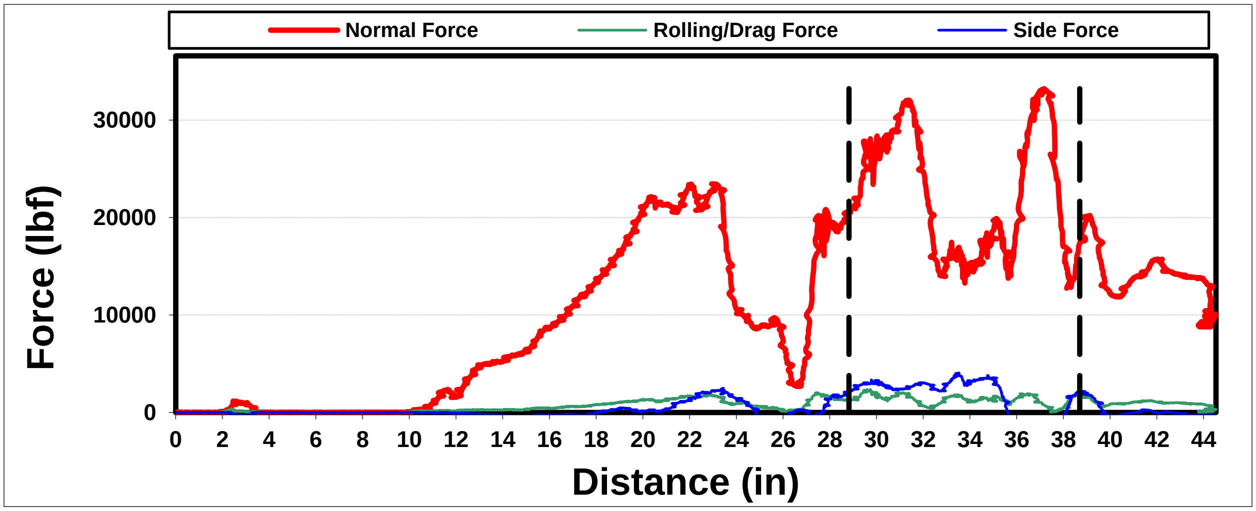

Normal Force
Rolling/Drag Force
Side Force
Force (lbf)
30000
20000
10000
0
0 2 4 6 8 10 12 14 16 18 20 22 24 26 28 30 32 34 36 38 40 42 44
Distance (in)

Pass 3 Line 10

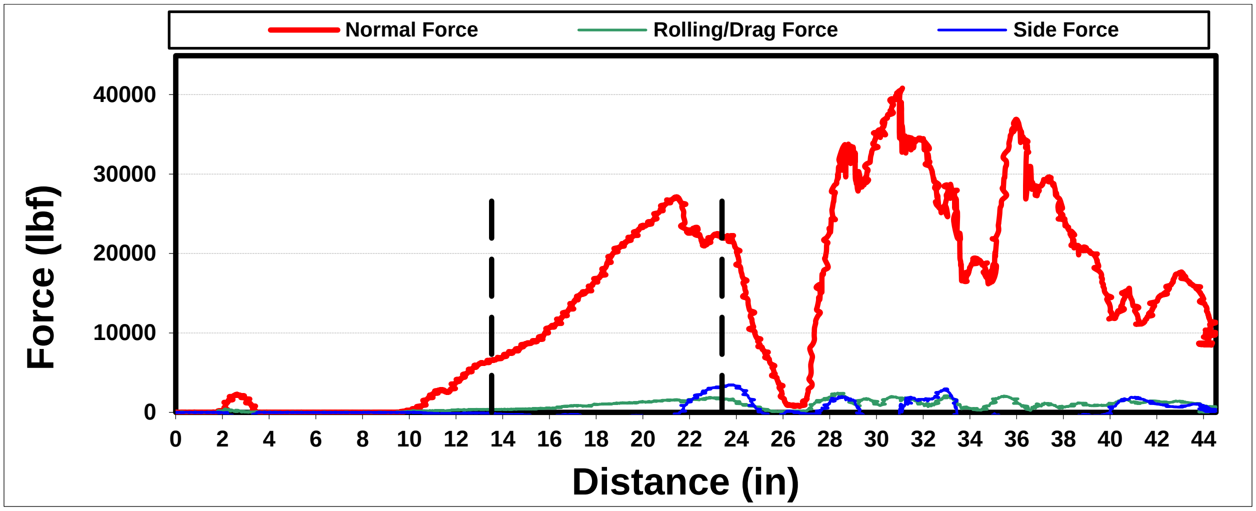

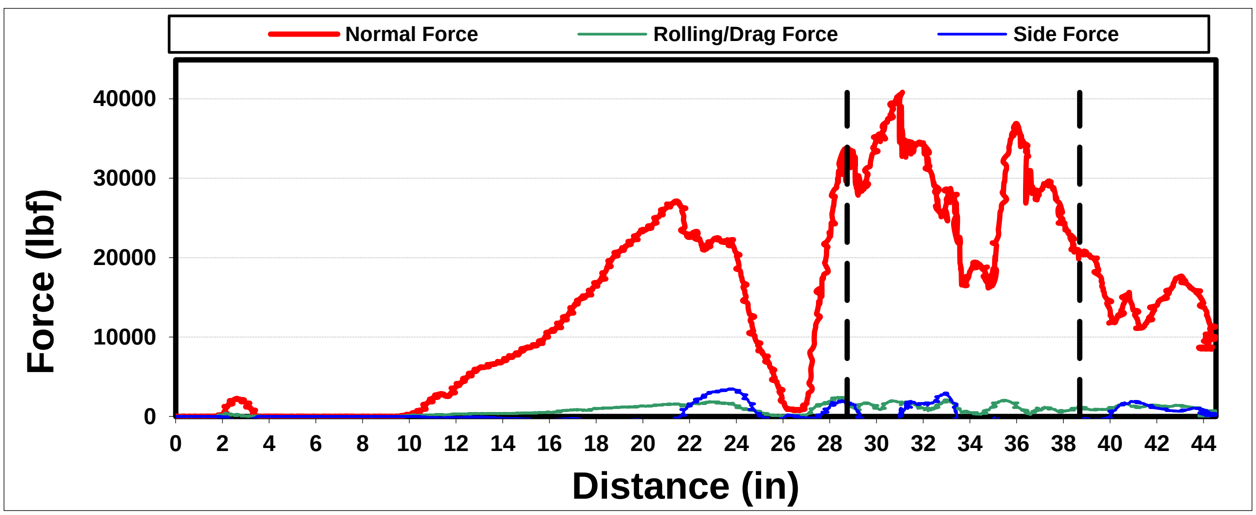

Pass 3 Line 11

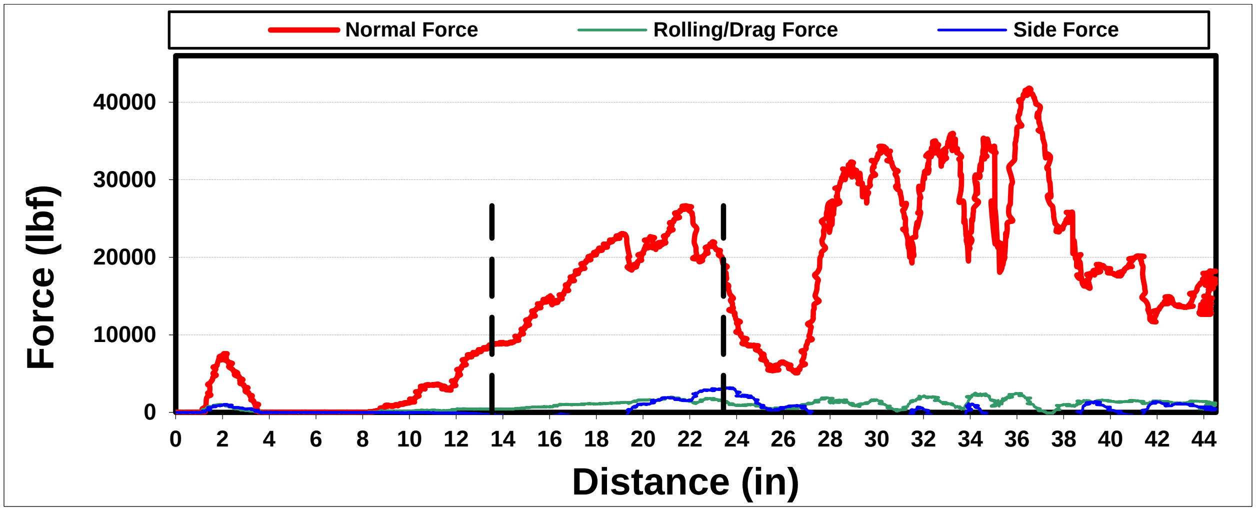

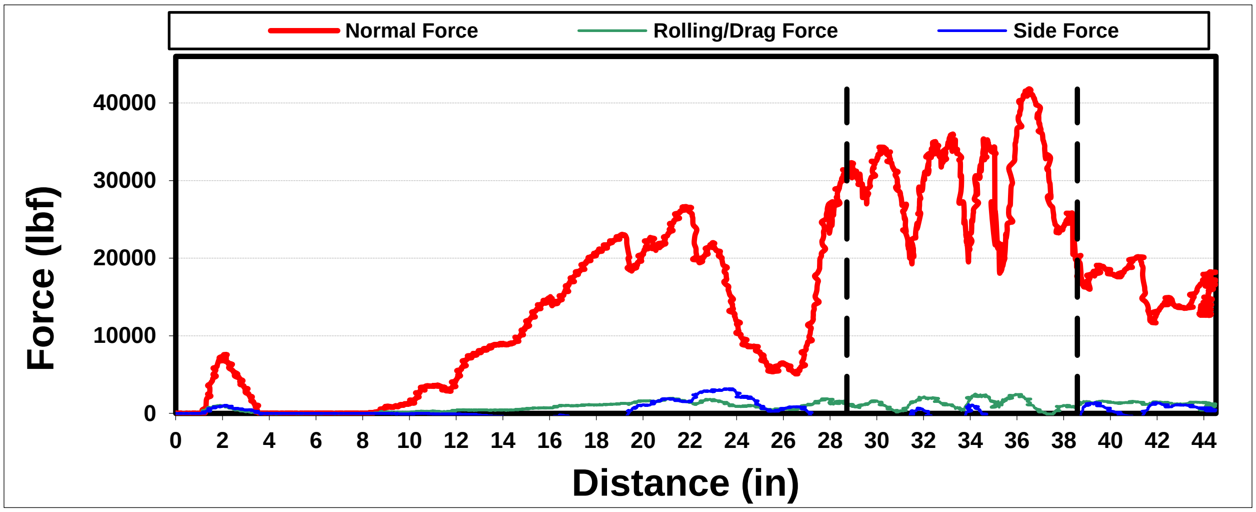

Pass 3 Line 12

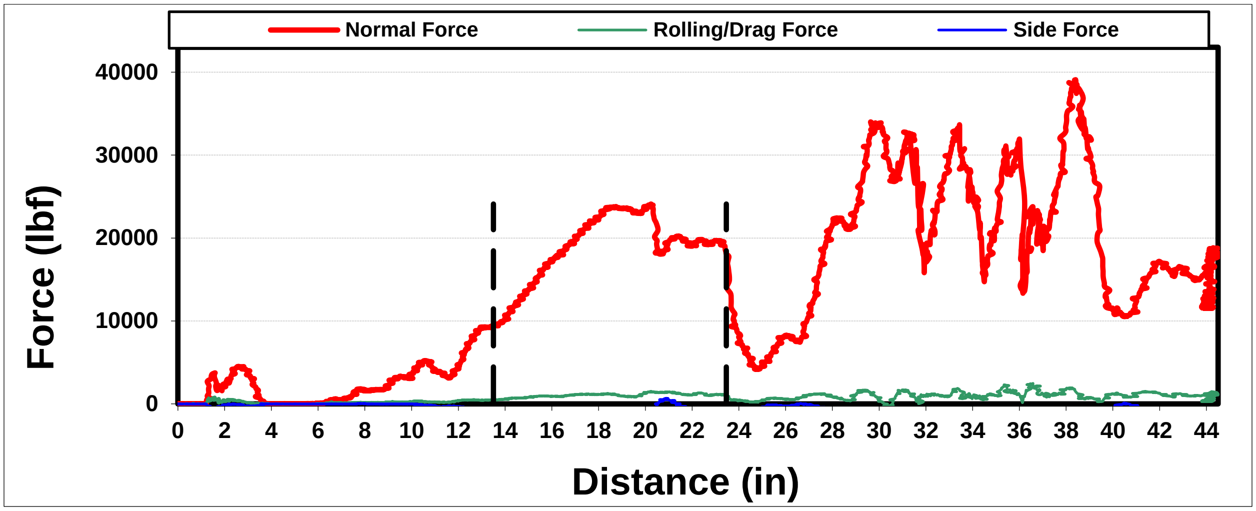

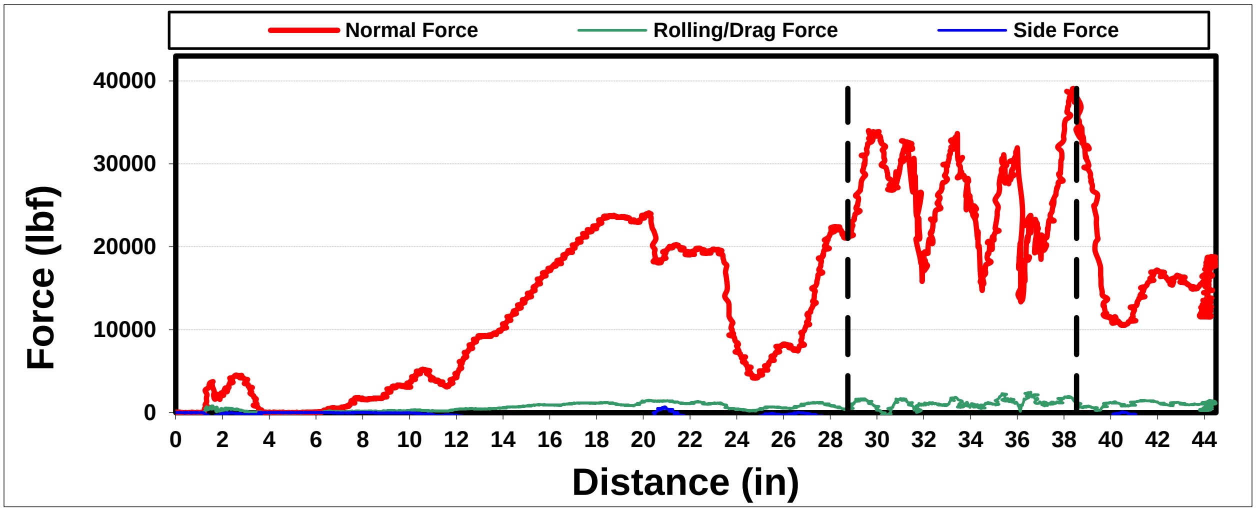

Post-Conditioning Passes:

Pass 1 Line 2

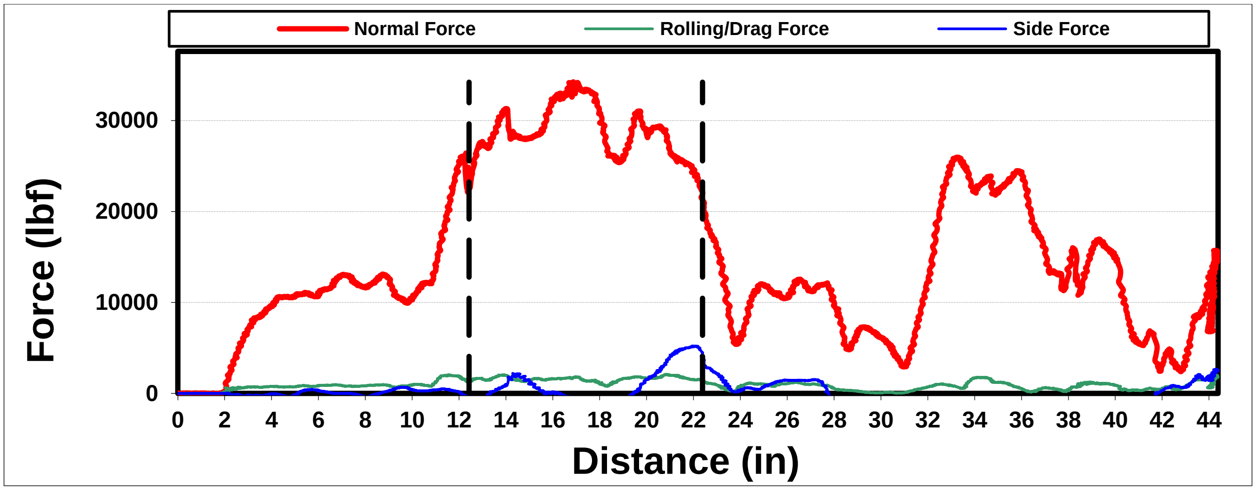

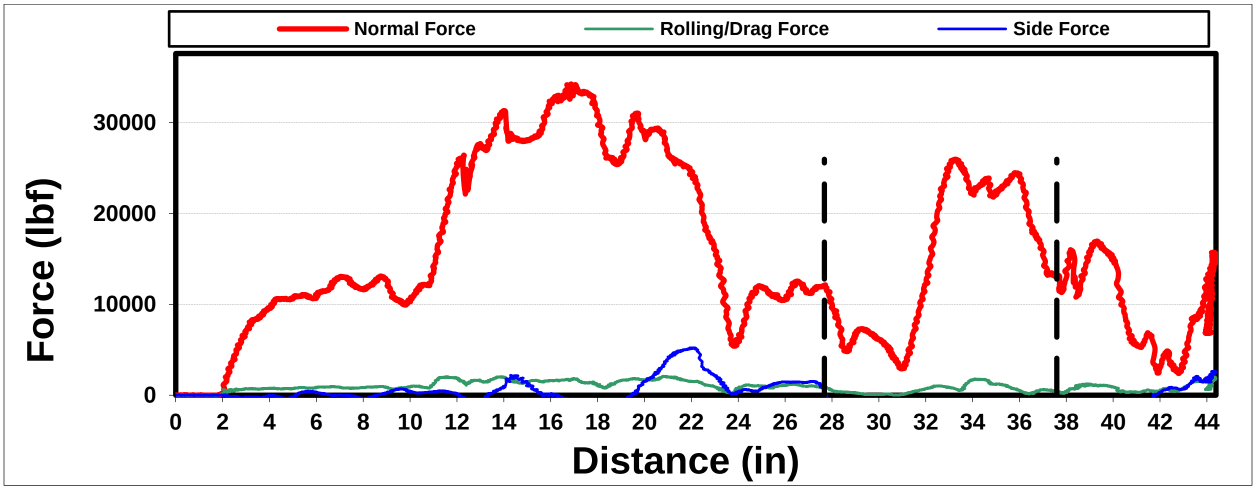

Pass 1 Line 3

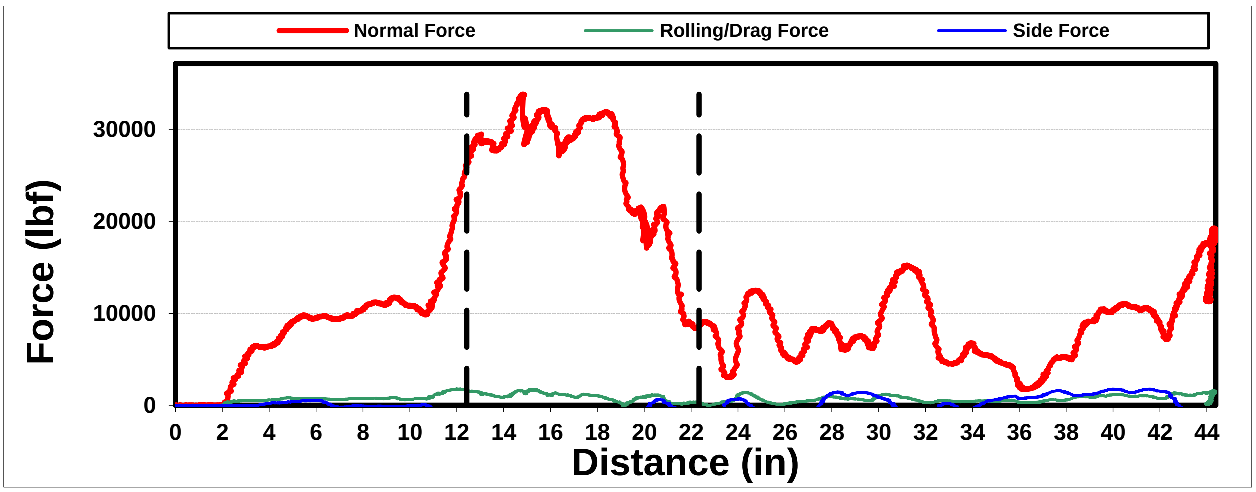

Normal Force
Rolling/Drag Force
Side Force
Force (lbf)
0
10000
20000
30000
0 2 4 6 8 10 12 14 16 18 20 22 24 26 28 30 32 34 36 38 40 42 44
Distance (in)

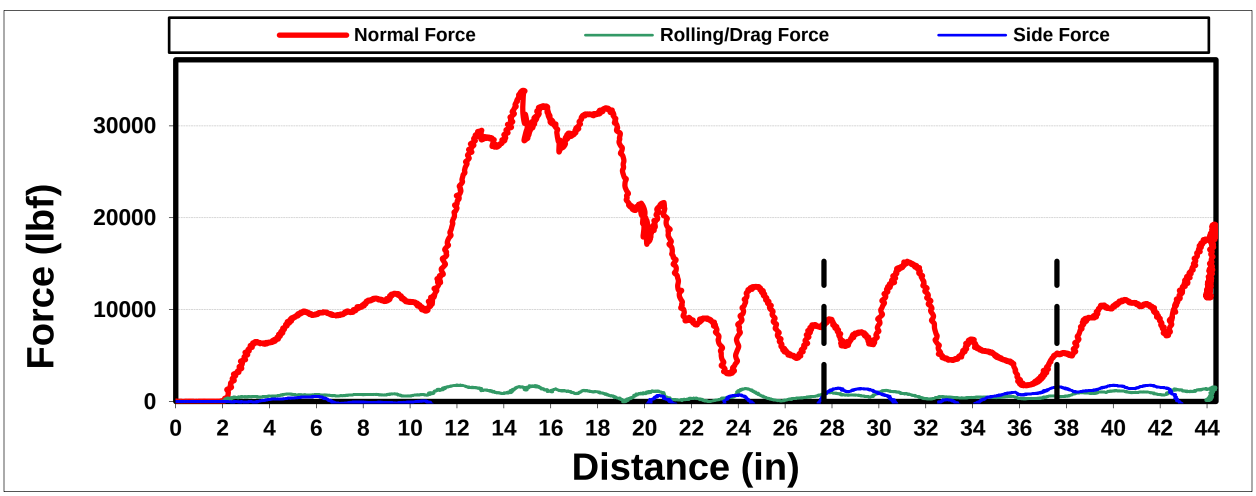

Normal Force
Rolling/Drag Force
Side Force
Force (lbf)
0
10000
20000
30000
0 2 4 6 8 10 12 14 16 18 20 22 24 26 28 30 32 34 36 38 40 42 44
Distance (in)

Pass 1 Line 5

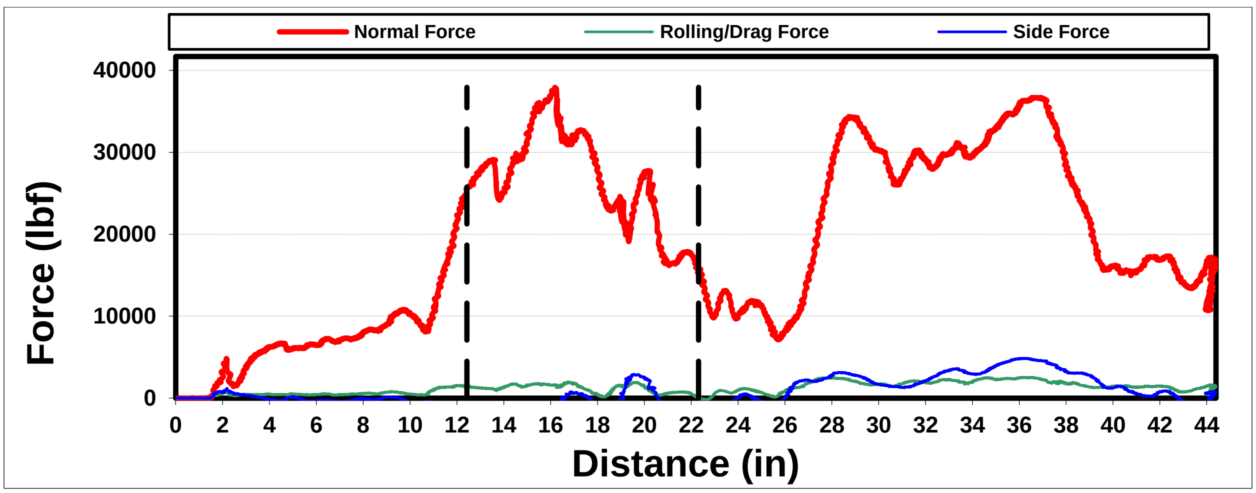

Normal Force
Rolling/Drag Force
Side Force
Force (lbf)
40000
30000
20000
10000
0
0 2 4 6 8 10 12 14 16 18 20 22 24 26 28 30 32 34 36 38 40 42 44
Distance (in)

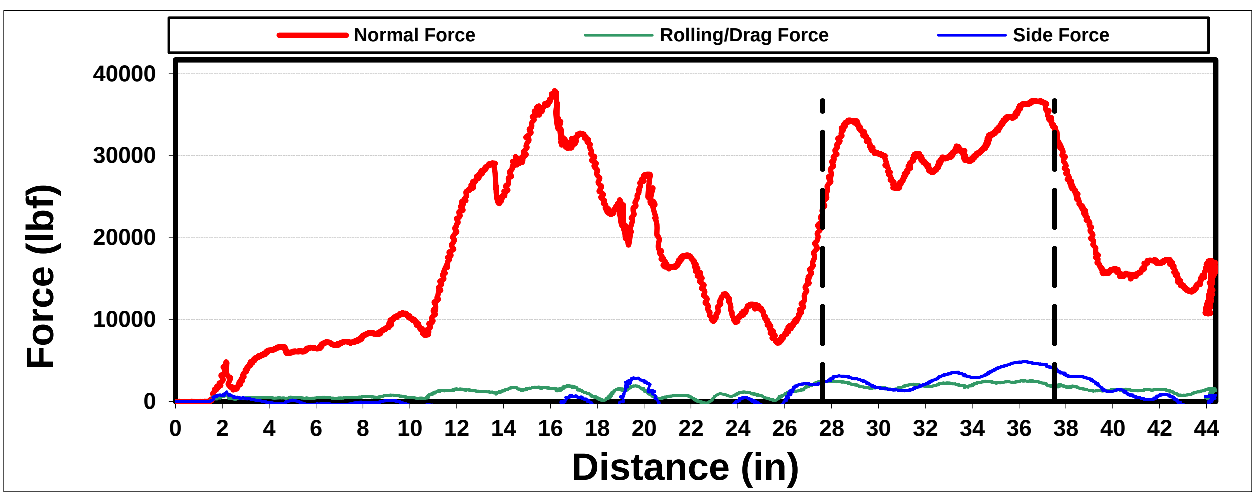

Normal Force
Rolling/Drag Force
Side Force
Force (lbf)
40000
30000
20000
10000
0
0 2 4 6 8 10 12 14 16 18 20 22 24 26 28 30 32 34 36 38 40 42 44
Distance (in)

Pass 1 Line 9

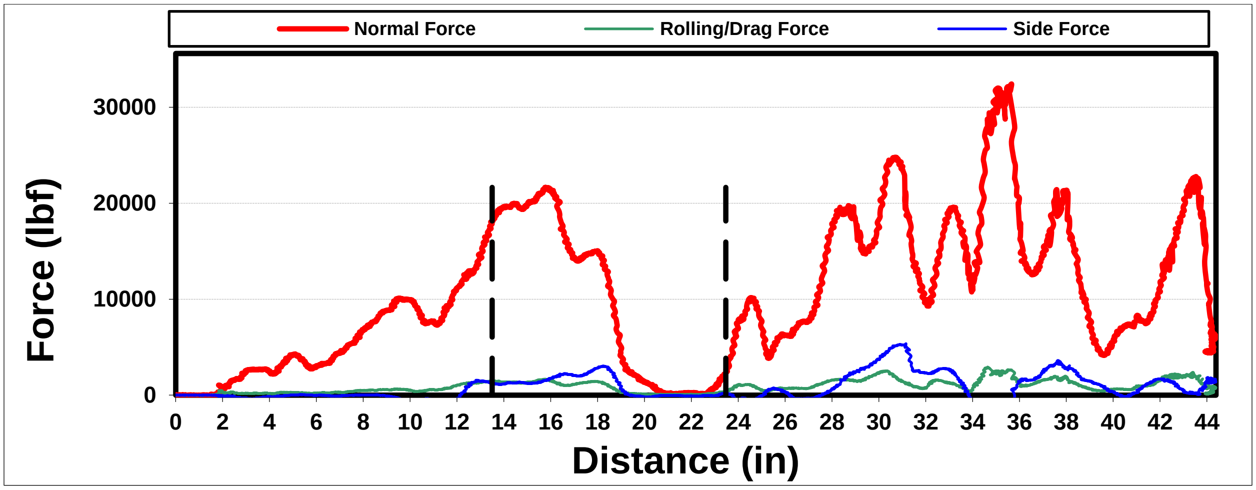
Normal Force
Rolling/Drag Force
Side Force
Force (lbf)
30000
20000
10000
0
0 2 4 6 8 10 12 14 16 18 20 22 24 26 28 30 32 34 36 38 40 42 44
Distance (in)

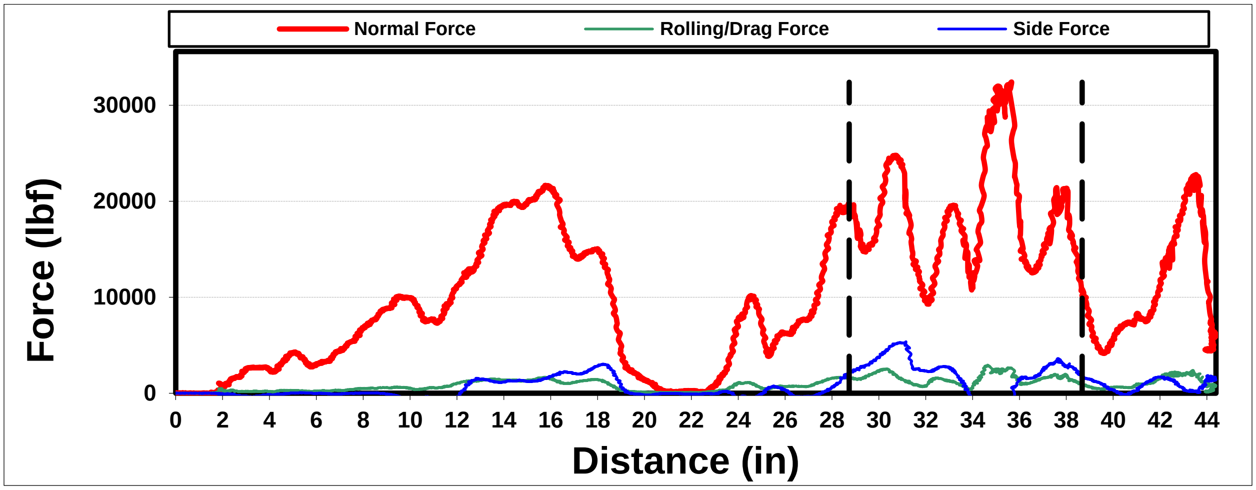
Normal Force
Rolling/Drag Force
Side Force
Force (lbf)
30000
20000
10000
0
0 2 4 6 8 10 12 14 16 18 20 22 24 26 28 30 32 34 36 38 40 42 44
Distance (in)

Pass 1 Line 10

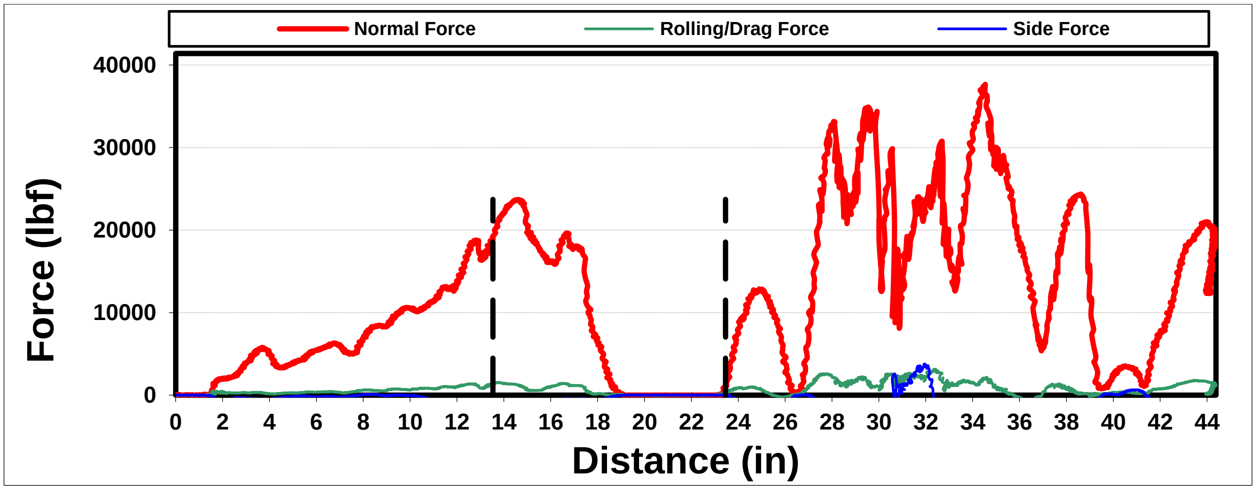

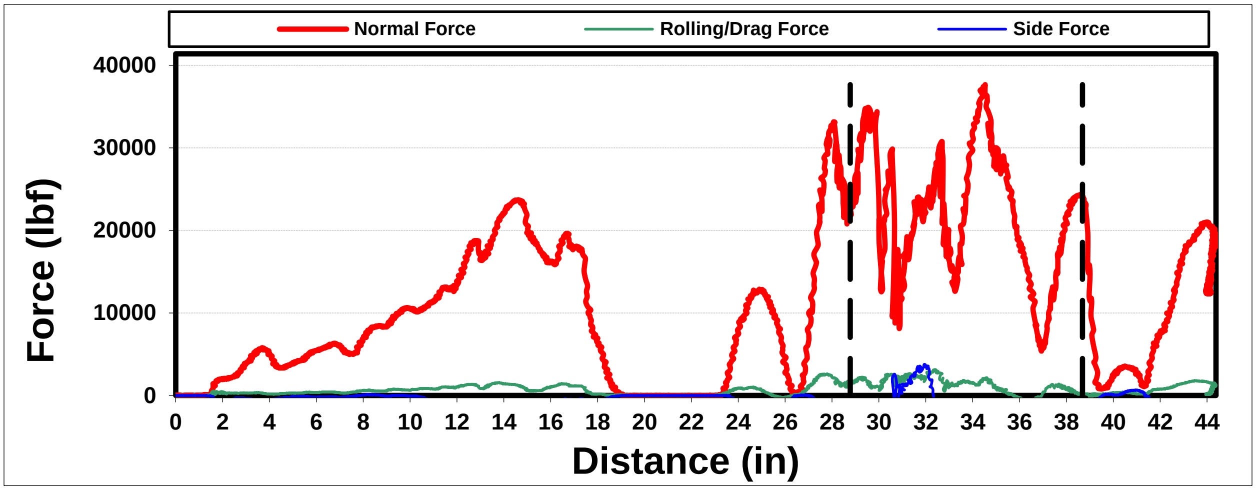

Pass 1 Line 11

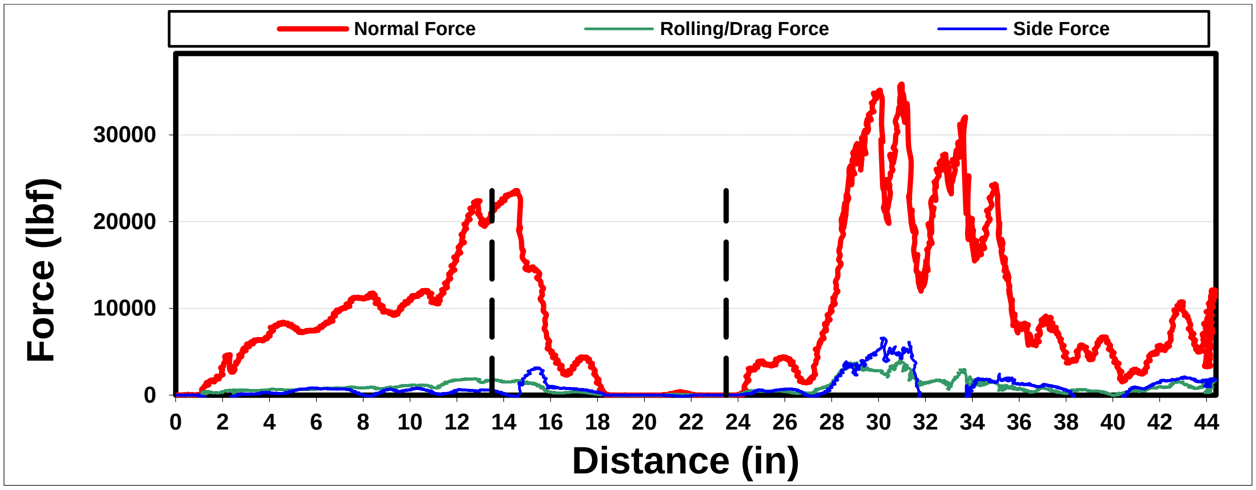

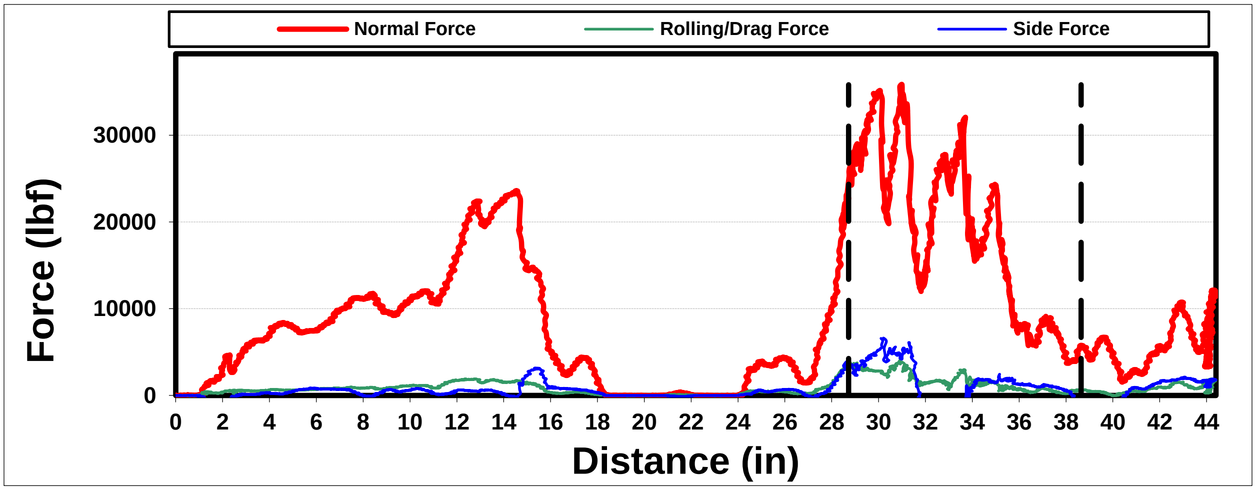

Pass 1 Line 12

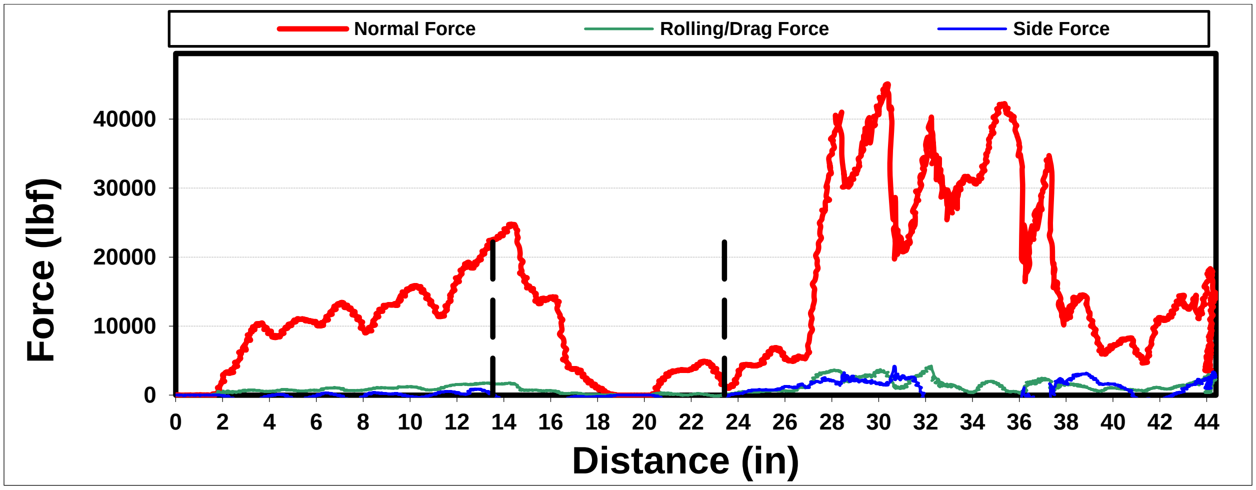

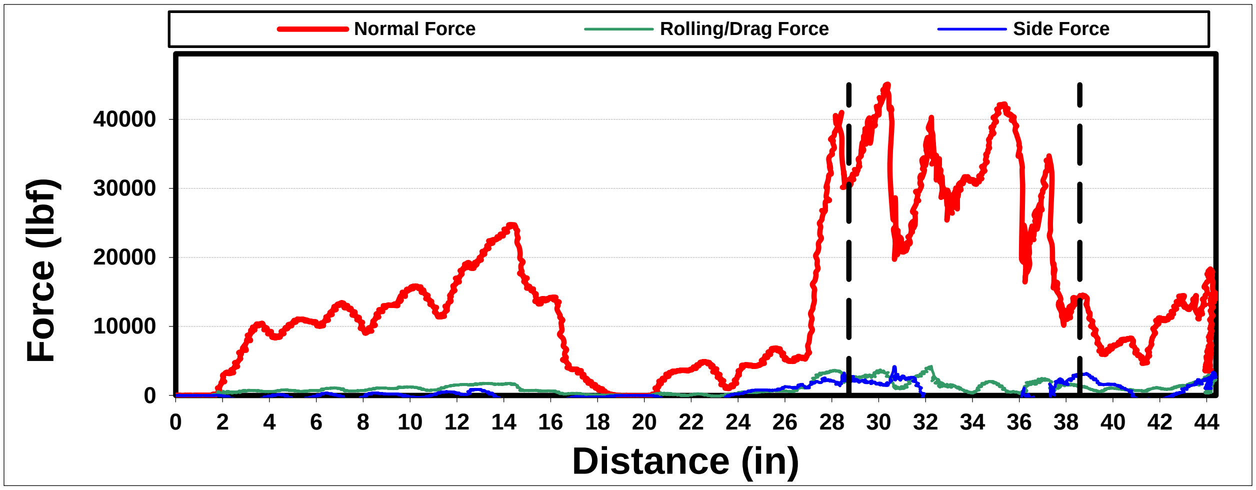

Pass 2 Line 2

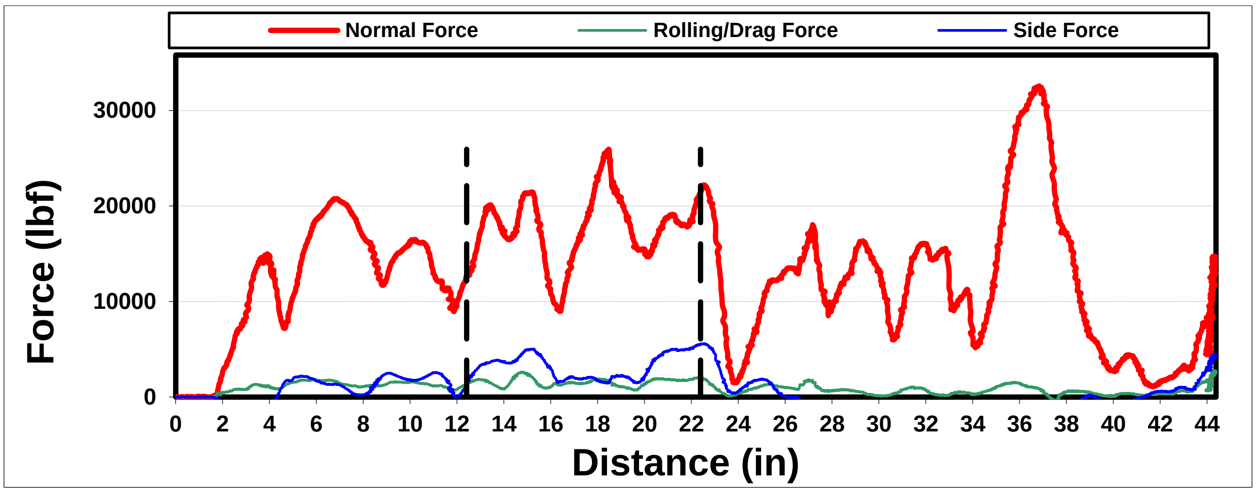

Normal Force
Rolling/Drag Force
Side Force
Force (lbf)
30000
20000
10000
0
0 2 4 6 8 10 12 14 16 18 20 22 24 26 28 30 32 34 36 38 40 42 44
Distance (in)

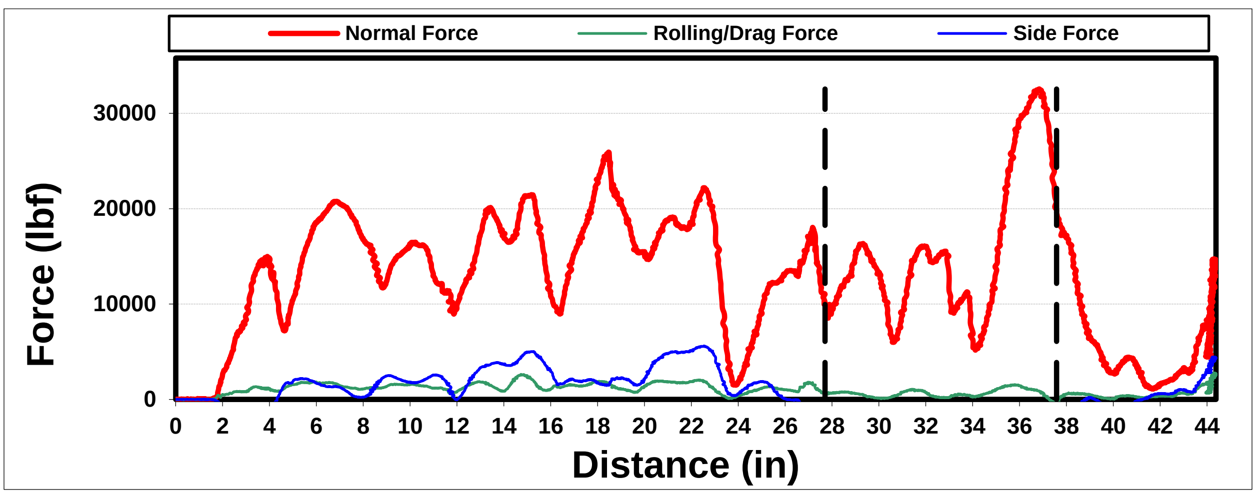

Normal Force
Rolling/Drag Force
Side Force
Force (lbf)
30000
20000
10000
0
0 2 4 6 8 10 12 14 16 18 20 22 24 26 28 30 32 34 36 38 40 42 44
Distance (in)

Pass 2 Line 3

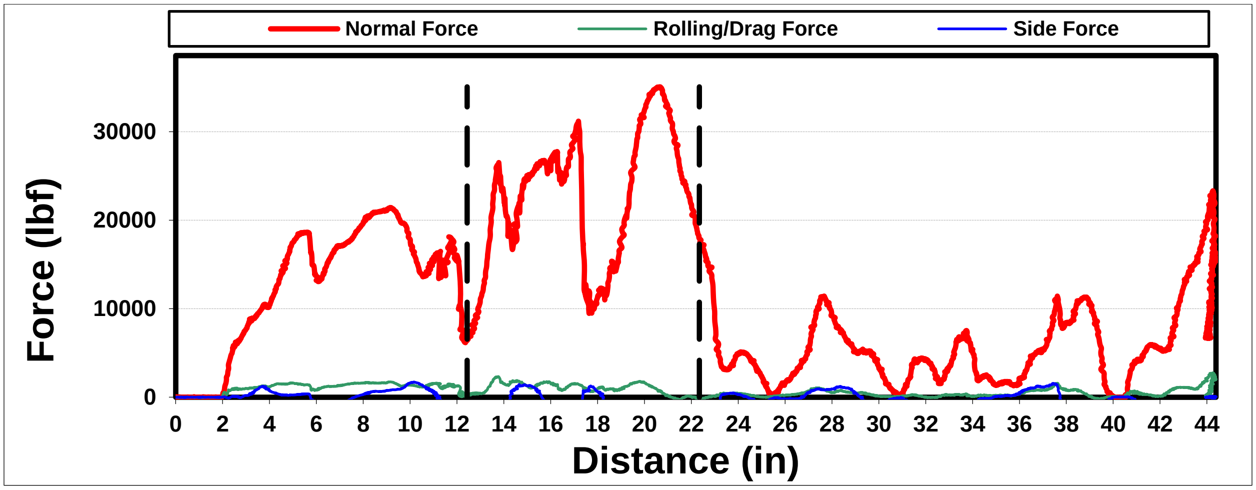

Normal Force
Rolling/Drag Force
Side Force
Force (lbf)
0
10000
20000
30000
0 2 4 6 8 10 12 14 16 18 20 22 24 26 28 30 32 34 36 38 40 42 44
Distance (in)

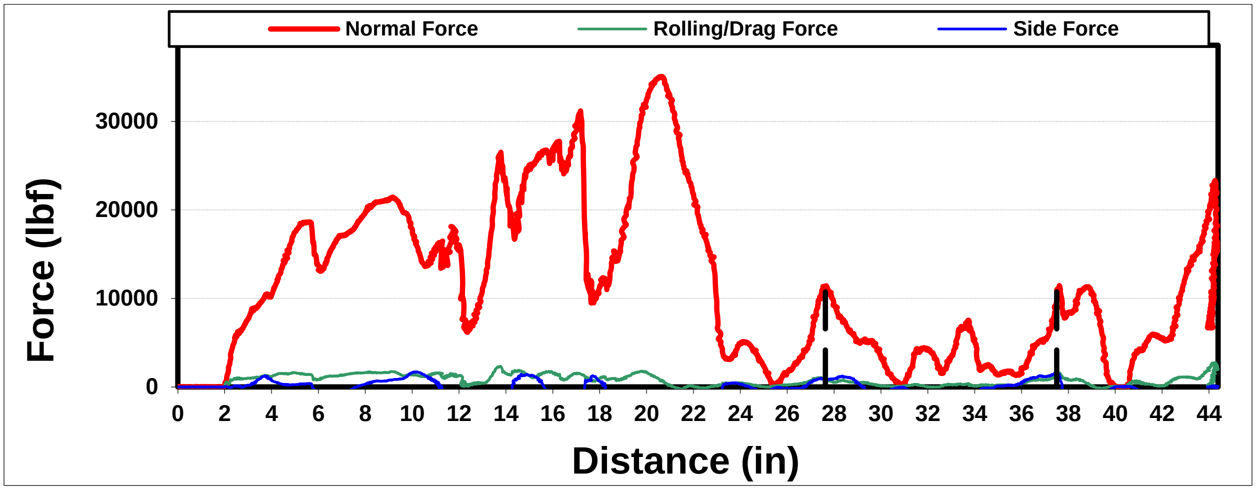

Normal Force
Rolling/Drag Force
Side Force
Force (lbf)
0
10000
20000
30000
0 2 4 6 8 10 12 14 16 18 20 22 24 26 28 30 32 34 36 38 40 42 44
Distance (in)

Pass 2 Line 5

Line – 5

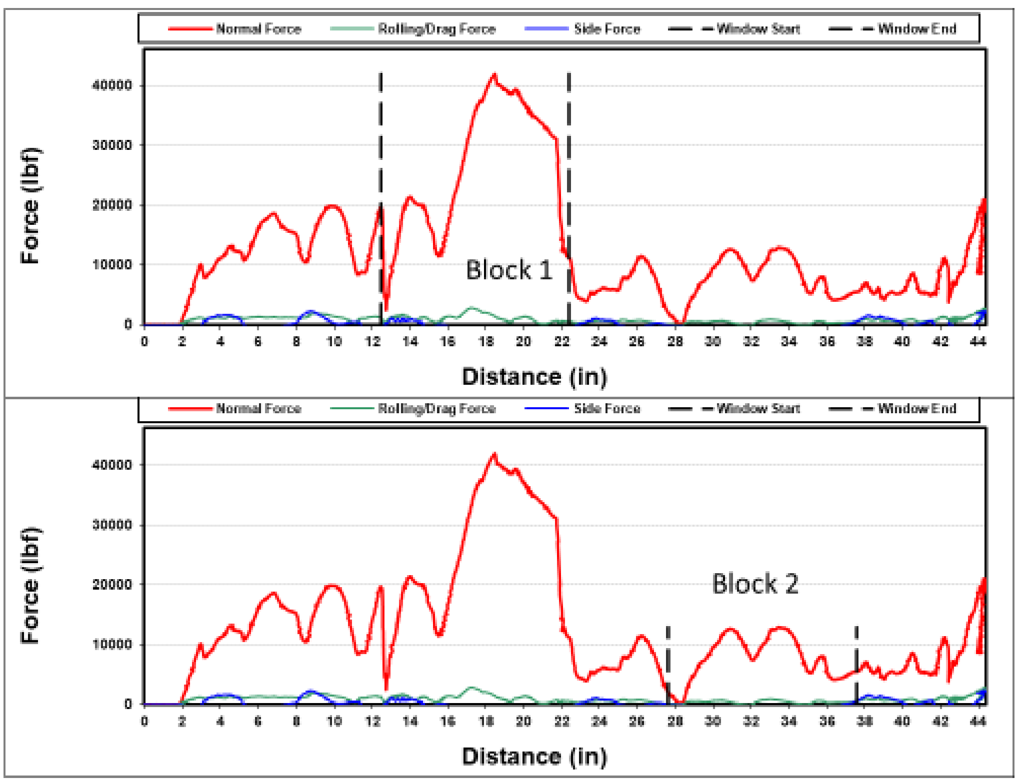

Pass 2 Line 9

Line – 9

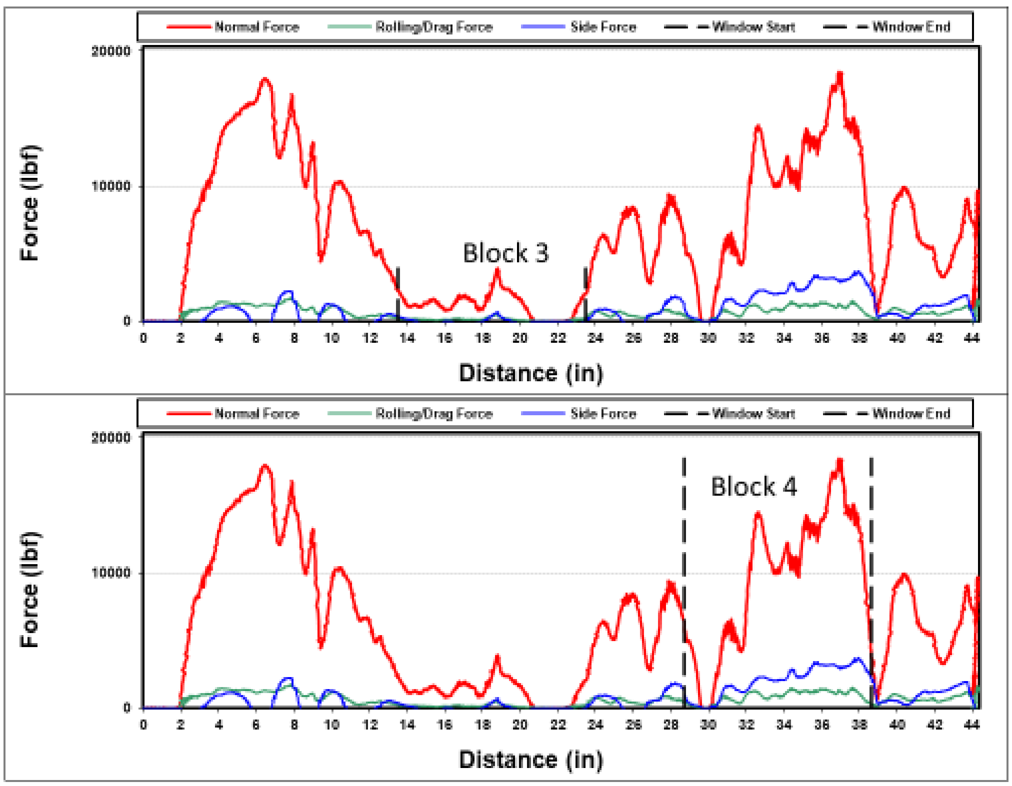

Pass 2 Line 10

Line – 10

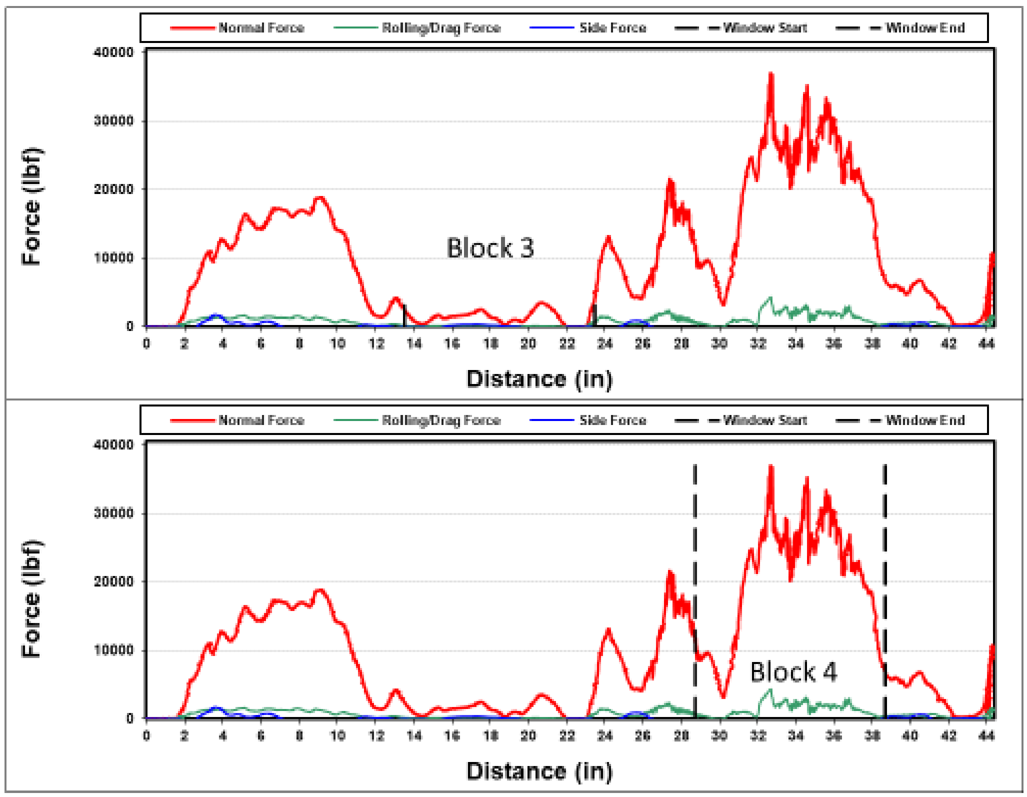

Pass 2 Line 11

Line – 11

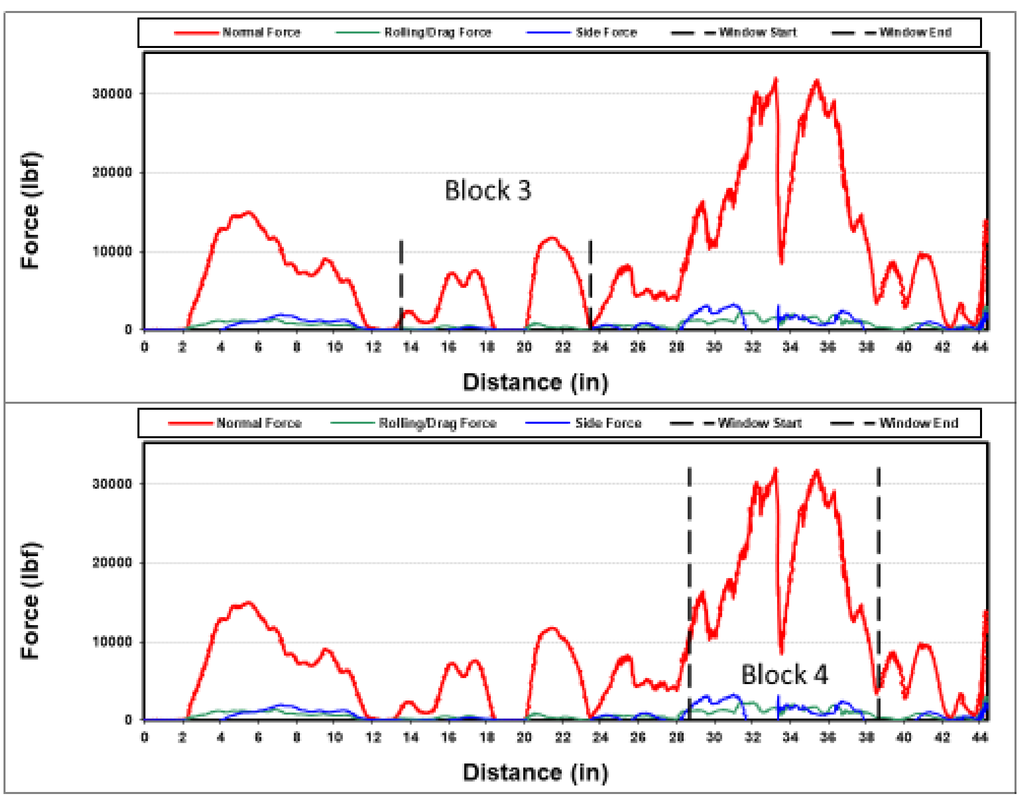

Pass 2 Line 12

Line – 12

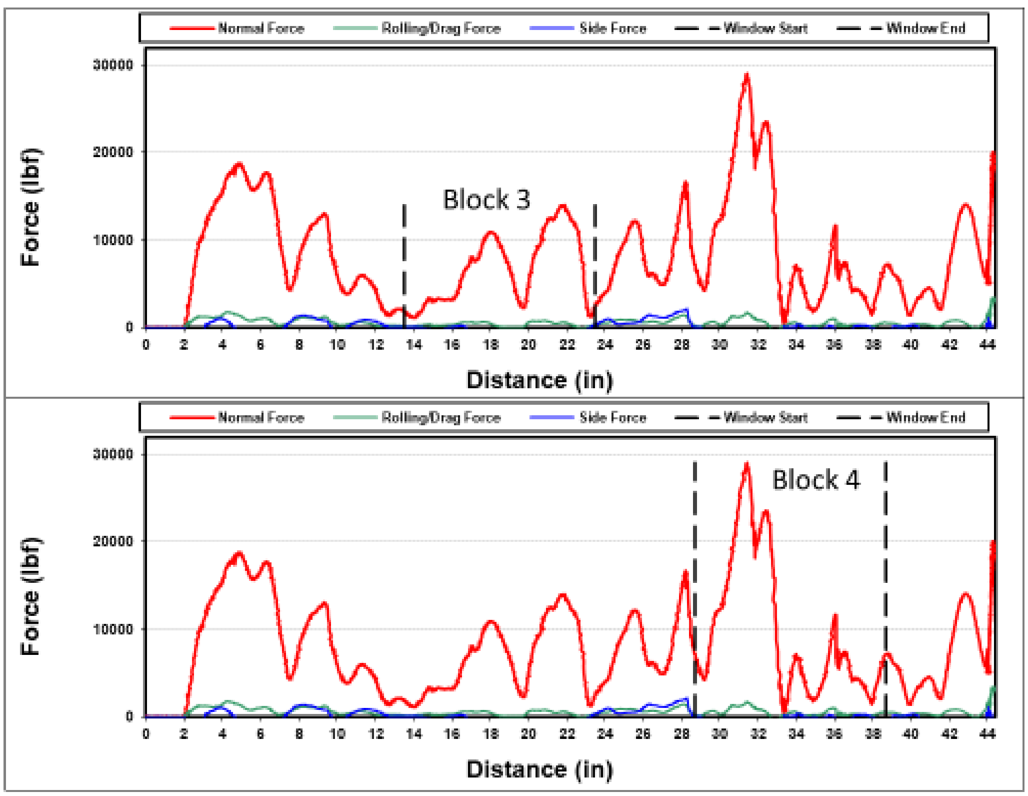

Pass 3 Line 2

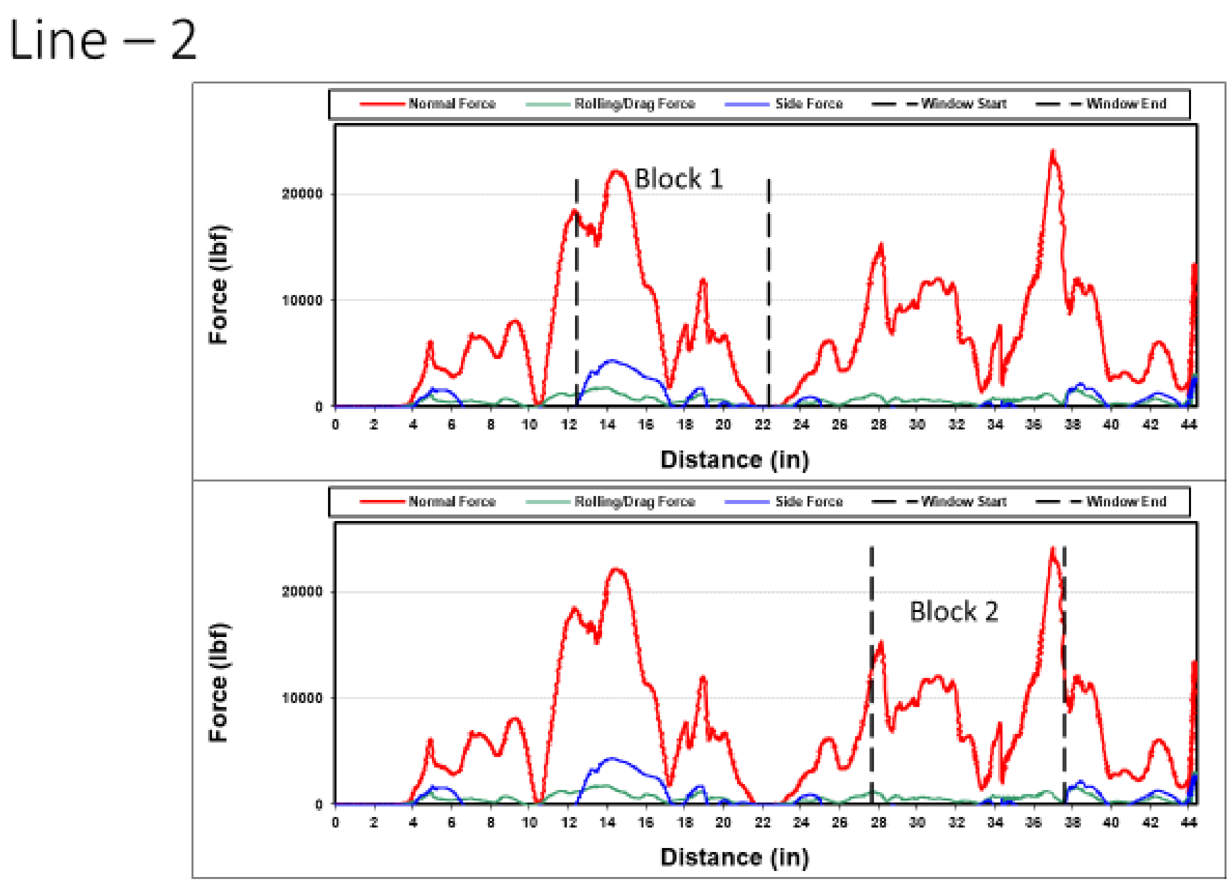

Line – 2
Normal Force
Rolling/Drag Force
Side Force
Window Start
Window End
Block 1
Force (lbf)
Distance (in)
Block 2

Pass 3 Line 3

Line – 3

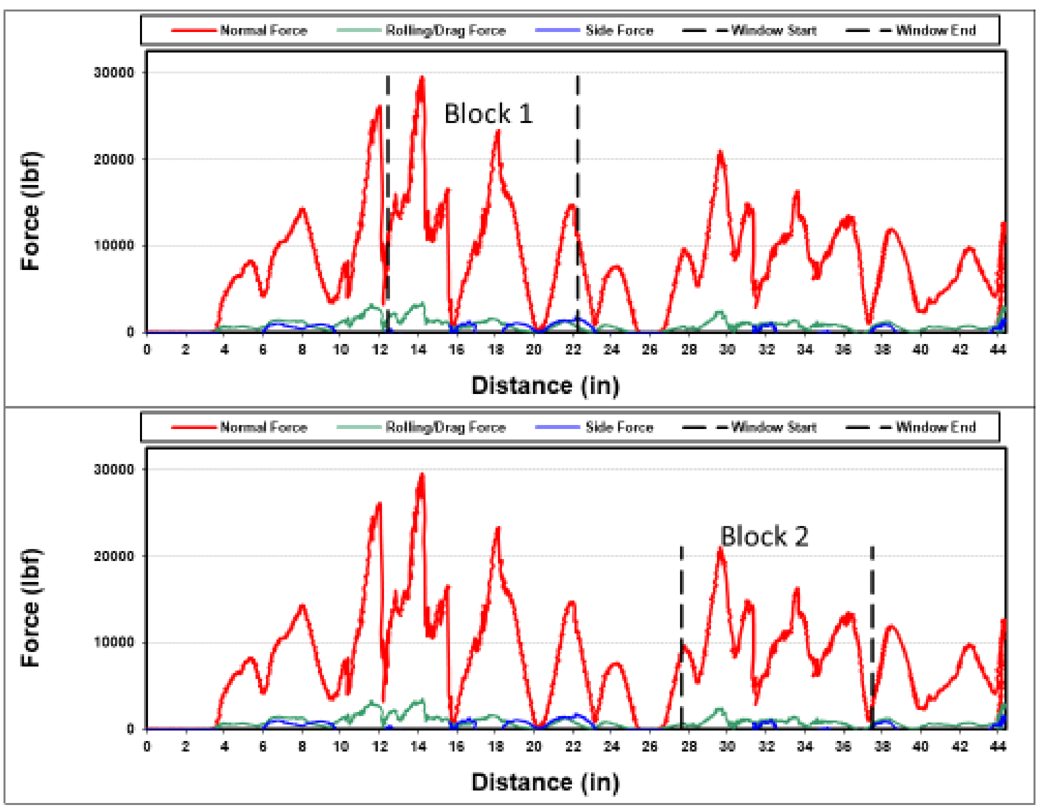

Pass 3 Line 5

Line – 5

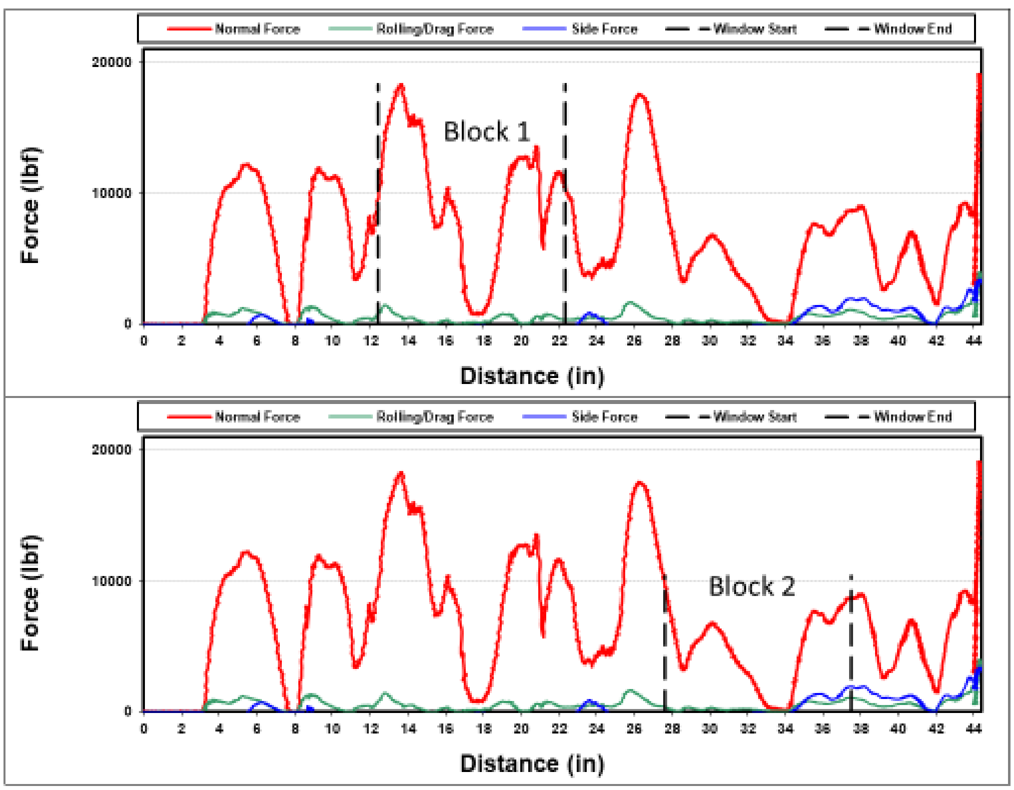

Pass 3 Line 9

Line – 9

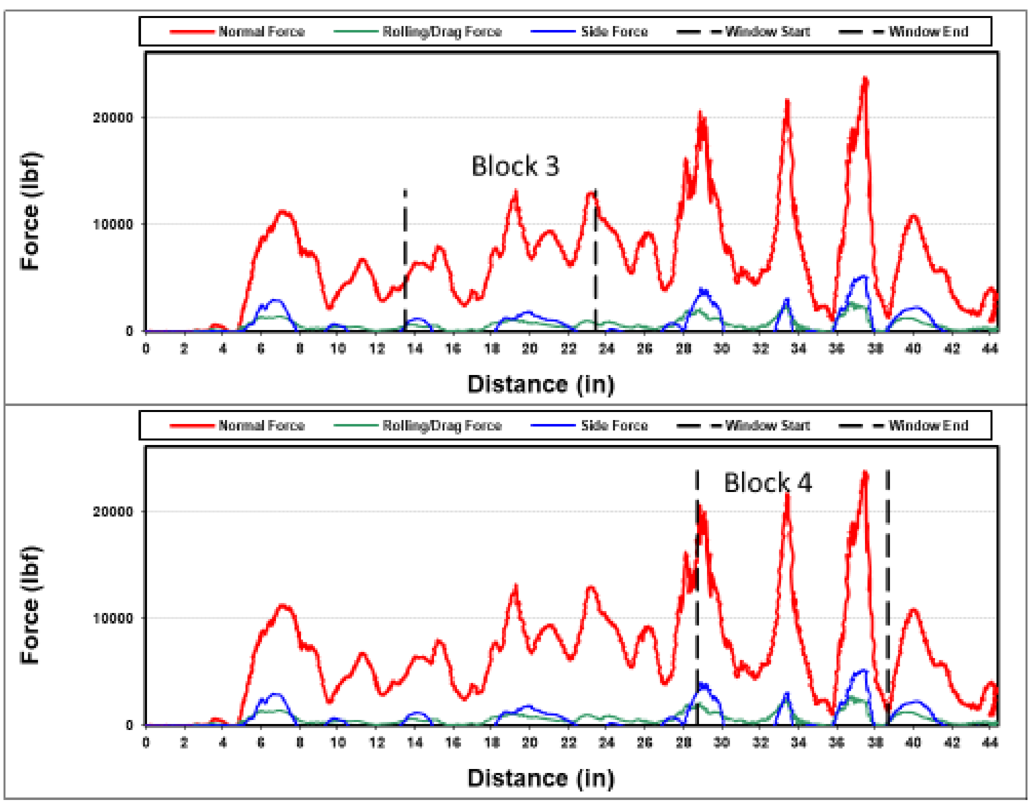

Pass 3 Line 10

Line – 10

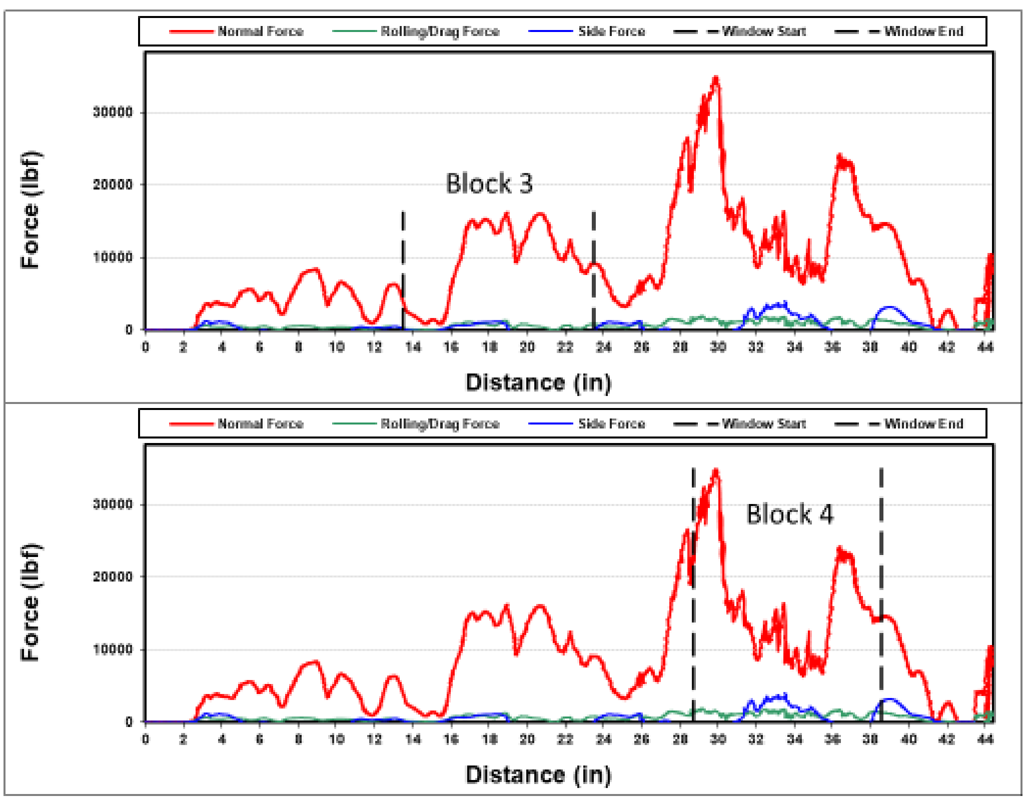

Pass 3 Line 11

Line – 11

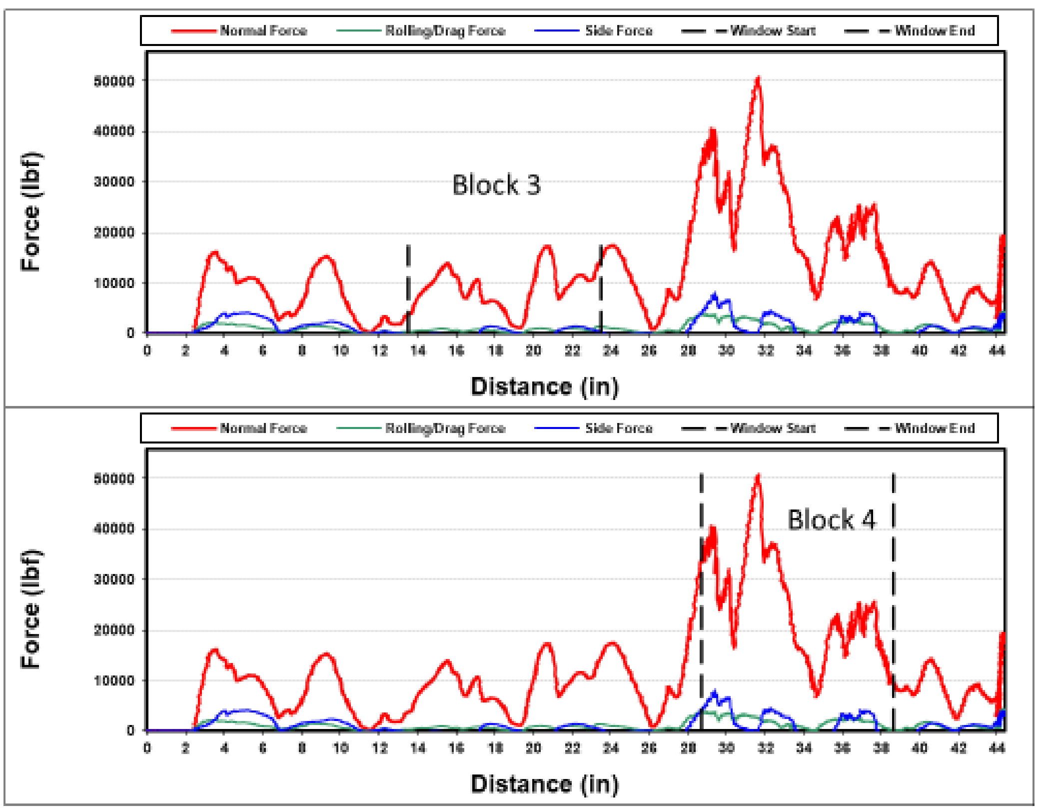

Pass 3 Line 12

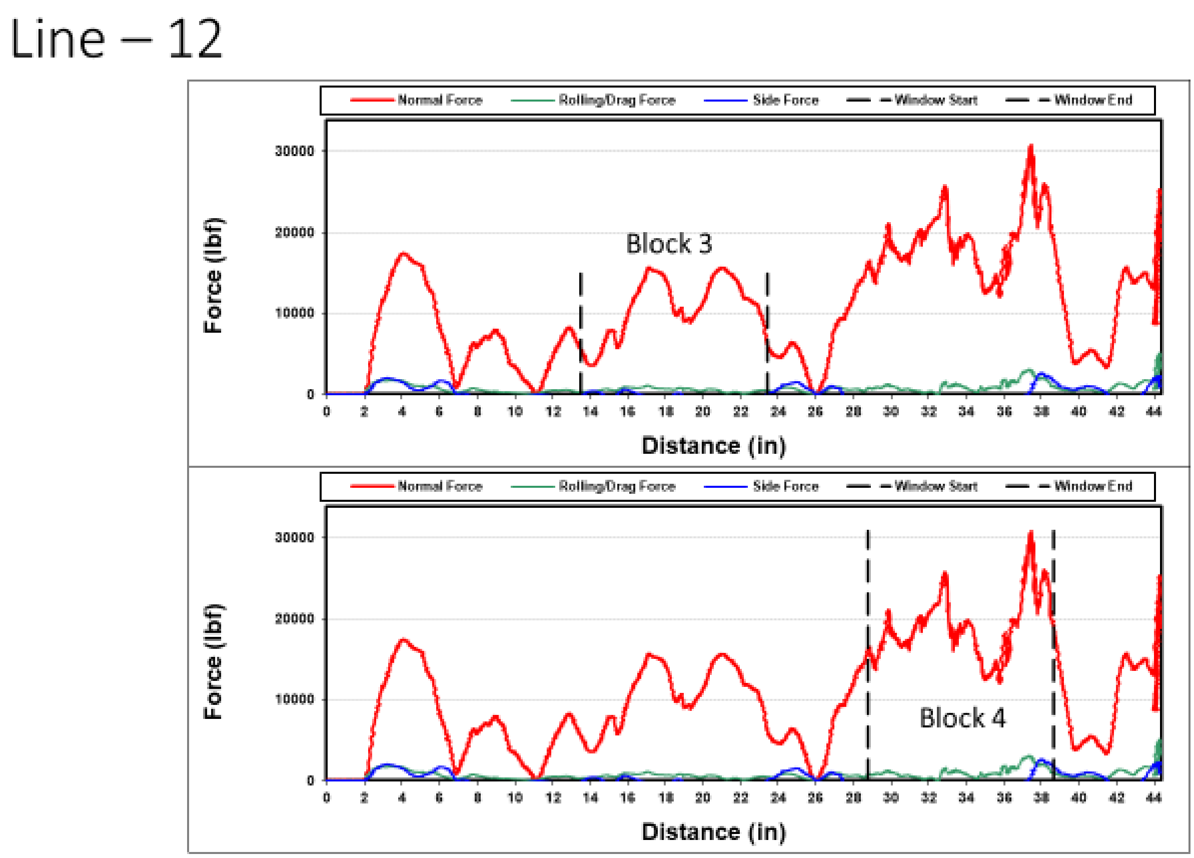

Pass 4 Line 2

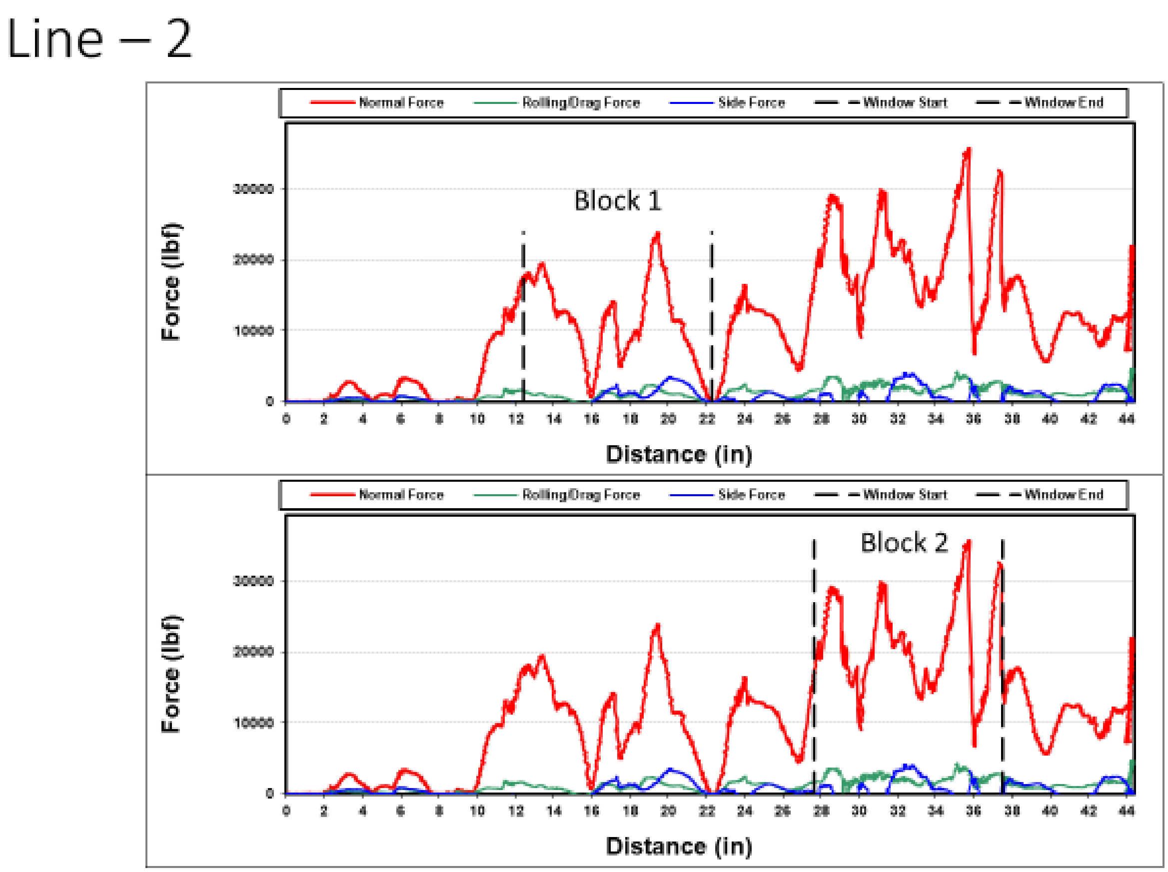
Line – 2
Normal Force
Rolling/Drag Force
Side Force
Window Start
Window End
Block 1
Force (lbf)
Distance (in)
Normal Force
Rolling/Drag Force
Side Force
Window Start
Window End
Block 2
Force (lbf)
Distance (in)

Pass 4 Line 3

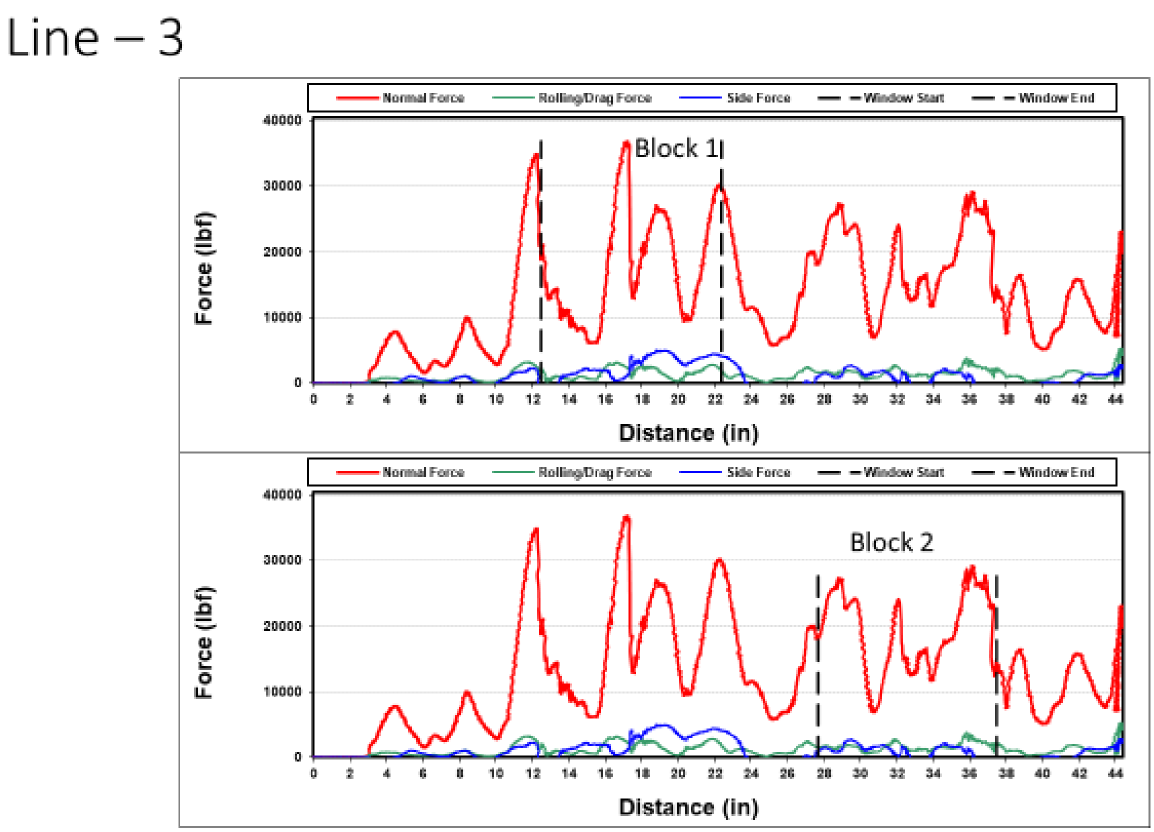
Line – 3
Normal Force
Rolling/Drag Force
Side Force
Window Start
Window End
Block 1
Block 2
Force (lbf)
Distance (in)
0
10000
20000
30000
40000
0 2 4 6 8 10 12 14 16 18 20 22 24 26 28 30 32 34 36 38 40 42 44

Pass 4 Line 5

Line – 5

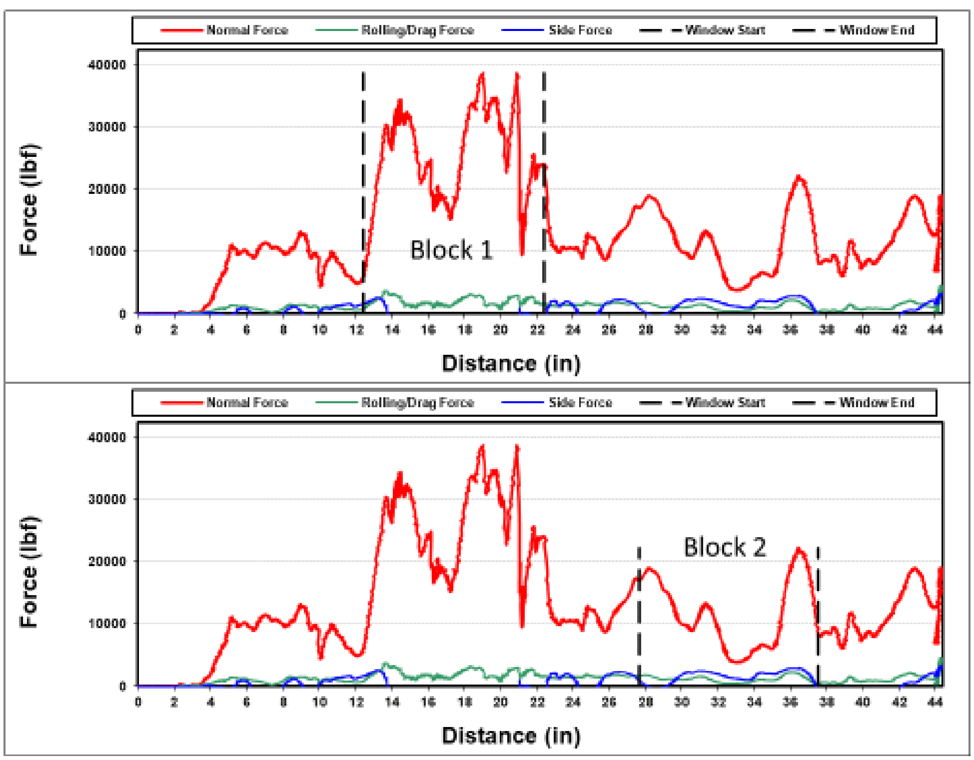

Pass 4 Line 9

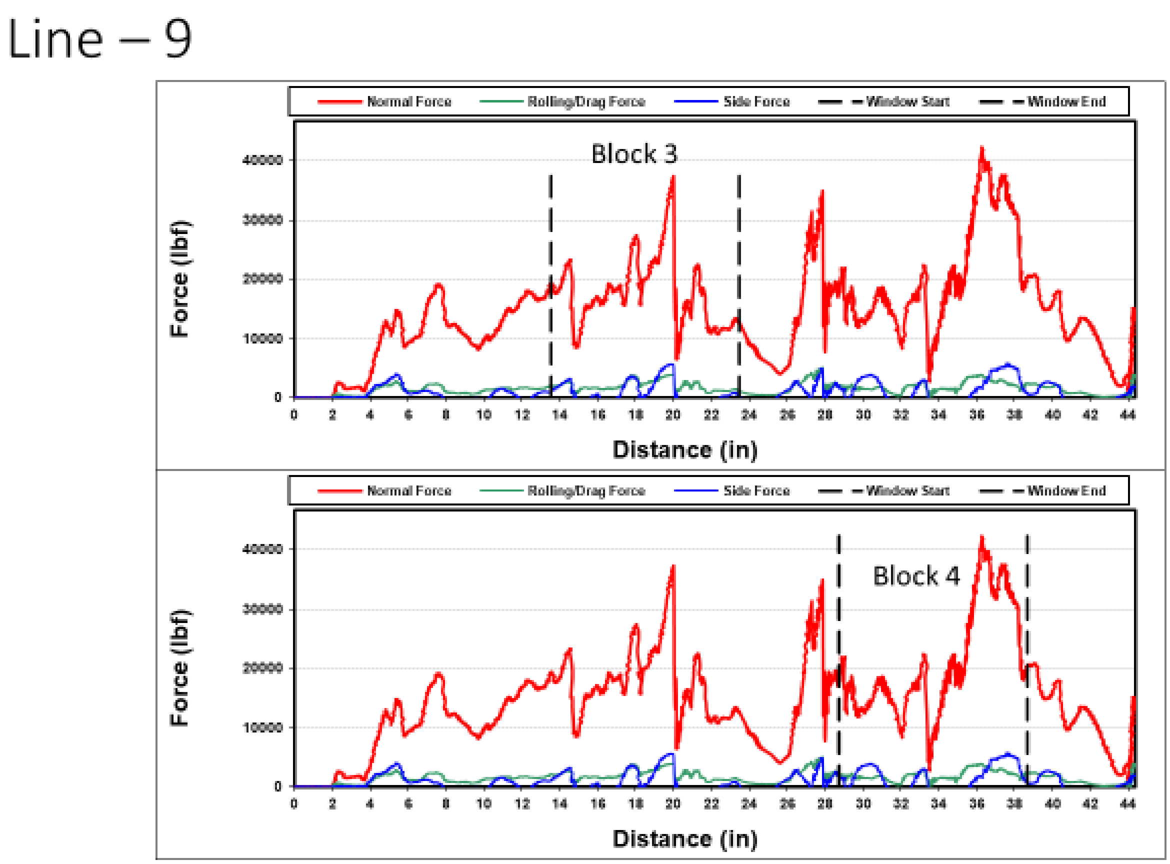

Line – 9
Normal Force
Rolling/Drag Force
Side Force
Window Start
Window End
Block 3
Force (lbf)
Distance (in)
Normal Force
Rolling/Drag Force
Side Force
Window Start
Window End
Block 4
Force (lbf)
Distance (in)

Pass 4 Line 10

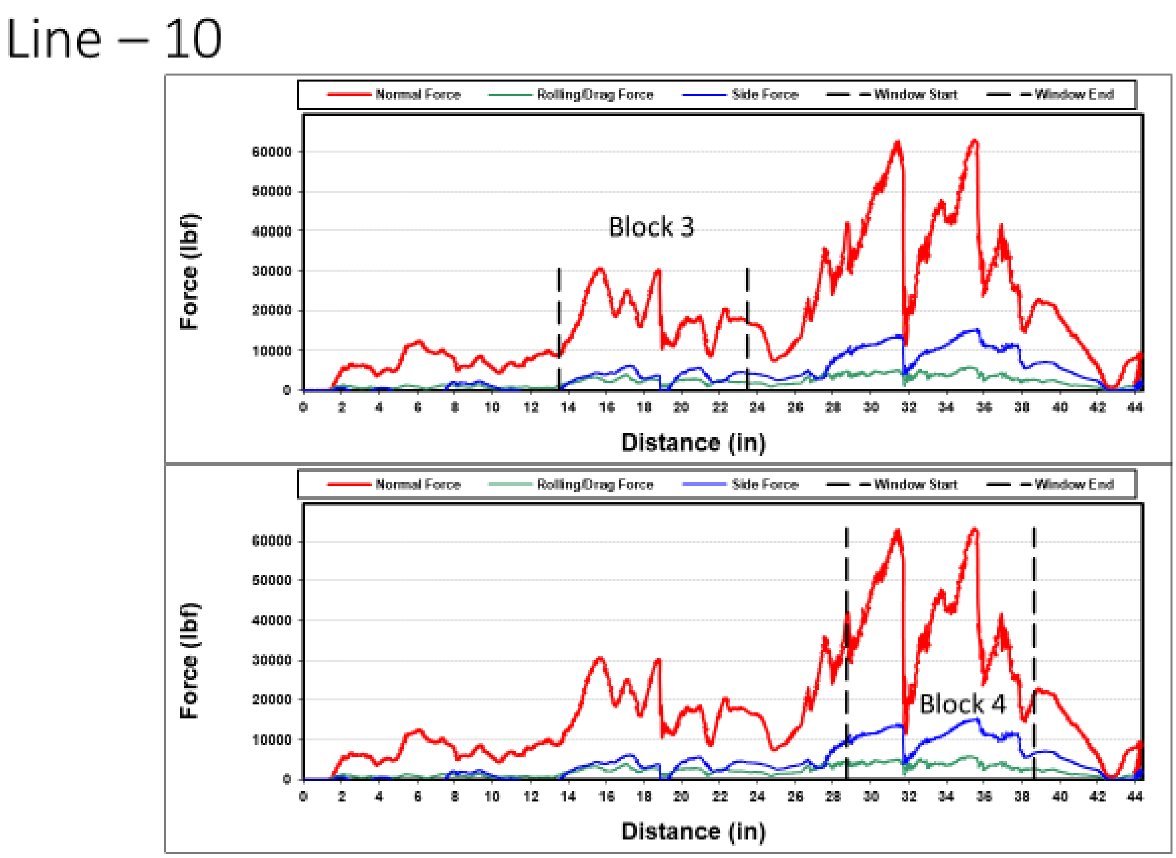

Pass 4 Line 11

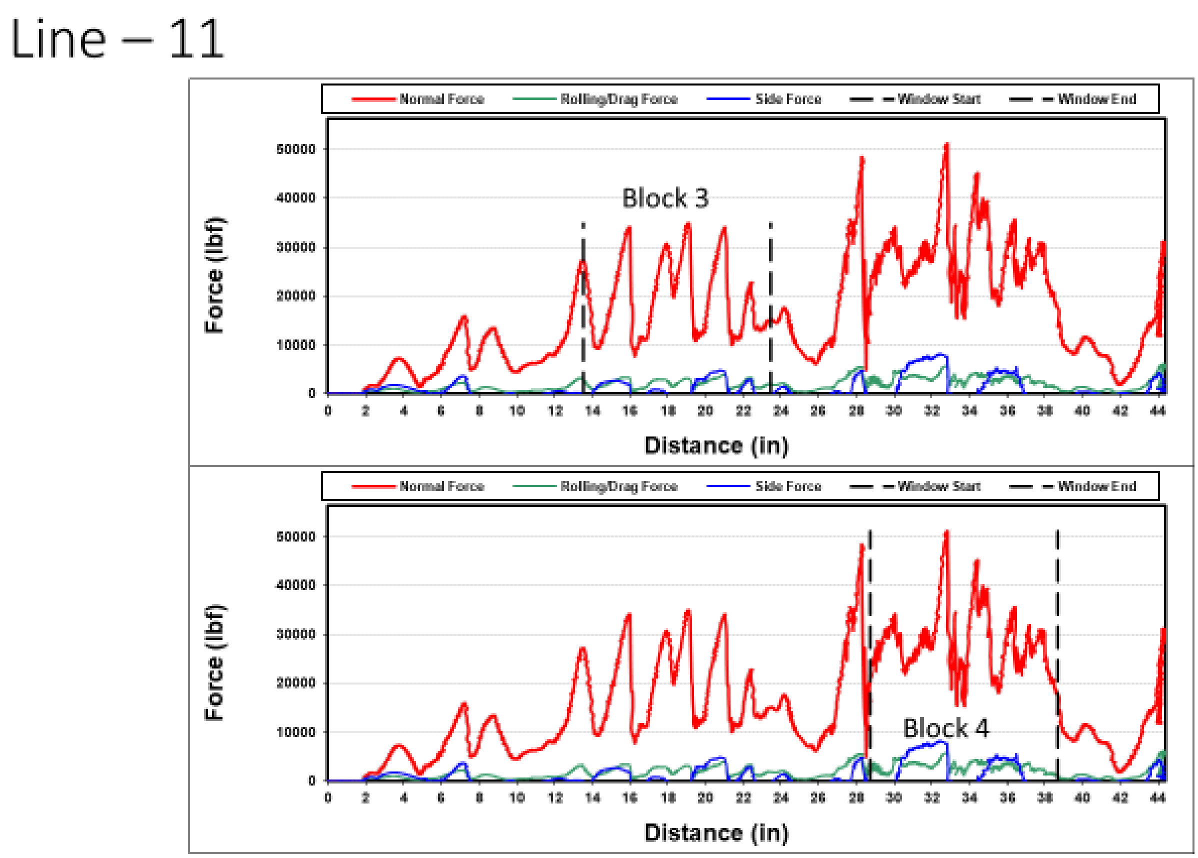

Pass 4 Line 12

Line – 12

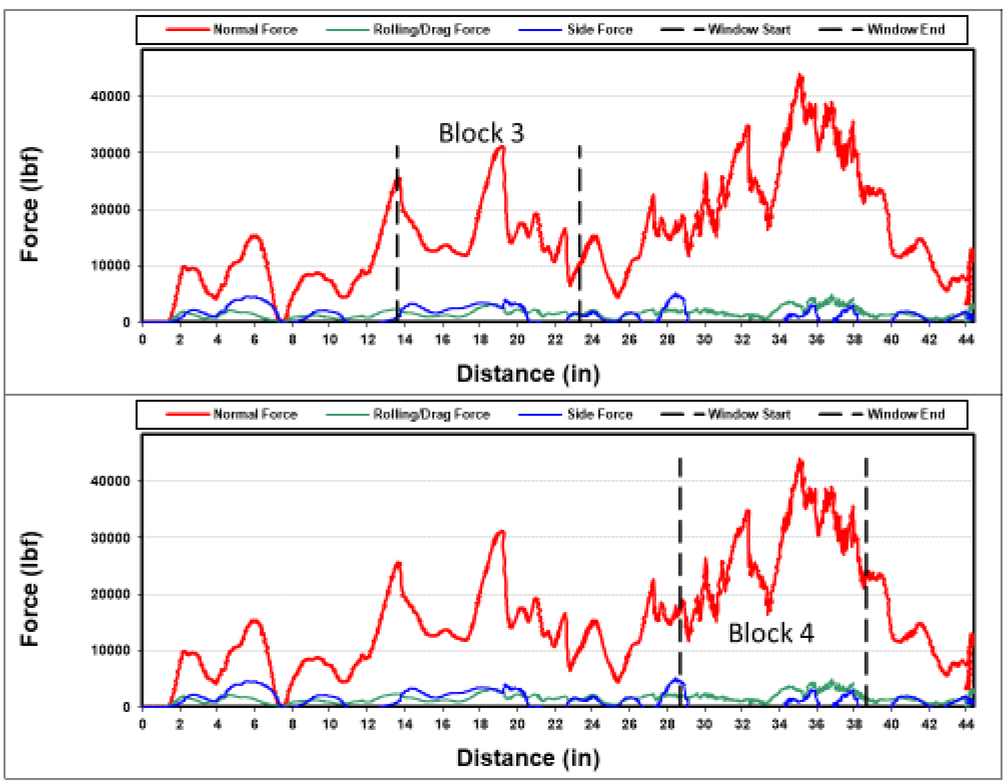

Pass 5 Line 2

Line – 2

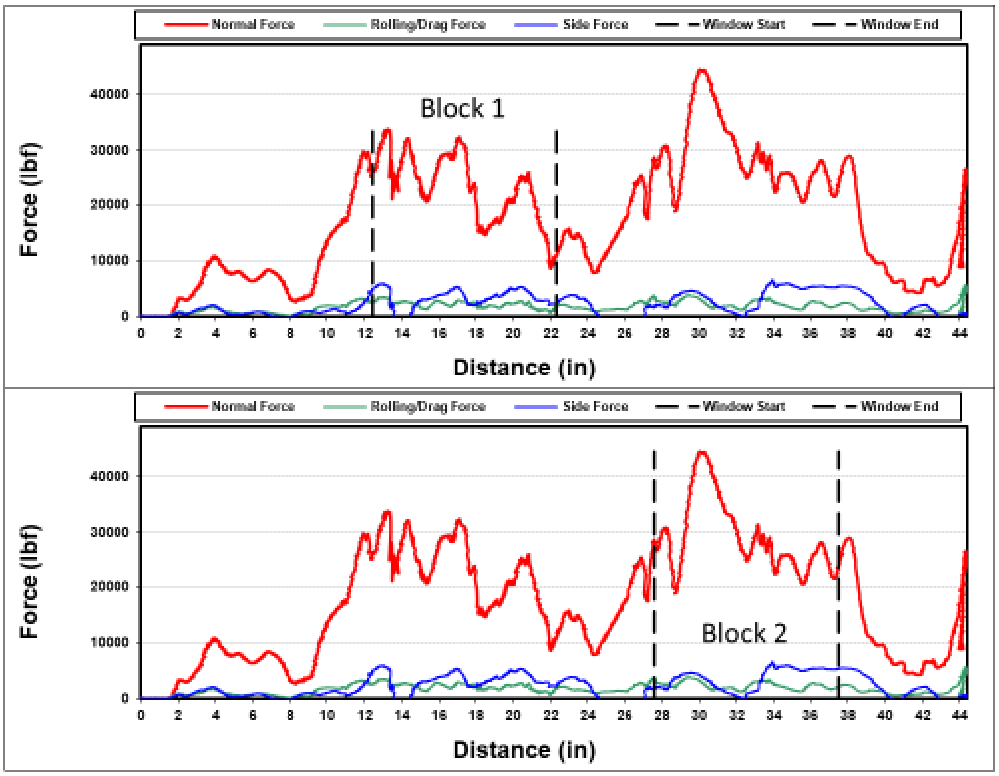

Pass 5 Line 3

Line – 3

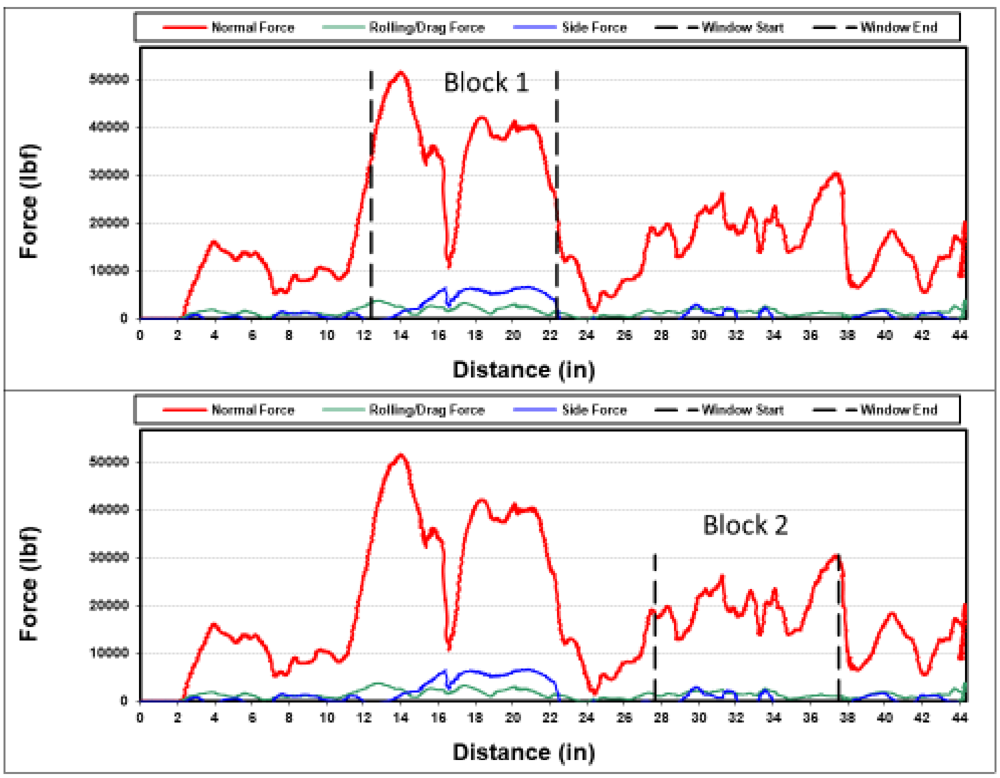

Pass 5 Line 5

Line – 5

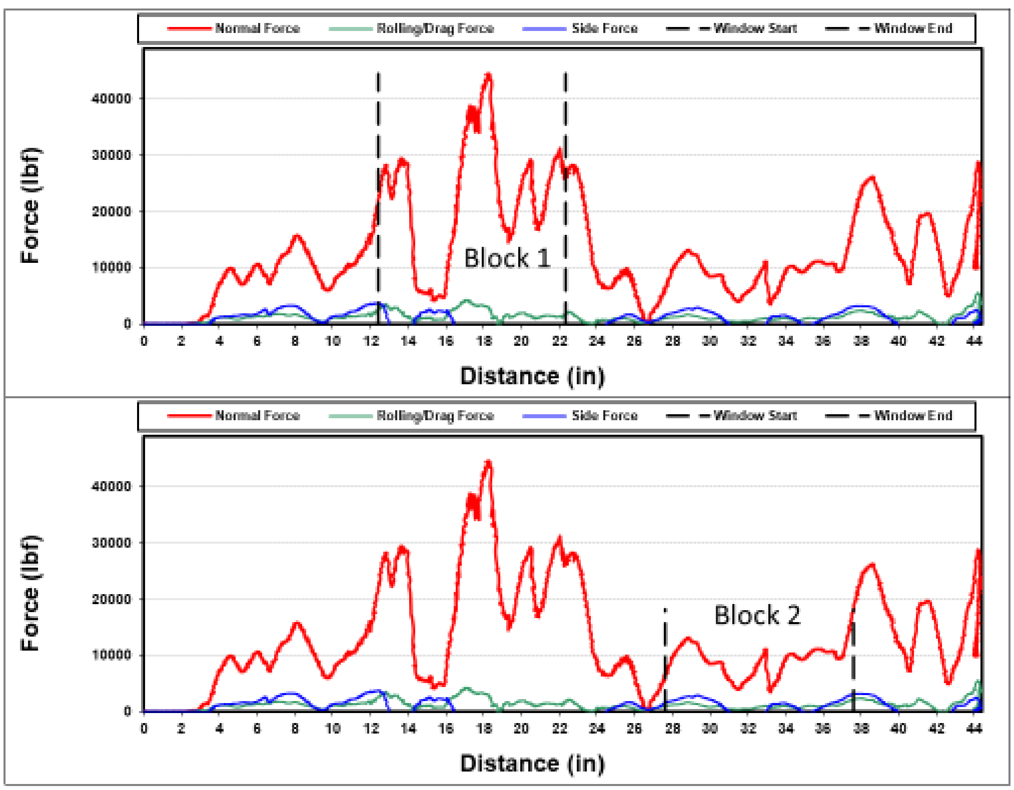

Pass 5 Line 9

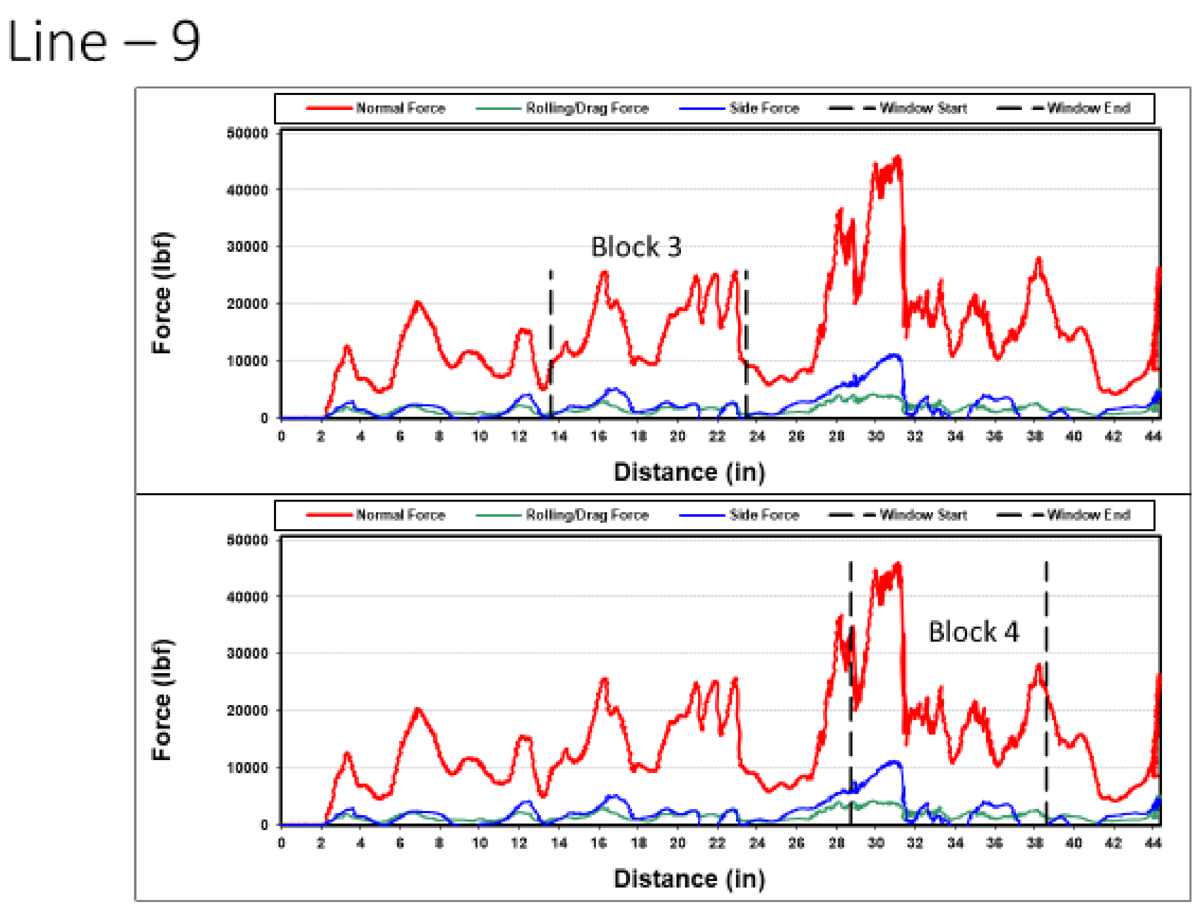
Line – 9
Normal Force
Rolling/Drag Force
Side Force
Window Start
Window End
Force (lbf)
Distance (in)
Block 3
Block 4

Pass 5 Line 10

Line – 10

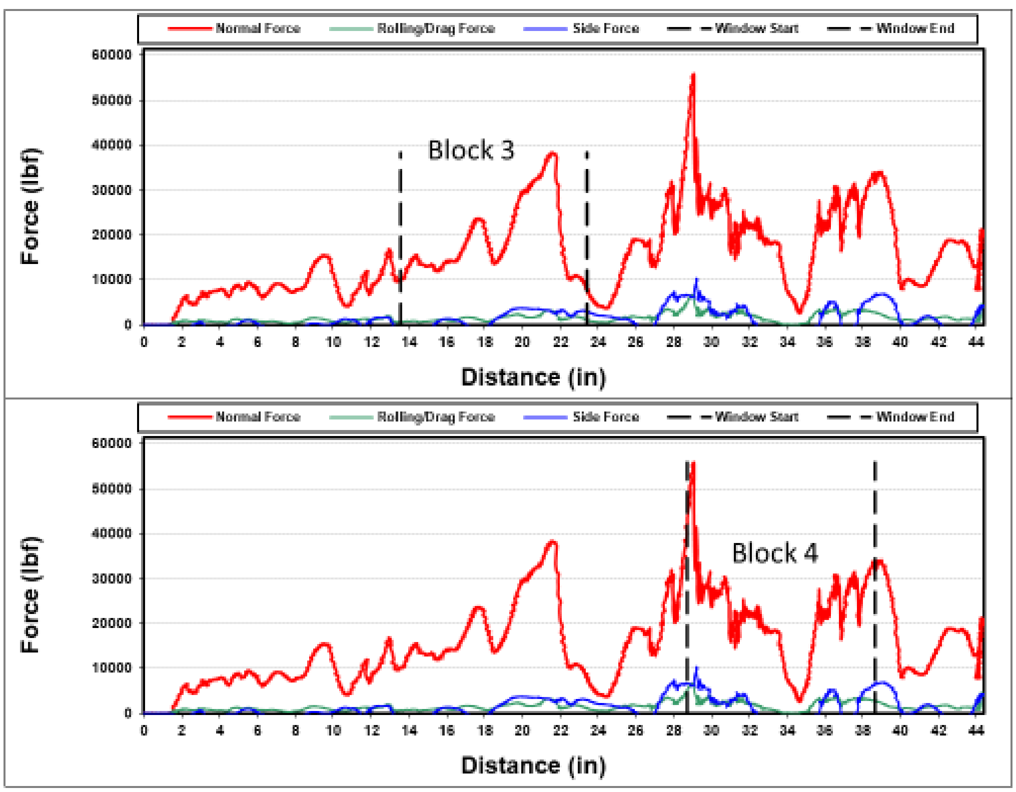

Pass 5 Line 11

Line – 11

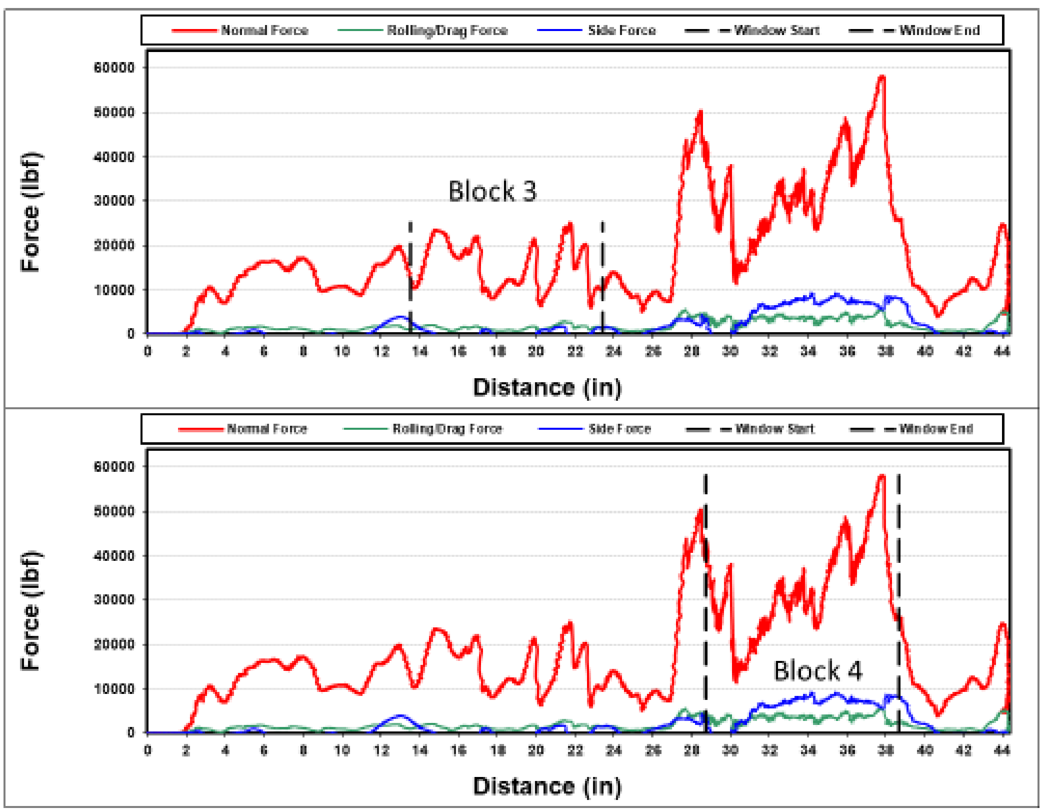

Pass 6 Line 2

Line – 2

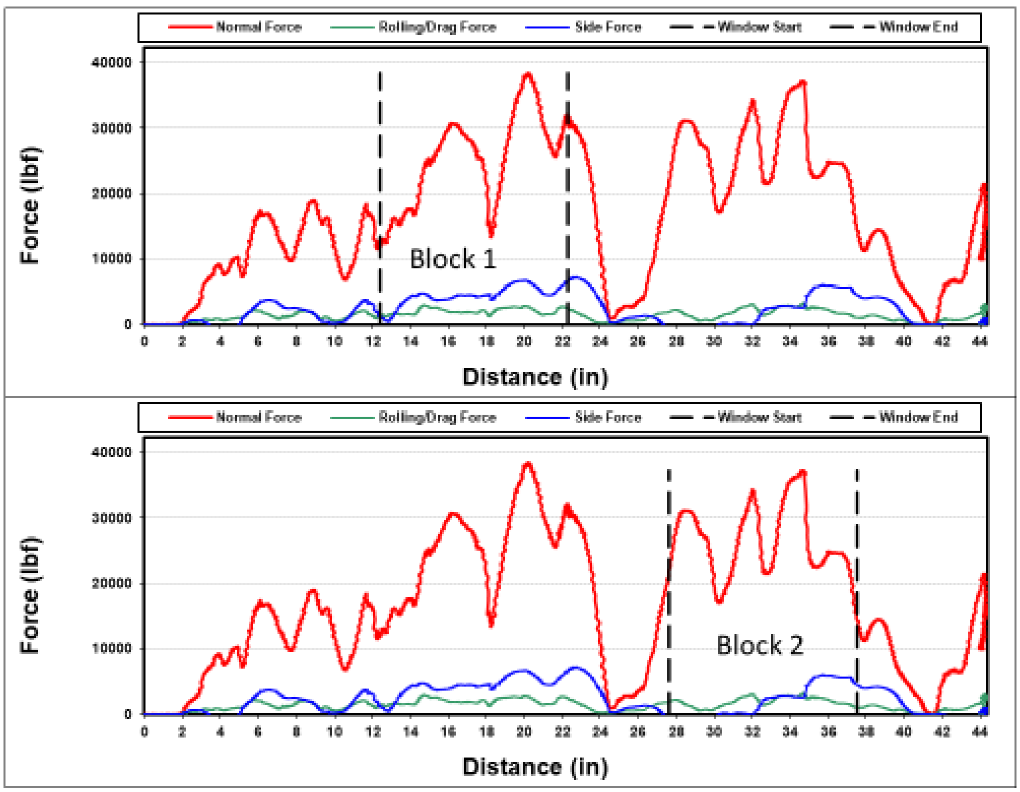

Pass 6 Line 3

Line – 3

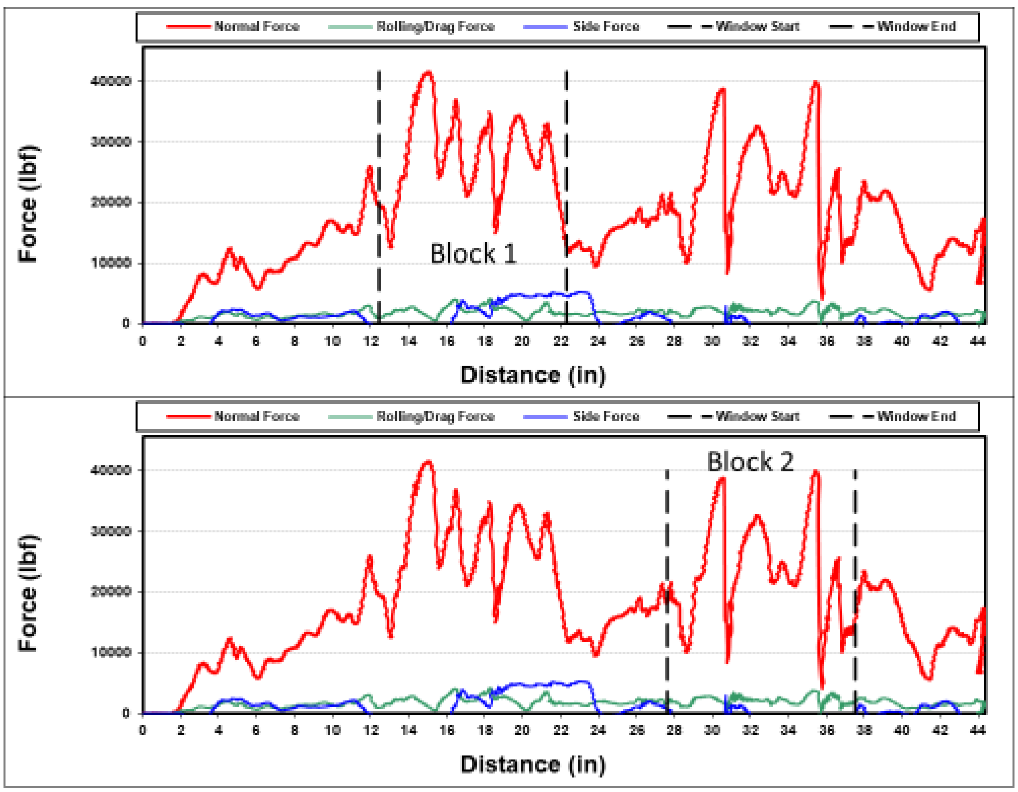

Pass 6 Line 5

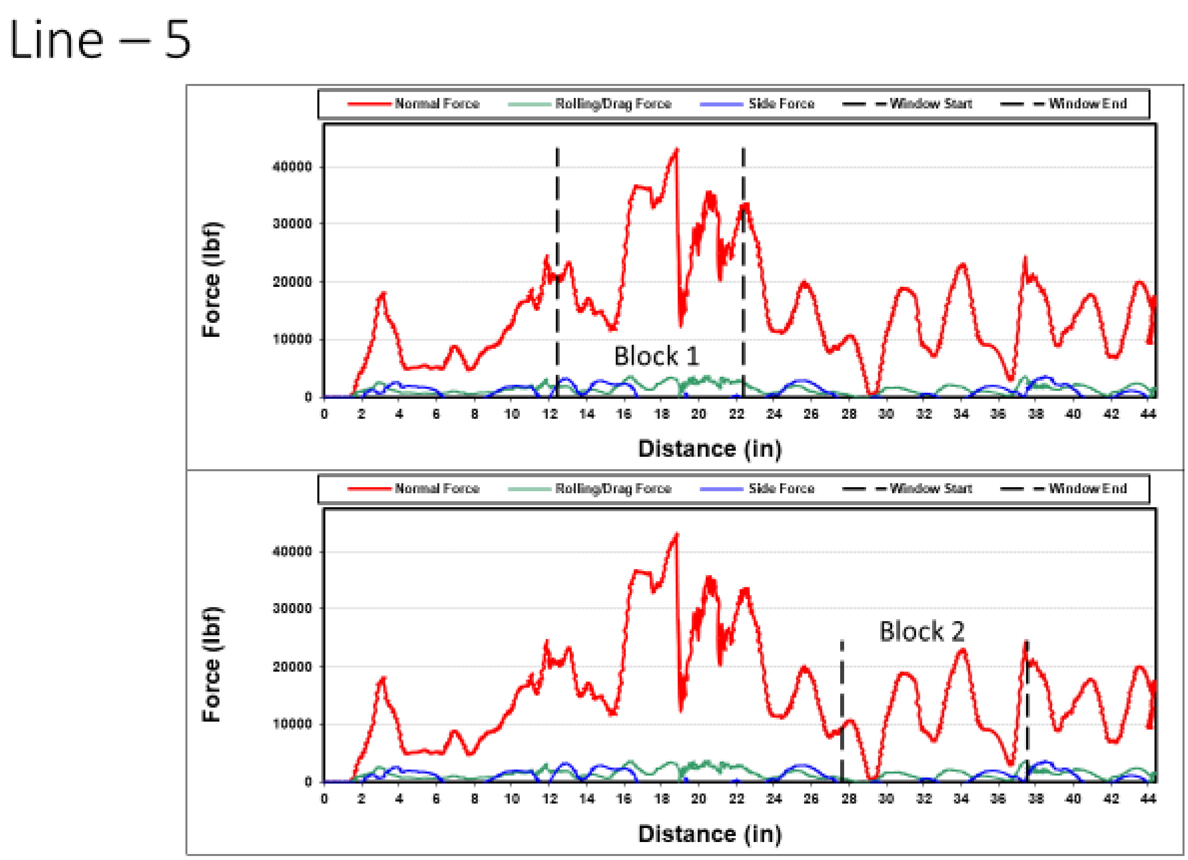
Line – 5
Normal Force
Rolling/Drag Force
Side Force
Window Start
Window End
Force (lbf)
Distance (in)
Block 1
Normal Force
Rolling/Drag Force
Side Force
Window Start
Window End
Force (lbf)
Distance (in)
Block 2

Pass 6 Line 9

Line – 9

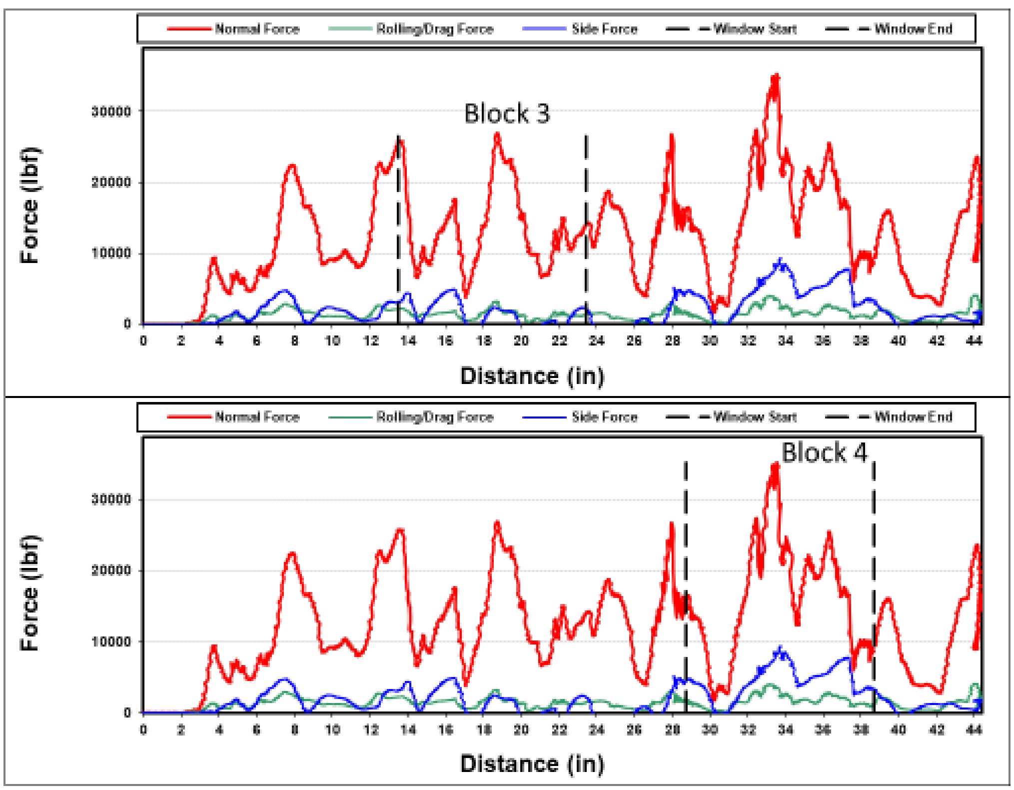

Pass 6 Line 10

Line – 10

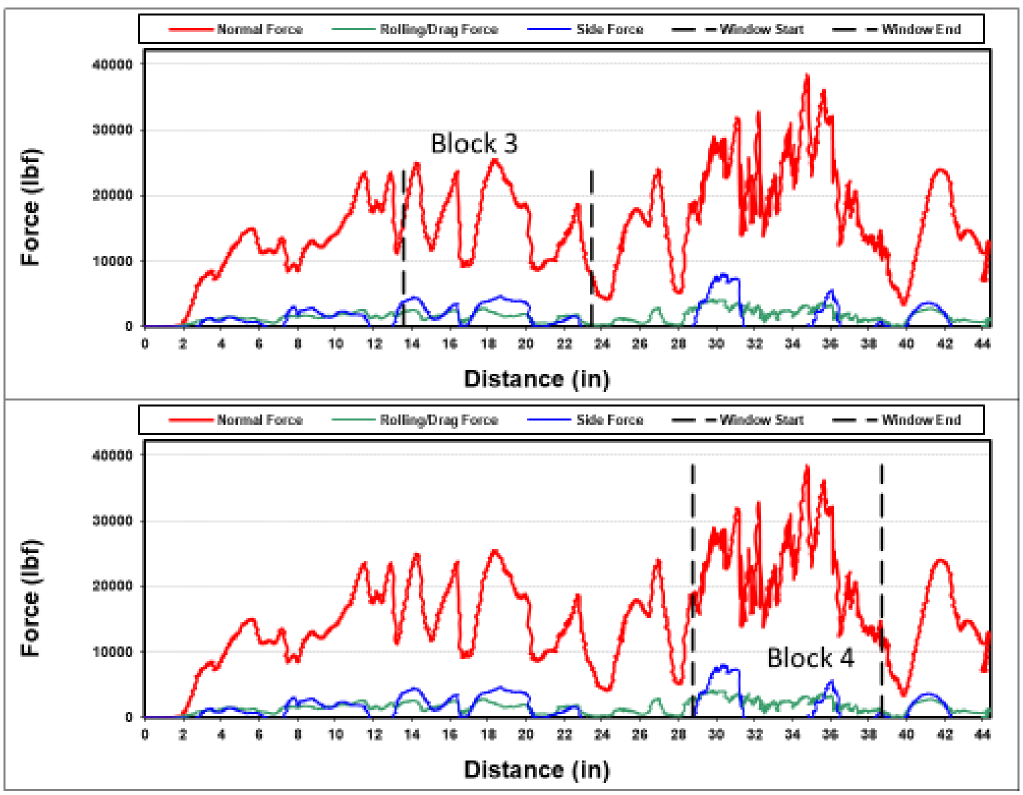

Pass 6 Line 11

Line – 11

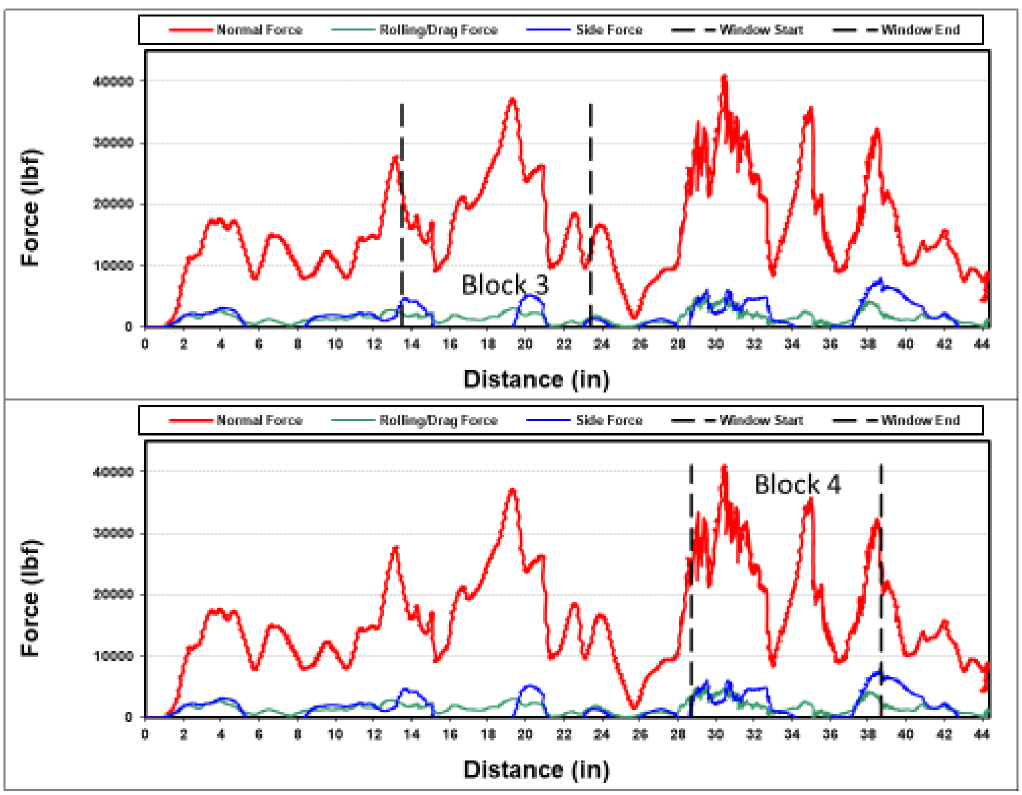

Pass 6 Line 12

Line – 12